

SELECTED METHODS OF SURFACE ENGINEERING APPLIED TO MATERIALS
SCIENCE

by
GÖZDE İPEK ÖZTÜRK

Submitted to the Graduate School of Engineering and Natural Sciences
in partial fulfillment of
the requirements for the degree of
Master of Science

Sabancı University
Summer 2004

© Gzde İpek ztrk

All Rights Reserved

TABLE OF CONTENTS

	Page No:
Acknowledgements.....	iii
Abstract.....	iv
Özet.....	vi
List of Figures	viii

CHAPTER 1

1. Selected methods for surface engineering

1.1. Overview of surface engineering.....	1
1.1.1 Commercial areas of interest.....	1
(i) Biotechnology	
(ii) Synthesis	
(iii) Engineering	
1.2. Surface modification of polyolefins.....	3
1.2.1. Overview.....	3
1.2.2. Types of surface modifications.....	4
(i) Flame treatments	
(ii) Corona Treatments	
(iii) Plasma treatments	
(iv) Wet chemistry	
1.3. The relative oxidation rates of polymers.....	9
1.4. Thermal degradation of polypropylene.....	10
1.5. Tailoring surfaces with silanes.....	12
1.5.1. Silanization procedures.....	13
1.6. Oxidation induced patterning of polypropylene.....	16
1.6.1. Polymer mixtures.....	16
1.6.2. Thermodynamics of polymer mixtures.....	16
1.6.3. Phase separation phenomena.....	17
1.6.4. Phase separation mechanisms	19

(i)	Nucleation and growth	
(ii)	Spinodal decomposition	
	Uphill diffusion	
1.6.5.	Surface directed phase separation.....	22

CHAPTER 2

2. Synthesizing and anchoring organosiloxane film on injection molded polypropylene by intercalation strategy

2.1.	Introduction.....	24
2.2.	Materials.....	25
2.3.	Methods.....	25
2.3.1.	Rationale.....	25
2.3.2.	General methods.....	28
	(i) Ninhydrin Reaction	
2.3.3.	Synthetic Methods.....	28
	(i) Characterizing tube extension due to toluene perfusion	
	(ii) Verifying the co-perfusion of aminopropyltrimethoxysilane-toluene.	
	(iii) Characterizing the product of co-perfusion and subsequent activation-crosslinking	
	(iv) Characterizing the product of concurrent co-perfusion-activation-crosslinking	
	(v) Validating non-adsorptive mode of product retention	
2.4.	Results.....	31
2.5.	Discussion.....	33
	(i) Evidence supporting perfusion of toluene and co-perfusion of aminopropylsilyl species.	
	(ii) Evidence supporting co-perfusion, activation and crosslinking of aminopropylsilyl species in the matrix and pendant to the surface	

(iii)	Evidence ruling out non-covalent modes of aminopropylsilyl retention in the matrix and along the surface	
2.6.	Conclusion.....	36

CHAPTER 3

3. Chemical Modification of Polypropylene Surface by Ammonium Peroxydisulfate Oxidation and Oxidation induced Mesopattern Formation

3.1.	Introduction.....	37
3.2.	Materials.....	38
3.3.	Methods.....	38
3.3.1.	Reaction method.....	38
(i)	Time course reactions	
(ii)	Gravimetric Analysis	
3.3.2.	General Methods.....	39
(i)	Preparation of Persulfate and Control Solutions	
(ii)	Washing and Drying Method for Modified Samples	
(iii)	Preparation and ATR-FTIR Analysis of Samples	
(iv)	Preparation and Scanning Electron Spectroscopic Analysis of Samples	
(v)	Preparation and Differential Scanning Calorimetry Analysis of Samples	
3.4.	Results.....	41
(i)	FTIR measurements of time course samples	
(ii)	Scanning Electron Microscope analyses	

3.5.	Discussion.....	51
	(i) Persulfate-initiated surface reactions and spectroscopic characterization	
	(ii) Rationalizing Cracking Mechanism	
	(iii) Rationalizing Pattern formation	
3.6.	Conclusion.....	64
	REFERENCES.....	65

ACKNOWLEDGEMENTS

I would like to thank my supervisor Asst. Prof Dr. Alpay Taralp for his support and encouragement throughout my education and thesis studies. He was always supportive. It was a pleasure to work with his guidance.

I would also like to thank to Asst. Prof. Dr. Mehmet Ali Gülgün, Assoc. Prof. Dr. Yusuf Z. Menciloglu, Asst. Prof. Dr. Canan Baysal, Asst. Prof. Dr. Clewa Ow Yang, Prof. Dr. Yuda Yürüm for their support and guidance.

My friends were always there to support, humor and stimulate. In particular, I want to thank Dr. Kazim Acatay for being a very nice brother to all of us, for his patience and sharing his experience with all of us. I want to thank also my friends Dr. Mustafa M. Demir, Umut Soydaner and Funda Çelebi for their friendship, support and time they spent with me.

I want to thank my best friend Eren Simsek for his continuous encouragement, trust and patience.

Last but not least, I want to thank my family for their support, not only during my graduate education, but also throughout my whole life.

ABSTRACT

Two approaches were developed to surface-functionalize commercially available injection molded isotactic polypropylene tubes:

Non-reactive method: A novel technique, in which organosiloxane films were fabricated and anchored on low-surface-energy polymer without invoking chemical pretreatment of the surface, was developed to surface-functionalize injection molded polypropylene tubes. In envisaging a non-reactive approach, polypropylene tubes were incubated in solutions that encouraged inter-molecular chain separation of surface-positioned polymeric chains and entry of small, monomeric silane precursors into the sub-layers. During precursor activation, the reaction conditions encouraged activated silane species potentially in and above the plastic matrix to crosslink, in principle affording a thin coating whose bulk was partially submerged and entangled within the plastic matrix. The binary network afforded, for example, polyaminopropylsiloxane entangled within polypropylene, described a system in which two interconnected polymers shared no formal covalent bonds but nevertheless were inseparable.

Reactive method: In surface-engineering of injection-molded polypropylene tubes by oxidative activation, native, mesoscopically flat tubes were oxidized using aqueous ammonium peroxydisulfate. When evaluated in the context of the conditions employed for oxidation, FTIR-ATR spectral analysis indicated that the activated plastics predominantly bore carboxyl, ketone and possibly hydroxyl groups as major surface products and an approximate uniform increase of matrix-bound oxidation products up to 16 hours reaction time. Scanning electron microscopy analyses showed insignificant changes of mesoscale topology up to 8 hours reaction time, sparsely distributed bulges of approximate 400nm diameter developed by 12 hours reaction time, and a sudden and marked transformation thereafter to give the sponge-like mesoscale topology. The main mechanisms envisaged to rationalize the topology included organized pitting of the surface, oxidation-mediated phase separation, or a combination of the two. While

degradative loss of polymer chains clearly pointed to the former mechanism, it by itself could not rationalize the topology, as pitting would have been anticipated gradually in time. In fact, the dramatic change of topology, which suddenly developed late in the oxidation process, could only be consistent with a phase separation. This deduction was corroborated in conducting the parallel experiment with gradually oxidized melt-blown fibers. Mesopatterning induced by oxidation described an alternative to current methods based on lithography, self-organization and solvent casting.

ÖZET

Enjeksiyonla kalıplanmış izotaktik polipropilen tüp yüzeyi reaktif olan ve reaktif olmayan iki yöntem ile modifiye edilmiştir.

Reaktif olmayan yöntem. Enjeksiyonla kalıplanmış polimerlerin yüzey modifikasyonunda çalışılmamış bir strateji olarak, reaktif öncü monomerlerin polimer matrisi içine sokulması ve bunu takiben aktive edilip kendi içinde çapraz bağlanmasının sağlanması esasına dayalı bir yaklaşım takip edilmiştir. Enjeksiyonla kalıplanmış polipropilen tüpler, yüzey zincirlerinin moleküller arası seviyede ayrılmasını ve öncü silan monomerlerin bu zincirler arasına girmesini teşvik eden bir kimyasal olan toluen ile ısıtılmıştır. Bir sonraki basamakta suyun ortama sokulmasıyla polimer zincirlerinin arasına girmiş olan aminopropiltrimetoksisilan gibi öncü organosilan monomerleri aktif silanole dönüştürülmesiyle aktif monomerlerin polipropilen matrisi içerisinde çapraz bağlanacağı ortam hazırlanmıştır. Bunun sonucunda polipropilen ile poliaminopropylsiloxane, kovalent bağ içermeyen, birbirinden ayrılamaz durumda, iç içe geçmiş ikili ağ oluşturmuştur. Ninhidrin analizleri tüp yüzeyinde amino gruplarının varlığını göstermiştir. Diğer yüzey modifikasyon yöntemlerinden farklı olarak, polipropilenin kimyasal yapısını değiştirmeden yüzeyine fonksiyonel gruplar eklenmesi sağlayan yeni bir yöntem sunmuştur.

Reaktif yöntem. Enjeksiyonla kalıplanmış izotaktik polipropilen tüpler, amonyum peroksidisülfat çözeltisi kullanılarak kimyasal yolla modifiye edilmiştir ve bu işlemi takiben yüzeyde oluşan desenin temel nedeni ve potansiyel uygulamaları araştırılmıştır. Oksidasyon işlemi yüzey boyunca sadece polar fonksiyonel gruplar değil, daha önemlisi, topolojide mezoskopik seviyede önemli değişikliğe yol açmıştır. FTIR-ATR spektroskopik analizleri sonucunda yüzeye bağlı oksidasyon ürünlerinde 16 saatlik reaksiyona kadar düzgün bir artış olduğu gözlemlenmiştir. Buna karşın, taramalı elektron mikrografları analizleri göstermiştir ki, 8. saate kadar topolojide önemli değişiklikler olmamakta; 8 ve 12 saat arasında, seyrekçe dağılmış, yaklaşık 400nm çaplı tümsekler şekillenmeye başlamakta ve ilerleyen aşamalarda mezoskopik seviyede

süngerimsi görünümler oluşmaktadır. Topolojide meydana gelen bu değişikliğin açıklanmasında yüzeyin kimyasal reaksiyon sonucu oyulması, oksidasyon sonucu faz ayrımı oluşumu gibi mekanizmalar öngörülmüştür. Polimer zincirlerinin reaksiyon sonucu kaybı, önerilen ilk mekanizmaya işaret etse de oyma işlemi zamanla kademeli olarak beklendiği için, topolojideki değişikliğin nedenini tek başına açıklamaya yeterli değildir. Oksidasyon sonrası topolojide meydana gelen çarpıcı değişiklikler faz ayrımıyla ve stresin serbest kalmasıyla tutarlıdır. Bu çıkarım, polipropilen fiberlerle yapılan paralel deneyle kuvvetlendirilmiştir. Oluşan yeni topolojinin altında yatan mekanizmanın açıklanması kimyasal olarak aktif yeni yüzeyler elde edilmesinde ve yüzey modifikasyonunda alternatifler sunmaktadır.

LIST OF FIGURES

Figure 1.1. Free radical chain reaction involved in polypropylene thermal oxidation.....	11
Figure 1.2. Modification of silica gel with aminopropyltriethoxysilane.....	15
Figure 1.3. Free energies of mixing as a function of composition for conditions under which two species are miscible (a) and immiscible(b)	17
Figure 1.4. Schematic phase diagrams illustrating the different pathways which may lead to phase separation A. Temperature quench, B. Removal of common solvent, C. Polymerization of one or both of the components.....	18
Figure 1.5. Spinodal decomposition. A. In the unstable part of the phase diagram, random concentration fluctuations are unstable and grow in amplitude. Long-wavelength fluctuations (b) grow slowly because of the large distances through which material needs to be transported, while short fluctuations (c) are suppressed, because of the free energy penalty associated with sharp concentration gradient.....	21
Figure 1.6. The behavior of the interface width w and the average domain size R at various stages of spinodal decomposition: (a) early stage, (b) intermediate stage, (c) late stage.....	23
Figure 2.1. Two approaches to anchor organosilanes onto plastics using intercalation and activation. A. Aminopropyltrimethoxysilane in dry toluene is co-infused into the matrix (Step 1); water-saturated toluene is delivered to intercalated and surface-residing organosilanes (Step 2); reactive organosilanols form siloxane bridges to one another with heating and concomitant loss of toluene (Step 3). B. Simultaneous co-infusion and activation of aminopropyltrimethoxysilane (<i>Step 1</i>) followed by decantation and heat-induced cross-linking (<i>Step 2</i>).....	27

Figure 2.2. Distention of polypropylene during solvent treatment is depicted. A. Image of Eppendorf Safe-Twist tubes treated (3h) with propanol control (left) and water-reduced toluene (right); B. Graph of elongation versus time in toluene, reporting the top-to-bottom length of an Eppendorf Safe-Lock tube.....31

Figure 2.3. A. Native tube; B. Control tube incubated with aminopropyltrimethoxysilane in non-perfusing propanol; C. Trial tube incubated with aminopropyltrimethoxysilane in water-reduced toluene.....32

Figure 2.4. A. Native tube; B. Control tubes treated with aminopropyltrimethoxysilane in water-reduced toluene solution; C. Trial tubes treated with aminopropyltrimethoxysilane in water-saturated toluene solution.....32

Figure 3.1. Cutting steps for sample preparation for ATR-FTIR 40

Figure 3.2. ATR FTIR spectrum of vacuum dried samples before (dashed line) and after (solid line) reaction (1M, 70°C, 16h).....41

Figure 3.3. ATR- FTIR spectra of the time course reaction.....44

Figure 3.4. SEM image of A. Native Eppendorf tube; B. Eppendorf Tube treated with ammonium sulfate(1M, 70°C, 16h) ; C. Eppendorf Tube treated with ammonium persulfate (1M, 70°C, 16h)..... 45

Figure 3.5 Photograph of A. Native Eppendorf tube; B. Oxidized Eppendorf Tube, showing the change in optical clarity after oxidation.....45

Figure 3.6. A. Schematic drawing of an Eppendorf half-full with the oxidant solution ammonium peroxydisulfate; B. Optical microscope image of oxidized Eppendorf Tube showing the air-solution boundary..... 46

Figure 3.7. Scanning electron micrograph of APS treated Eppendorf tube taken from the cross-sectional viewpoint, tilted slightly towards the inner face.....	47
Figure 3.8. Scanning electron micrographs of gold-coated surfaces of Eppendorf tubes oxidized with APS (1M, 70°C, 42h) at different magnifications.....	47
Figure 3.9. Scanning electron micrographs of injection-molded polypropylene oxidized for: (A) 8h; (B) 10h; (C) 12h; and (D) 16h. The negative reaction control surface appeared identical to the 8h time point (A).....	48
Figure 3.10. Scanning electron micrographs of oxidized melt-blown polypropylene at different magnifications.....	49
Figure 3.11. Scanning electron micrographs and EDS analysis of oxidized PP fiber; lines intensities corresponding to: yellow line: base fiber; redline: amorphous, green line: particles on the surface..	50
Figure 3.12. Scanning electron micrographs A. Polypropylene fiber, B. Polypropylene tubes, treated with APS showing two structures separated by a boundary.....	51
Figure 3.13. A. Homolytic decomposition of persulfate B. Hydrogen abstraction from a tertiary carbon.....	52
Figure 3.14. Chain scission under anoxic conditions.....	52
Figure 3.15. Hydroperoxidation of primary and secondary carbon centers.	53
Figure 3.16. A. Unimolecular thermolysis of hydroperoxides B. Bimolecular thermolysis of hydroperoxides C. Decomposition of alkoxyl radical by β -scission.....	53
Figure 3.17. General acid catalyzed hydroperoxide decomposition.....	54

Figure 3.18. Acid catalyzed decomposition of polypropylene hydroperoxides.....	55
Figure 3.19. Decomposition of peroxides induced by A. peroxy radical B. hydroxyl radical.....	56
Figure 3.20. Reaction model illustrating formation of carboxylic acid , ester and alcohol via transfer pathway.....	56
Figure 3.21. Important reactions of termination step.....	57
Figure 3.22. Reaction model illustrating formation of functional groups in polypropylene during oxidation.....	58
Figure 3.23. Comparison of SEM micrographs(left) and FTIR(right) of time course samples.....	62

SELECTED METHODS OF SURFACE ENGINEERING APPLIED TO MATERIALS
SCIENCE

by
GÖZDE İPEK ÖZTÜRK

Submitted to the Graduate School of Engineering and Natural Sciences
in partial fulfillment of
the requirements for the degree of
Master of Science

Sabancı University
Summer 2004

© Gzde İpek ztrk

All Rights Reserved

TABLE OF CONTENTS

	Page No:
Acknowledgements.....	iii
Abstract.....	iv
Özet.....	vi
List of Figures	viii

CHAPTER 1

1. Selected methods for surface engineering

1.1. Overview of surface engineering.....	1
1.1.1 Commercial areas of interest.....	1
(i) Biotechnology	
(ii) Synthesis	
(iii) Engineering	
1.2. Surface modification of polyolefins.....	3
1.2.1. Overview.....	3
1.2.2. Types of surface modifications.....	4
(i) Flame treatments	
(ii) Corona Treatments	
(iii) Plasma treatments	
(iv) Wet chemistry	
1.3. The relative oxidation rates of polymers.....	9
1.4. Thermal degradation of polypropylene.....	10
1.5. Tailoring surfaces with silanes.....	12
1.5.1. Silanization procedures.....	13
1.6. Oxidation induced patterning of polypropylene.....	16
1.6.1. Polymer mixtures.....	16
1.6.2. Thermodynamics of polymer mixtures.....	16
1.6.3. Phase separation phenomena.....	17
1.6.4. Phase separation mechanisms	19

(i)	Nucleation and growth	
(ii)	Spinodal decomposition	
	Uphill diffusion	
1.6.5.	Surface directed phase separation.....	22

CHAPTER 2

2. Synthesizing and anchoring organosiloxane film on injection molded polypropylene by intercalation strategy

2.1.	Introduction.....	24
2.2.	Materials.....	25
2.3.	Methods.....	25
2.3.1.	Rationale.....	25
2.3.2.	General methods.....	28
	(i) Ninhydrin Reaction	
2.3.3.	Synthetic Methods.....	28
	(i) Characterizing tube extension due to toluene perfusion	
	(ii) Verifying the co-perfusion of aminopropyltrimethoxysilane-toluene.	
	(iii) Characterizing the product of co-perfusion and subsequent activation-crosslinking	
	(iv) Characterizing the product of concurrent co-perfusion-activation-crosslinking	
	(v) Validating non-adsorptive mode of product retention	
2.4.	Results.....	31
2.5.	Discussion.....	33
	(i) Evidence supporting perfusion of toluene and co-perfusion of aminopropylsilyl species.	
	(ii) Evidence supporting co-perfusion, activation and crosslinking of aminopropylsilyl species in the matrix and pendant to the surface	

(iii)	Evidence ruling out non-covalent modes of aminopropylsilyl retention in the matrix and along the surface	
2.6.	Conclusion.....	36

CHAPTER 3

3. Chemical Modification of Polypropylene Surface by Ammonium Peroxydisulfate Oxidation and Oxidation induced Mesopattern Formation

3.1.	Introduction.....	37
3.2.	Materials.....	38
3.3.	Methods.....	38
3.3.1.	Reaction method.....	38
(i)	Time course reactions	
(ii)	Gravimetric Analysis	
3.3.2.	General Methods.....	39
(i)	Preparation of Persulfate and Control Solutions	
(ii)	Washing and Drying Method for Modified Samples	
(iii)	Preparation and ATR-FTIR Analysis of Samples	
(iv)	Preparation and Scanning Electron Spectroscopic Analysis of Samples	
(v)	Preparation and Differential Scanning Calorimetry Analysis of Samples	
3.4.	Results.....	41
(i)	FTIR measurements of time course samples	
(ii)	Scanning Electron Microscope analyses	

3.5.	Discussion.....	51
	(i) Persulfate-initiated surface reactions and spectroscopic characterization	
	(ii) Rationalizing Cracking Mechanism	
	(iii) Rationalizing Pattern formation	
3.6.	Conclusion.....	64
	REFERENCES.....	65

ACKNOWLEDGEMENTS

I would like to thank my supervisor Asst. Prof Dr. Alpay Taralp for his support and encouragement throughout my education and thesis studies. He was always supportive. It was a pleasure to work with his guidance.

I would also like to thank to Asst. Prof. Dr. Mehmet Ali Gülgün, Assoc. Prof. Dr. Yusuf Z. Menciloglu, Asst. Prof. Dr. Canan Baysal, Asst. Prof. Dr. Clewa Ow Yang, Prof. Dr. Yuda Yürüm for their support and guidance.

My friends were always there to support, humor and stimulate. In particular, I want to thank Dr. Kazim Acatay for being a very nice brother to all of us, for his patience and sharing his experience with all of us. I want to thank also my friends Dr. Mustafa M. Demir, Umut Soydaner and Funda Çelebi for their friendship, support and time they spent with me.

I want to thank my best friend Eren Simsek for his continuous encouragement, trust and patience.

Last but not least, I want to thank my family for their support, not only during my graduate education, but also throughout my whole life.

ABSTRACT

Two approaches were developed to surface-functionalize commercially available injection molded isotactic polypropylene tubes:

Non-reactive method: A novel technique, in which organosiloxane films were fabricated and anchored on low-surface-energy polymer without invoking chemical pretreatment of the surface, was developed to surface-functionalize injection molded polypropylene tubes. In envisaging a non-reactive approach, polypropylene tubes were incubated in solutions that encouraged inter-molecular chain separation of surface-positioned polymeric chains and entry of small, monomeric silane precursors into the sub-layers. During precursor activation, the reaction conditions encouraged activated silane species potentially in and above the plastic matrix to crosslink, in principle affording a thin coating whose bulk was partially submerged and entangled within the plastic matrix. The binary network afforded, for example, polyaminopropylsiloxane entangled within polypropylene, described a system in which two interconnected polymers shared no formal covalent bonds but nevertheless were inseparable.

Reactive method: In surface-engineering of injection-molded polypropylene tubes by oxidative activation, native, mesoscopically flat tubes were oxidized using aqueous ammonium peroxydisulfate. When evaluated in the context of the conditions employed for oxidation, FTIR-ATR spectral analysis indicated that the activated plastics predominantly bore carboxyl, ketone and possibly hydroxyl groups as major surface products and an approximate uniform increase of matrix-bound oxidation products up to 16 hours reaction time. Scanning electron microscopy analyses showed insignificant changes of mesoscale topology up to 8 hours reaction time, sparsely distributed bulges of approximate 400nm diameter developed by 12 hours reaction time, and a sudden and marked transformation thereafter to give the sponge-like mesoscale topology. The main mechanisms envisaged to rationalize the topology included organized pitting of the surface, oxidation-mediated phase separation, or a combination of the two. While

degradative loss of polymer chains clearly pointed to the former mechanism, it by itself could not rationalize the topology, as pitting would have been anticipated gradually in time. In fact, the dramatic change of topology, which suddenly developed late in the oxidation process, could only be consistent with a phase separation. This deduction was corroborated in conducting the parallel experiment with gradually oxidized melt-blown fibers. Mesopatterning induced by oxidation described an alternative to current methods based on lithography, self-organization and solvent casting.

ÖZET

Enjeksiyonla kalıplanmış izotaktik polipropilen tüp yüzeyi reaktif olan ve reaktif olmayan iki yöntem ile modifiye edilmiştir.

Reaktif olmayan yöntem. Enjeksiyonla kalıplanmış polimerlerin yüzey modifikasyonunda çalışılmamış bir strateji olarak, reaktif öncü monomerlerin polimer matrisi içine sokulması ve bunu takiben aktive edilip kendi içinde çapraz bağlanmasının sağlanması esasına dayalı bir yaklaşım takip edilmiştir. Enjeksiyonla kalıplanmış polipropilen tüpler, yüzey zincirlerinin moleküller arası seviyede ayrılmasını ve öncü silan monomerlerin bu zincirler arasına girmesini teşvik eden bir kimyasal olan toluen ile ısıtılmıştır. Bir sonraki basamakta suyun ortama sokulmasıyla polimer zincirlerinin arasına girmiş olan aminopropiltrimetoksisilan gibi öncü organosilan monomerleri aktif silanole dönüştürülmesiyle aktif monomerlerin polipropilen matrisi içerisinde çapraz bağlanacağı ortam hazırlanmıştır. Bunun sonucunda polipropilen ile poliaminopropylsiloxane, kovalent bağ içermeyen, birbirinden ayrılamaz durumda, iç içe geçmiş ikili ağ oluşturmuştur. Ninhidrin analizleri tüp yüzeyinde amino gruplarının varlığını göstermiştir. Diğer yüzey modifikasyon yöntemlerinden farklı olarak, polipropilenin kimyasal yapısını değiştirmeden yüzeyine fonksiyonel gruplar eklenmesi sağlayan yeni bir yöntem sunmuştur.

Reaktif yöntem. Enjeksiyonla kalıplanmış izotaktik polipropilen tüpler, amonyum peroksidisülfat çözeltisi kullanılarak kimyasal yolla modifiye edilmiştir ve bu işlemi takiben yüzeyde oluşan desenin temel nedeni ve potansiyel uygulamaları araştırılmıştır. Oksidasyon işlemi yüzey boyunca sadece polar fonksiyonel gruplar değil, daha önemlisi, topolojide mezoskopik seviyede önemli değişikliğe yol açmıştır. FTIR-ATR spektroskopik analizleri sonucunda yüzeye bağlı oksidasyon ürünlerinde 16 saatlik reaksiyona kadar düzgün bir artış olduğu gözlemlenmiştir. Buna karşın, taramalı elektron mikrografları analizleri göstermiştir ki, 8. saate kadar topolojide önemli değişiklikler olmamakta; 8 ve 12 saat arasında, seyrekçe dağılmış, yaklaşık 400nm çaplı tümsekler şekillenmeye başlamakta ve ilerleyen aşamalarda mezoskopik seviyede

süngerimsi görünümler oluşmaktadır. Topolojide meydana gelen bu değişikliğin açıklanmasında yüzeyin kimyasal reaksiyon sonucu oyulması, oksidasyon sonucu faz ayrımı oluşumu gibi mekanizmalar öngörülmüştür. Polimer zincirlerinin reaksiyon sonucu kaybı, önerilen ilk mekanizmaya işaret etse de oyma işlemi zamanla kademeli olarak beklendiği için, topolojideki değişikliğin nedenini tek başına açıklamaya yeterli değildir. Oksidasyon sonrası topolojide meydana gelen çarpıcı değişiklikler faz ayrımıyla ve stresin serbest kalmasıyla tutarlıdır. Bu çıkarım, polipropilen fiberlerle yapılan paralel deneyle kuvvetlendirilmiştir. Oluşan yeni topolojinin altında yatan mekanizmanın açıklanması kimyasal olarak aktif yeni yüzeyler elde edilmesinde ve yüzey modifikasyonunda alternatifler sunmaktadır.

LIST OF FIGURES

Figure 1.1. Free radical chain reaction involved in polypropylene thermal oxidation.....	11
Figure 1.2. Modification of silica gel with aminopropyltriethoxysilane.....	15
Figure 1.3. Free energies of mixing as a function of composition for conditions under which two species are miscible (a) and immiscible(b)	17
Figure 1.4. Schematic phase diagrams illustrating the different pathways which may lead to phase separation A. Temperature quench, B. Removal of common solvent, C. Polymerization of one or both of the components.....	18
Figure 1.5. Spinodal decomposition. A. In the unstable part of the phase diagram, random concentration fluctuations are unstable and grow in amplitude. Long-wavelength fluctuations (b) grow slowly because of the large distances through which material needs to be transported, while short fluctuations (c) are suppressed, because of the free energy penalty associated with sharp concentration gradient.....	21
Figure 1.6. The behavior of the interface width w and the average domain size R at various stages of spinodal decomposition: (a) early stage, (b) intermediate stage, (c) late stage.....	23
Figure 2.1. Two approaches to anchor organosilanes onto plastics using intercalation and activation. A. Aminopropyltrimethoxysilane in dry toluene is co-infused into the matrix (Step 1); water-saturated toluene is delivered to intercalated and surface-residing organosilanes (Step 2); reactive organosilanols form siloxane bridges to one another with heating and concomitant loss of toluene (Step 3). B. Simultaneous co-infusion and activation of aminopropyltrimethoxysilane (<i>Step 1</i>) followed by decantation and heat-induced cross-linking (<i>Step 2</i>).....	27

Figure 2.2. Distention of polypropylene during solvent treatment is depicted. A. Image of Eppendorf Safe-Twist tubes treated (3h) with propanol control (left) and water-reduced toluene (right); B. Graph of elongation versus time in toluene, reporting the top-to-bottom length of an Eppendorf Safe-Lock tube.....31

Figure 2.3. A. Native tube; B. Control tube incubated with aminopropyltrimethoxysilane in non-perfusing propanol; C. Trial tube incubated with aminopropyltrimethoxysilane in water-reduced toluene.....32

Figure 2.4. A. Native tube; B. Control tubes treated with aminopropyltrimethoxysilane in water-reduced toluene solution; C. Trial tubes treated with aminopropyltrimethoxysilane in water-saturated toluene solution.....32

Figure 3.1. Cutting steps for sample preparation for ATR-FTIR 40

Figure 3.2. ATR FTIR spectrum of vacuum dried samples before (dashed line) and after (solid line) reaction (1M, 70°C, 16h).....41

Figure 3.3. ATR- FTIR spectra of the time course reaction.....44

Figure 3.4. SEM image of A. Native Eppendorf tube; B. Eppendorf Tube treated with ammonium sulfate(1M, 70°C, 16h) ; C. Eppendorf Tube treated with ammonium persulfate (1M, 70°C, 16h)..... 45

Figure 3.5 Photograph of A. Native Eppendorf tube; B. Oxidized Eppendorf Tube, showing the change in optical clarity after oxidation.....45

Figure 3.6. A. Schematic drawing of an Eppendorf half-full with the oxidant solution ammonium peroxydisulfate; B. Optical microscope image of oxidized Eppendorf Tube showing the air-solution boundary..... 46

Figure 3.7. Scanning electron micrograph of APS treated Eppendorf tube taken from the cross-sectional viewpoint, tilted slightly towards the inner face.....	47
Figure 3.8. Scanning electron micrographs of gold-coated surfaces of Eppendorf tubes oxidized with APS (1M, 70°C, 42h) at different magnifications.....	47
Figure 3.9. Scanning electron micrographs of injection-molded polypropylene oxidized for: (A) 8h; (B) 10h; (C) 12h; and (D) 16h. The negative reaction control surface appeared identical to the 8h time point (A).....	48
Figure 3.10. Scanning electron micrographs of oxidized melt-blown polypropylene at different magnifications.....	49
Figure 3.11. Scanning electron micrographs and EDS analysis of oxidized PP fiber; lines intensities corresponding to: yellow line: base fiber; redline: amorphous, green line: particles on the surface..	50
Figure 3.12. Scanning electron micrographs A. Polypropylene fiber, B. Polypropylene tubes, treated with APS showing two structures separated by a boundary.....	51
Figure 3.13. A. Homolytic decomposition of persulfate B. Hydrogen abstraction from a tertiary carbon.....	52
Figure 3.14. Chain scission under anoxic conditions.....	52
Figure 3.15. Hydroperoxidation of primary and secondary carbon centers.	53
Figure 3.16. A. Unimolecular thermolysis of hydroperoxides B. Bimolecular thermolysis of hydroperoxides C. Decomposition of alkoxyl radical by β -scission.....	53
Figure 3.17. General acid catalyzed hydroperoxide decomposition.....	54

Figure 3.18. Acid catalyzed decomposition of polypropylene hydroperoxides.....	55
Figure 3.19. Decomposition of peroxides induced by A. peroxy radical B. hydroxyl radical.....	56
Figure 3.20. Reaction model illustrating formation of carboxylic acid , ester and alcohol via transfer pathway.....	56
Figure 3.21. Important reactions of termination step.....	57
Figure 3.22. Reaction model illustrating formation of functional groups in polypropylene during oxidation.....	58
Figure 3.23. Comparison of SEM micrographs(left) and FTIR(right) of time course samples.....	62

CHAPTER 1

SELECTED METHODS OF SURFACE ENGINEERING APPLIED TO MATERIALS SCIENCE

1.1 Overview of surface engineering

Surface engineering, as a strategy of general scope, is a method to rationally modify the surface-pendant functional groups of starting materials, yielding products with altered surface characteristics and predictable macroscopic properties. It can be broadly classified into processes that improve corrosion resistance and wear resistance to extend useful component life; impart special properties such as lubricity enhancement; improve electrical conductivity, solderability; provide shielding for electromagnetic and radio frequency radiation [1-12]. Engineering surfaces or interfaces has become important in areas as diverse as biotechnology, chromatography, catalysis, construction, electrochemistry, electronics, photography, separation, gas storage, separation, synthesis and automobile industry, to name a few [13-28].

In most cases a surface layer comprised of functional groups constitutes a tiny fraction of the total material, however, the performance of metals, polymers, inorganics, composites and related products is reflected in part by the physico-chemical characteristics of such groups. Surface-related features such as adhesion strength, corrosion resistance and chemical reactivity are often manipulated by modifying the surface and in principle almost any surface trait is tunable [1-12]. By modifying surfaces, one can combine a material that may have useful bulk properties (e.g. mechanical, optical) with appropriate surface properties (e.g. corrosion resistance, low wear, low friction, biocompatibility, hydrophobicity). Therefore, the potential to improve the quality of materials by chemically transforming surfaces has attracted interest from industry.

1.1.1 Commercial areas of interest

(i) Biotechnology

Surfaces play a vital role in biology and medicine since most biological reactions occur at surfaces and interfaces. After the introduction of modern surface methods to study and modify materials and surfaces of biological interest, contemporary surface science has had considerable impact on biology and medicine. Three areas, in particular, have been influential in advancing biological applications for surface science: chromatographic separations, blood compatibility and cell culture. Implant biomaterials, blood oxygenators, hemodialysis, affinity chromatography, surface diagnostics, cell culture surfaces and biosensors as examples of surface technology applied to biological problems [29-32].

(ii) Synthesis

In catalysis, the surface properties of inorganic supports, predominantly oxides, influence the activity of supported catalyst and properties of product obtained. The morphology as well as the type, concentration and arrangement of ion sites over the oxide surface, inclusive of OH groups, can be changed by varying the conditions of their thermal pre-treating and by the chemical modification [33-35].

(iii) Engineering, processing

In metallurgy, the performance and service life of metal parts, e.g. cutting tools, machinery parts such as bearing pins for motor timing chains, punch pins, tooth of root of spur gears depends on the surface characteristics. Upon modification of the surface by means of various techniques, higher wear resistance and longer service life is achieved. In some cases abrasive and impact resistance is improved [36,37].

1.2 Surface modification of polyolefins

1.2.1 Overview

Polymers are becoming increasingly attractive materials for a series of applications so far dominated by metals, semiconductors and glasses due to their mechanical characteristics, chemical stability, light weight and design possibilities.

Surface chemistry and structure play a significant role in defining the physical properties and ultimate uses of polymers. Interfacial chemistry of polymers is relevant to many applications of polymer materials, such as adhesion, wetting, compatibility, and gas/liquid permeability. However, their surface properties often do not meet the demands of engineering and biotechnological applications. Therefore, in order to fulfill the requirements for some applications, e.g. medical applications, surface modification is often employed to achieve desired properties, while maintaining the characteristics of the bulk. As a consequence, the possibility of selective surface tailoring while keeping bulk characteristics unchanged extends the application of polymers. The chemistry of polymer surfaces is important also in terms of polymer degradation and fabrication of biocompatible devices. Therefore, surface modification of polymers is an important field both in applied as well as in basic research and it is an area of scientific and commercial interest.

Polyolefins display relatively poor adhesivity due to low-surface-energy. Relative low surface energy and relative high chemical resistance of polyolefins impede their materials applications, particularly those which require adhesive bond between a polyolefin and another condensed phase. Thus, the modification of polyolefins to impart polar functionality has been a long standing scientific challenge and an industrially important area. High polarity is important for the use of polyolefins in solution (dispersancy) or in the solid phase (adhesion, printability). Polypropylene, for instance, exemplifies many features that are shared amongst the polyolefins, in particular, low surface tension and chemical reactivity due to absence of polar surface groups. The dearth of polar, chemically reactive groups, in turn precludes the formation of covalent bonds, resulting in weak surface interactions and the familiar problem of poor surface adhesion. Therefore, modification of the surface that produces a more polar surface is obligatory to improve properties such as wettability, adhesion, dyeability and printability or to provide functionalities for further reactions. However, in some

applications such as paper release mechanisms, surface of polypropylene need to be modified to reduce the wettability and adhesion. Such a modification can be achieved by hydrosilylation of terminal double bonds in polypropylene through reactive processing [38-41].

The surface treatment of polymers can be accomplished by various methods ranging from wet chemical process to dry processes. At present, several established methods of surface modification such as plasma treatment, light and radiation initiated grafting, chemical etching and controlled oxidation, peroxide initiated radical transformation, electron bombardment, surface grafting and corona discharge have been used to introduce polar functional groups that are capable of substantial interactions with adhesive molecules yielding improved wetting and adhesive. A recently reported perfusion-activation-crosslinking approach also shows potential. Persulfate-induced oxidation of polypropylene, in particular, has been used successfully [41-43].

Most of these surface modification methods lead to the introduction of different functional groups in different extent and the resulting surface is chemically and structurally heterogeneous. Even in the case of chemical treatment, often the modified surface is chemically heterogeneous. Most of the reactions used are often accompanied with some side reactions and it is not possible to remove these side products from the surface. Further, the mechanism of the surface reaction may differ from the analogous solution reaction. Thus, in order to extend the applicability of established organic reactions to polymer surfaces, it is important to characterize the modified surface in terms of the nature of functional groups introduced on the surface, chemical environment of the functional groups and occurrence of any side reactions. This information greatly increases understanding of the interfacial reactions partially in relation to the reactivity of surface functional groups. This information, in turn, may be used to design better surface reactions.

1.2.2 Types of surface modifications

The principles of physically modifying polymer surfaces involves chemically altering the surface layer and deposition an extraneous layer on top of existing material, thereby generating a well-defined interphase. As polymer surfaces have a low chemical activity, generation of high energy species such as radicals, ions, molecules in excited

electronic states is required to chemically alter the surface. Methods that generate high energy species include flame treatments, corona and plasma treatments. Coating via physical treatment involves generation of fundamental materials, such as atoms or atomic clusters, to be deposited on polymer surface. Suitable techniques involve plasmas (sputtering, plasma polymerization) or energy-induced sublimation (e.g. thermally or ion beam-induced evaporation) [44]. Methods are described below in detail.

(i) Flame treatments

Flame treatments, which introduce oxygen-containing functions at the polyolefin surfaces, are widely applied in industry mainly to improve printability and paintability (adhesion properties). Flame treatment can be used to oxidize extremely thin layer of (~5–10 nm) the polymer surface in a controlled way. A large number of studies on flame-modified polyolefin surfaces has appeared in the literature [45-50].

Oxidation at the polymer surface is attributed to high flame temperatures (1000°C-2000°C) or reaction with excited species in the flame. These active species, which include radicals, ions and molecules in excited states, are formed by the high temperatures. The combined XPS/SIMS study of Garbassi *et al* on flame treated polypropylene revealed oxygen containing functional groups such as hydroxyl, carbonyl, carboxyl along the surface and a consequent improvement in adhesion and wettability [51].

From the literature, it is clear that the surface chemistry of a flame modified, as well as of a plasma modified or electrical-discharge modified polyolefin surface, is very complex and under certain conditions susceptible to changes. The likely oxidation mechanism by these flame treatments as well as by the other oxidation processes can be described by initiation, propagation and termination. A new computational model, SPIN, was used to determine the chemical composition of the impinging flames used to modify polypropylene. The SPIN model indicated that the species primarily responsible for the surface oxidation of the polypropylene are OH, H₂O₂, and O₂. Atomic force microscopy study of flame treated polypropylene indicated generation of a 'nodular' surface topography which is probably the result of the agglomeration of intermediate-molecular-weight materials [45-47].

(ii) Corona Treatments

Corona treatment is widely used in industry to increase the wettability or the adhesion of polymer films or fibers. The improvement achieved in adhesion after corona treatment is related to both chemical and physical changes. Several important facts about oxidation and adhesion of polyolefins can be found in the studies of Owens, Briggs *et al* and Lanauze *et al* in which ink adhesion and self-adhesion after corona treatment have been studied [52-54].

Corona treatments exploit the corona effect, i.e. formation of high energy electromagnetic fields close to charged thin wires or points, with consequent ionization in their proximity. This process involves a dielectric barrier controlled discharge (DBD) which develops between two parallel electrodes. One of these electrodes is in the form of a bar and the other is a cylindrical roller of radius large enough to treat the gas gap as constant. The material to be treated is placed on the roller. To treat polymer, at least one of the two electrodes is covered by a solid dielectric barrier (silicone rubber or ceramic), which controls the discharge. To simplify the utilization of the process, the discharge is usually carried out in atmospheric air.

In the ion-rich region, excited species, (e.g. ions, radicals, electrons, molecules in excited states, etc) can react with surface groups to form radicals. These radicals rapidly react with oxygen and functionalize the polymer surface with and without chain scission. In the literature it has been reported that during air corona treatment, chain scission produces low molecular weight oxidized materials on the surface of polyolefins. On severely corona treated samples, the formation of roughening is attributed to the agglomeration of low molecular weight oxidized materials at relatively high humidity. Despite those risks, the corona treatment can be used to promote further surface chemistry, namely graft polymerization.

The reason why the corona treatment is so widely employed is because of its facility to be implemented in a film production line at the end of the forming process, or just before an inking or coating device enters into action. However, there are some drawbacks: such surface treatment is surface ageing, uniformity and the control of the treatment is limited due to a lack of discharge homogeneity, and the nature of the surface transformations are limited due to the use of air as the plasma gas. The major transformations taking place are surface cleaning and oxidation, which are not always the most desirable of chemistry. To minimize such problems, industrial systems that allow careful control of the atmosphere have been developed [41, 44, 55-57].

(iii) Plasma treatments

Plasma treatments have been used in a range of applications, from improving the poor adhesion associated with hydrocarbon polymers, to optimizing the surface properties of potential polymeric biomaterials [58-60].

A plasma can be broadly defined as a gas containing charged and neutral particles, including electrons, positive ions, negative ions, radicals, atoms and molecules resulting from ionization, fragmentation, and excitation processes. Reactions between gas-phase and surface species produce functional groups and crosslinking at the surface. Plasma treatment grants the flexibility to use different types of gas which results diverse chemical functionalization of the surface. Examples gases include argon, ammonia, carbon monoxide, fluoride, hydrogen, nitrogen, nitrogen dioxide, oxygen and water. At the present time most of the plasma treatments of polymers are run with oxygen which is used widely in industry for hydrophilic surface modification of. Air, oxygen, nitrogen, argon, water, carbon dioxide, CF₄, plasmas have been used to modify polypropylene surfaces to provide the required physical and chemical surface properties for various applications [41,44, 61-66].

The major reactions known to occur along the polymer surface are etching, cleaning, crosslinking, grafting and other classic reactions leading to addition, substitution, formation of functional groups. Under certain conditions, surface functionalization is not the only modification; a morphologic transformation is also noticed. With semicrystalline polymers, it is known that the amorphous phase is preferentially removed during an oxygen-mediated etch. Besides the obvious chemical changes caused by the plasma, it has been shown that the surface roughness of polypropylene increases substantially after air-plasma treatment, possibly as a result of preferential attack of the amorphous regions of the polypropylene. In principle, a gas plasma treatment used to etch selectively can be used to tailor the surface structure of phase-separated polymeric systems, i.e., semicrystalline homopolymers, polymer blends, or block copolymers. For example, plasma processes have been optimized to sterilization and to transfer geometric micro-patterns at the surface of biomedical polymers with the aim of driving the behavior of the cells in tissue engineering. The architecture of the resulting surfaces is ultimately determined by the initial phase-separated surface/bulk structure and the difference of etching rate between the two polymer phases. Using this approach, it follows to reason that surfaces can be created

which contain tubular or spherical holes, ridges, or tubular or spherical protuberances. The size of these holes/protuberances will likely be determined by the domains present in the phase-separated polymer system and can vary between tens of nanometers and a few micrometers [41, 67-70].

The possibility of altering the surface of polymer materials at room temperature and uniqueness of the modified surfaces are the particularly appreciated advantages of low-pressure plasma processing for the surface modification applications. Many studies have been devoted to the characterization of plasma-treated polymer surfaces, but much remains to be learned about the complex interactions at the plasma-polymer boundary during plasma treatment processes.

Other types of related modifications are low-pressure plasma treatments, electron beam treatment, UV treatments, ion beam treatments, laser treatments, metallization and sputtering [71-77].

(iv) Wet chemistry

Wet treatments were the first modification techniques used in order to improve surface properties of the polymers. The most common wet treatment of polymer surfaces are sodium etching of fluoropolymers and oxidation of several different polymers based on chromic acid solutions, methane sulfonic acid and nitric acid solutions. Strong oxidants such as $\text{CrO}_3/\text{H}_2\text{SO}_4$, $\text{K}_2\text{Cr}_2\text{O}_7/\text{H}_2\text{SO}_4$, $\text{KClO}_3/\text{H}_2\text{SO}_4$, $\text{KMnO}_4/\text{H}_2\text{SO}_4$, HNO_3 and H_2SO_4 can provide surface functionalization. Sulfuric acid and chromic-sulfuric acid treatments introduce sulfonic acid, carboxylic acid and other less oxidized functional groups. Sulfonation, using fuming sulfuric acid or using gaseous SO_3 introduces SO_3H groups on the polymer surfaced by. In the former case, there can be substantial polymer degradation. A more controlled method of surface sulfonation involves the use of latter method, suitably diluted with nitrogen to moderate the reactivity of the sulfonating agent. Gas phase sulfonation of polyethylene is industrially practiced to impart superior hydrocarbon barrier properties to high-density polyethylene (HDPE) and to improve the gas barrier properties of polyethylene. Early investigations showed that oxidation of polypropylene and ABS with sulphuric acid solution saturated with chromium trioxide at 80°C yields strongly adhesive polypropylene surfaces [41,78-85].

1.3 The relative oxidation rates of polymers

Hydrocarbon polymers vary in their inherent resistance to oxidation. Principal determinants include chemical structures and their physical and morphological characteristics. Increased chain branching, for example, leads to more rapid auto-oxidation, and indeed polypropylene is the most oxidizable polymer of the major commercial polyolefins, rendering the use of heat and light stabilizers mandatory in commercial plastic preparations. Oxidative degradation processes of polypropylene are normally accelerated under the influence of temperature, ultraviolet light and other factors such as mechanical stress, atmospheric pollutants, adventitious metal ion contaminants. The effect of the first two parameters is, by far, the more important.

The different reactivity of chemically related polymers, such as polyolefins towards the etching solution has been investigated in literature. The surface of polypropylene, low density polyethylene, high density polyethylene has been reacted with chromic acid solution and the effect of etching solution was assed by scanning electron microscope, transmission electron microscope, FTIR-ATR and contact angle measurement. The result of relative oxidation studies showed that polypropylene was etched more readily than other polymers and an explanation of this result was related to the solution chemistry. It was observed that tertiary hydrogens were attacked much more rapidly than primary hydrogen and the relative rate of reaction of $\equiv\text{C}-\text{H}$, $-\text{CH}_2-$ and $-\text{CH}_3$ is about 4600:75:1. According to the information about the relative rate of reaction given in the literature, the number of tertiary carbons on the molecular chain is the rate determining feature, at least during the onset of reaction [86,87].

1.4 Thermal degradation of polypropylene

Degradation may occur at all stages of the lifecycle of polypropylene (polymerization, storage, processing fabrication an in-service) but its initiation is most pronounced during high-temperature, high shear conversion processes (extrusion, injection molding, blow molding, internal mixing). Such processes, which include reprocessing and recycling, are used to produce the final fabricated article, including reprocessing and recycling processes. The high temperatures required to achieve these

polymer conversion processes are detrimental to the stability of the macromolecular structure [88].

With due consideration to the fact that different polymers have different physico-chemical traits, a considerable number of decomposition pathways may be envisaged. Decomposition is seldom a one step process, and it typically describes a reaction series in each pathways. For instance, decomposition usually proceeds via reactions between various oxidation products such as aldehydes and hydroperoxides. Hydroperoxides may also decompose via acid catalysis or thermolysis. Special structures can be formed in polyethylene as well as in polypropylene. Their contribution can be important in explaining chain scission and some of the final oxidation products. Ultimately, product distribution depend not only on the polymer type, e.g. polyethylene, polypropylene, but also on the conditions of the oxidation. In this respect significant differences are expected between oxidation of the polymer melt and oxidation of solid phase polymers, both at low and high temperature.

The oxidation mechanisms of polymers and low molecular weight analogs share many essential features, however, additional constraints imposed by polymeric state influence the former process. To better understand this statement, a look at thermal oxidation is required. Thermal oxidation of polypropylene is a free radical chain process characterized by three basic steps:

1. initiation, leading to the production of the first free radicals in the chain sequence;
2. propagation, giving the most important molecular product of oxidation, the hydroperoxide; and
3. termination, eliminating the radical species and sometimes leading to crosslinking of polymer chains.

In a polymer, any reaction may proceed either inside the same molecule or between two neighboring molecules. With oxidative chain propagation, for instance, an intra molecular reaction results in formation of the structure in which the hydroperoxide group and the free radical group are positioned within a short distance of the same molecule. These can easily react with each other in the confines of the polymer matrix.

The nature of the primary oxidative insertion reaction of molecular oxygen with polypropylene is complicated by other reactions such as hydroperoxide initiation or metal catalysis (*Figure 1.1, Reactions 1,4*). The propagation reaction (*Reaction 3*) is

typically 20% faster at a tertiary carbon atom than at a secondary carbon atom. Furthermore, this reaction, which is the most important accelerator of auto-oxidation and the rate determining step, is particularly facilitated by intramolecular hydrogen abstraction, affording adjacent peroxides along the polymer chain. These products are less stable than isolated hydroperoxides and lead to an increased rate of initiation. Consequently, the kinetic chain length (i.e. the average number of oxidation cycles, reactions 3 and 4, that precede termination) for polypropylene oxidation is quite high, i.e. approximately 100. Polyethylene, in contrast, displays a kinetic chain length one order of magnitude less and a correspondingly higher oxidative stability.

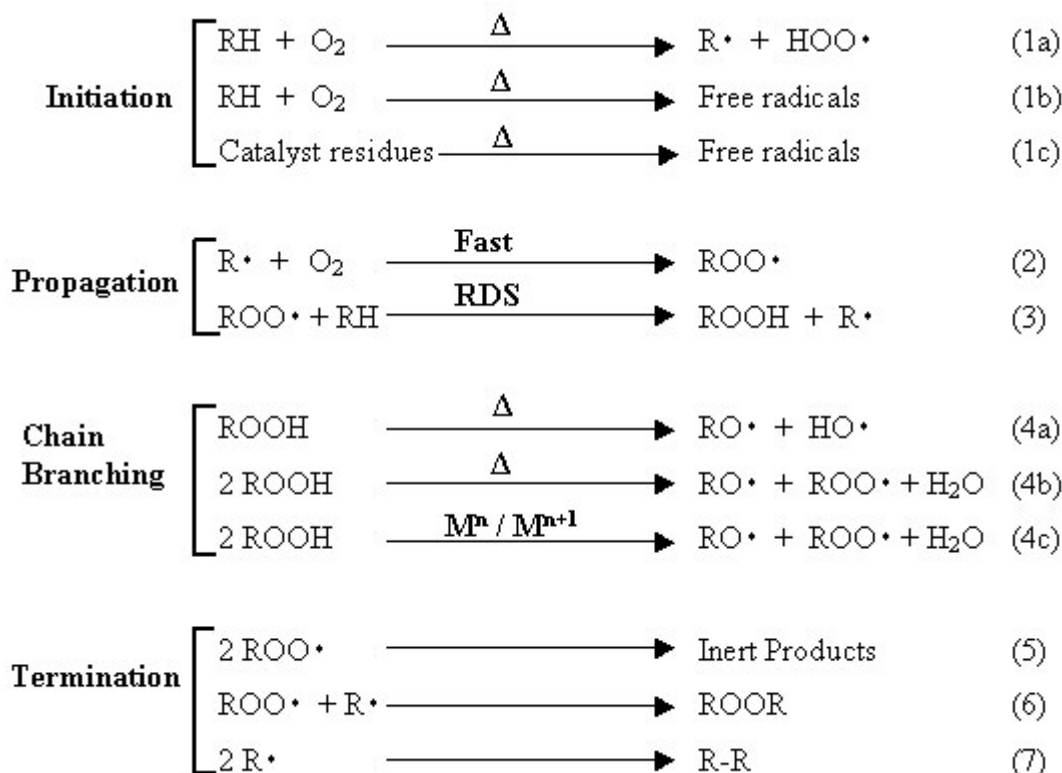


Figure 1.1. Free radical chain reaction involved in polypropylene thermal oxidation.

Thermal oxidation of polypropylene and polyethylene yields significant hydroperoxide concentrations. In polypropylene these hydroperoxides accumulate to a large extent as clusters of two to six groups. There is much less intramolecular hydrogen abstraction by peroxy radicals in polyethylene than in polypropylene. As a consequence, the labile structures formed in polyethylene and polypropylene are often significantly different. The ultimate fate of hydroperoxides is related to intramolecular and intermolecular pseudo-monomolecular decomposition modes involving a carbon–hydrogen bond from the polymer. The latter mode normally does not contribute below

300 °C. Other hydroperoxide decomposition modes include bimolecular reactions that can be intermolecular as well as intramolecular [41,88-95]. The yield of hydroperoxides in polypropylene oxidation depends on oxygen pressure among other conditions and never reaches the relative value of 1. Competing reactions and radical migration introduces a structural dependency to the formation of hydroperoxides particularly including the rate constant of its decomposition, and on oxygen pressure at which the hydroperoxide has been prepared [90].

1.5 Tailoring surfaces with silanes

Silanes have been used to modify surfaces both to reduce nonspecific adsorption and to provide moieties suitable for covalent attachment. Silane coupling agents are capable of providing chemical bonding between an organic material and an inorganic material. Depending on the type of silane coupling agent used and the purpose of the material to be obtained, the surface properties vary between hydrophilic and hydrophobic. This advantageous property of silanes is widely utilized to treat the surfaces of glass products, particularly to improve the performance of reinforced plastics, paints, adhesives, other coating materials and inorganic fillers. Silanes are also used to prime various substrate materials.

Surface silylation with chloro- and alkyl silanes has become established over the last two decades as a method to enhance the applicability of the product a number of high-tech areas such as chromatography, catalysis and proteomics. In biochemistry, it is used to immobilize enzymes. In the analytical field it is used to adsorb organic compounds and metal ions selectively, whereas in chemical field it is used to immobilize metal complexes for use as catalysts. The choice of chemical modification depends on the target molecule to be immobilized and the specific application in which the modified surface will be used [96-101].

Silane reactions can be used to modify hydroxylated or amine-rich surfaces. Since glass, silicon, germanium, alumina, and quartz surfaces as well as many metal oxide surfaces, are all rich in hydroxyl groups, silanes are particularly useful for modifying these materials. Direct evidence for surface modification on these substrates is observed by an increase of contact angles, particularly when alkyl and fluoroalkyl silanes are

used. A wide range of different silanes are available, permitting many different functionalities to be incorporated on the surfaces.

Organofunctional silanes are best suited to attach biological moieties onto surfaces. Organofunctional groups have an advantage over comparable organic compounds in the sense that the silanes can potentially bond via several mechanisms. To attach biological materials, such as DNA and proteins, to surfaces, the major approach involves the reaction with organofunctional silanes followed by covalent attachment of the biological molecule to the newly introduced functional group on the surface. Examples of organofunctional silanes used this way include (3-glycidyloxypropyl)trimethoxysilane (3-GPS), (3-aminopropyl)triethoxysilane, aminophenyltrimethoxysilane, (3-mercaptopropyl)trimethoxysilane (3-MPTS), and the general class of haloacetamidossilanes. All of these have been successfully employed to modify glass surfaces and formed a basis to immobilize oligonucleotides via various cross-linking reagents [102-104].

1.5.1 Silanization Procedures

The primary procedures used to silanize solid supports are based upon liquid phase and gas phase methods. In the liquid phase method, substrate is immersed into solutions silane and solvent, i.e., water, water/ethanol or water/acetone. In the vapor phase method, vapor deposition and curing of the silane onto the solid support takes place at elevated temperatures.

In hydrated solvents, silanes undergo hydrolysis and partial condensation before deposition on the surface. In contact with water halogen or alkoxy groups are hydrolyzed. The incrementally forming silanol groups engage in hydrogen-bonding interactions with neighboring hydrolyzed silane molecules and surface hydroxyl groups. Siloxane bonds eventually form with the release of water. The molecular coat does not describe a monolayer, in fact, a three-dimensional polymeric silane network is formed along the surface. Trichlorosilanes or trialkoxysilanes are typically used in this type of modification.

Apart from the alkoxy or chloro group, the rate of hydrolysis of silanes is influenced by the functionality of the organic group. The stability of the silanol groups increases with increasing size of the organic group. Acyloxy- and aminofunctional

silanes are far more susceptible to hydrolysis than other alkoxy silanes. They hydrolyze in minutes in water, whereas others are stable in water for several hours. The increased rate of hydrolysis of the former is due to the acid or basic character of the functional group. Hydrolysis of the other alkoxy silane molecules may be catalyzed by the addition of a base or an acid. Covalent bond formation is not an immediate process. The silane pre-coat bears a considerable amount of chemisorbed molecules. These chemisorbed molecules, which are typically hydrogen-bonded, condense slowly. To accelerate chemical stabilization of the coating layer, a post-reaction curing step is often employed in which the modified substrate is thermally treated at temperatures in the range of 353-473 K.

If a modification with silanes is performed in fully dry conditions (dry organic solvent, dehydrated surface), hydrolysis is prevented. Chemical bonding with the substrate should result from the direct condensation of the chloro- or alkoxy groups with the surface groups. From experiments using methoxymethylsilanes, it has been concluded that direct condensation does not take place. Post-reaction curing only results in evaporation of the adsorbed molecules. Alkoxy silanes may only bond chemically to the silica surface if water is present at the interface. Hydrolysis, however also causes polymerization and therefore non-monolayer coverage are obtained. Aminosilanes contain the catalyzing amine function in the organic chain. The reaction of aminosilanes with substrates in dry conditions are therefore self catalyzed. They show direct condensation even at completely dry conditions. Upon addition of aminosilane to the silica substrate, the amine group may form hydrogen bonds or proton transfer complexes with surface silanols. This results in a very fast adsorption, followed by direct condensation. This reaction mechanism of aminopropyltriethoxysilane with silica gel in dry conditions is illustrated in *Figure 1.2* given below.

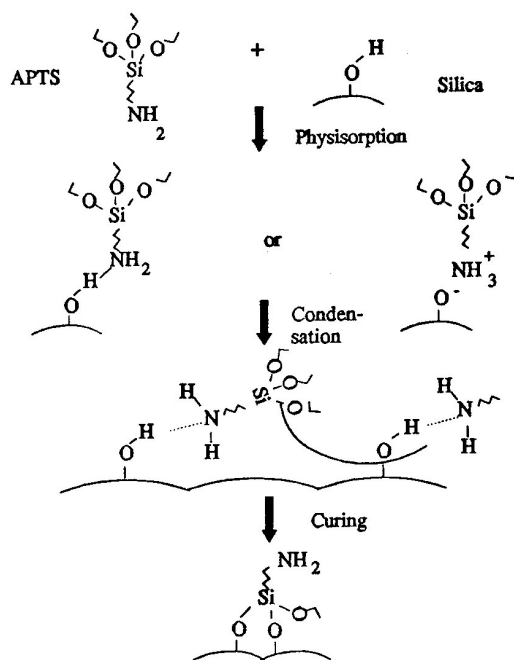


Figure 1.2. Modification of silica gel with aminopropyltriethoxysilane [9].

The polymerization reactions are hard to control and a layer of irreproducible thickness results. The control is ameliorated with the addition of a variable amount of a polar organic solvent such as ethanol or acetone. A number of strategies have been developed to limit the formation of heterogeneous polymeric layers relative to homogeneous monolayers. These include limiting the concentration of alkoxy silane prior to surface modification by performing silanization in the vapor phase, the use of anhydrous conditions, post-silanization curing, and the use of monoalkoxysilanes. However, monoalkoxysilanes are readily cleaved from modified surfaces due to rapid hydrolysis. Dialkoxy silanes have been shown to possess the disadvantages of both, i.e., the polymerization associated with trialkoxysilanes and the instability to hydrolysis of monoalkoxysilanes. Therefore, despite the problems of heterogeneity, trialkoxysilanes are the most extensively used silanization reagents. While postsilanization curing has been shown to limit the hydrolysis of silane films by cross-linking of the free silanols, these silanol groups are also free to polymerize and hence form heterogeneous silane layers, unless conditions favoring curing and limiting polymerization are rigorously enforced [9,105,106].

1.6 Oxidation Induced Patterning of Polypropylene

1.6.1 Polymer Mixtures

One of the fundamental problems of polymer science is to establish the mechanism of self organization in polymer systems under non-equilibrium conditions. A large part of application-oriented research is devoted to the study of polymer blends, since mixing provide a means to incorporate different properties. The properties of polymer blends (mechanical strength, surface bonding, and resistance) have a strong dependency on blend morphology. This morphology and the associated phase behavior in turn depend on the miscibility between the components of the blend. Thus, a fundamental understanding of the miscibility of the components in the blend is crucial to effectively design the end applications.

It is generally difficult or even impossible to correctly predict the mechanical properties of a mixture. The factors that determine if the polymer is in a one phase or multiple phase system include polymer molecular weight, blend composition, and molecular-level physico-chemical. In semicrystalline polymers, the phase behavior is even more complicated since these polymers crystallize between their glass transition and melting temperatures. The rates of phase separation and the resulting morphology depend on many parameters, e.g. time of heat treatment, temperature, concentration, and physical properties of the blend constituents. Understanding polymer miscibility will thus better define the conditions two polymers might form a homogeneous phase or a two-phase structure, will introduce the possibility to better control and manipulate the morphology of polymer blends [107-111].

1.6.2 Thermodynamics of polymer mixtures

The criterion that determines whether two species will mix or not is the free energy of mixing. Suppose a single phase has a composition ϕ_0 . At equilibrium the system assumes a state of minimum free energy, so if there existed a pair of compositions ϕ_1 and ϕ_2 such that the total energy is lowered, then the system will separate into two phases, and the single phase at composition ϕ_0 would not be stable.

The figure given below shows the free energies of mixing as a function of composition for conditions under which two species are miscible and immiscible. As it is shown in the *Figure 1.3.a*, if the relationship of free energy with composition has a convex-down shape, then every single composition has a lower total free energy than the phase-separated composition. The free energy curve would have a single minimum and the original total free energy of mixing is F_0 . The hypothetical free energy of the intermediate composition can be found by drawing a straight line between the free energies of the two constituent phases. Thus, the total free energy of mixing of the equivalent system can be equated to F'_0 .

On the other hand, in *Figure 1.3.b* the free energy profile is different. Between a certain range of intermediate compositions the curve is convex-down; a system of composition ϕ_0 will lower its free energy from F_0 to F'_0 by separating into two phases with compositions ϕ_1 and ϕ_2 . The lowest possible free energy is obtained when the phase separated compositions are defined by the points at which a line is tangential to the free energy curve in two places; these extremes define the limits of composition within which a single phase is not stable [110].

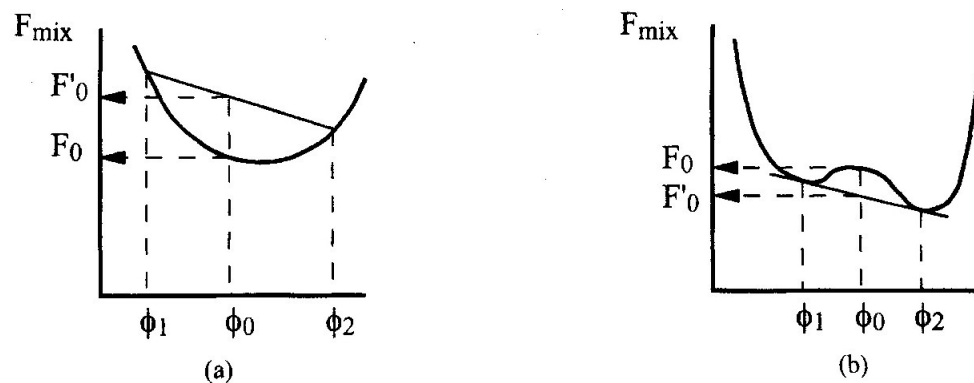


Figure 1.3. Free energies of mixing as a function of composition for conditions under which two species are miscible (a) and immiscible(b) [110].

1.6.3 Phase separation phenomena

Phase separation is important in the field of applied polymer chemistry and the behavior of number of different polymers has been studied in several different solvents. In experimental biochemistry this phenomenon has found widespread application in the separation and purification of organelles. Recent studies of protein solutions have

provided new and promising insights into the structural properties and phase behavior of soft matter [112-113].

Phase separation is induced when a sample is transferred from one-phase region into miscibility gap. Usually this is accomplished by a change in temperature, upward or downward depending on the system under study. There are many ways of starting with a single phase and arriving at a phase-separated structure. The schematic diagrams in *Figure 1.4* illustrates the different paths which may lead to phase separation. The *Figure 1.4.a* shows a phase diagram that has both one phase and two phase regions of the phase diagram at an experimentally accessible temperature. The sample is prepared in the one-phase region of the phase diagram as a homogeneous mixture and then the temperature is suddenly changed to bring the sample into two-phase region. Phase separation is initiated by the mechanism of spinodal decomposition or nucleation and growth, leading to the formation of domains of one phase in a matrix of the other. In *Figure 1.4.b*, a phase diagram of ternary solution of the two polymers in a suitable solvent that dissolves both well is shown. At low polymer concentration the unfavorable polymer-polymer interactions are diluted by the solvent, and the system forms a single phase. When the solvent is removed, the system phase separates. In *Figure 1.4.c*, one or both components are originally present as low relative molecular mass unit. An example of the former case might be a polymer of high relative molecular mass dissolved by monomers of a second polymer. As monomers are polymerized, the relative molecular mass of the second component reaches a value such that the degree of incompatibility exceeds a critical value and phase separation is initiated. Among the typical methods of reaching a phase separated state, temperature quench induced phase separation is simple to deal with theoretically. Consequently, it has been most extensively studied [114-117].

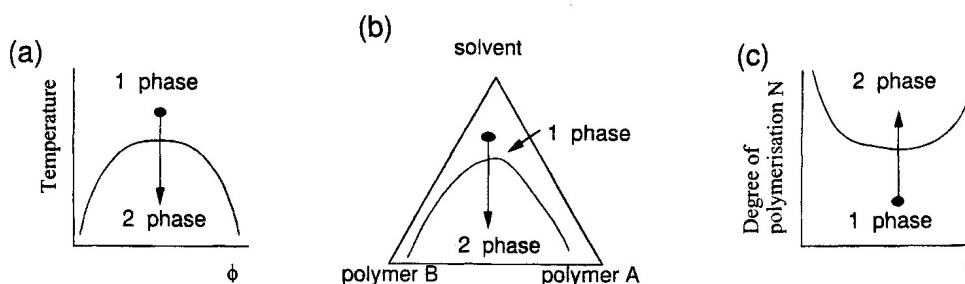


Figure 1.4. Schematic phase diagrams illustrating the different pathways which may lead to phase separation **A.** Temperature quench, **B.** Removal of common solvent, **C.** Polymerization of one or both of the components [110].

The phase-separated structures that result are normally characterized by the presence of interfaces between the coexisting phases. However, with polymer mixtures, it would be very rare indeed to achieve the situation in which the phase separation is complete and two macroscopic domains of the two phases are separated by a single interface. Rather, as a result of the slow dynamics of the polymers, an equilibrium situation will not be reached and the structure will yield a more complicated morphology consisting of much smaller domains of the two phases, which, although not at full equilibrium, may be considered stable for practical purposes.

1.6.4 Phase Separation Mechanisms

The mechanisms of phase separation is different in regions of metastability and instability of the phase diagram. Inside each region, depending on the closeness to binodal, spinodal or critical point, qualitative and quantitative distinctions in the kinetics of phase separation is observed. Two mechanisms of phase separation is usually considered: nucleation and growth, and spinodal decomposition. Nucleation and growth occurs if the unmixing is induced at a temperature near to the binodal, where the system is still stable with regard to small concentration fluctuations. Further away from the binodal this restricted 'metastability' is lost and spinodal decomposition sets in.

(i) Nucleation and Growth

The transition of the system from one-phase to two-phase state is related to amplification of fluctuations in composition and the development of microregions of new phase. This transition proceeds when the system is quenched into metastable region of the phase diagram. In the metastable part of the phase diagram, a small fluctuation in composition raises the free energy and the phase separation proceeds according to the mechanism of nucleation and growth.

The diffusion flows of components in the metastable region are directed towards diminishing fluctuations. The evolution of a new phase starts in this region. The energetically unfavorable effect of the appearance of a new interface determines the system instability only in relation to fluctuations whose sizes exceed some critical values. The composition of fluctuations is close to composition for a new phase. In

order to begin the phase separation process a droplet of minority size, which is greater than a critical size, has to be nucleated. Thus this mechanism of phase separation is called nucleation and growth.

(ii) Spinodal decomposition

Under the spinodal line, any small fluctuation in composition will lead to a lowering of the free energy. Under these conditions, phase separation will proceed immediately by mechanism of amplification of random composition which is called spinodal decomposition.

The theory of spinodal decomposition of homogeneous system at the initial stages of the process was developed in the fundamental works done by Cahn and Hillard. According to this theory at the initial stages of phase separation, the concentration fluctuations appear. They can be considered as a set of sinusoidal waves with fixed wavelength. Wavelengths represent the dimensions of the structures formed during the course of spinodal decomposition. Cahn theory forms the fundamental basis for studying kinetics of phase separation by spinodal mechanisms in aging of metal alloys, inorganic glasses, etc.

Uphill diffusion

The mutual diffusion of a polymer mixture is important for the mechanism that is operative in the unstable part of the phase diagram.

$$D_{\text{mutual}} = D_0 \phi (1 - \phi) \frac{d^2 F}{d\phi^2}$$

The prefactor D_0 which contains all the information about the dynamics of the two polymers is always positive. The curvature is negative within the spinodal line thus the mutual diffusion within the spinodal line is negative and it changes sign as the spinodal line is crossed. According to Fick's first law of diffusion, the negative mutual diffusion means that the material diffuses from regions of low concentration to high concentration (uphill diffusion). Any random, thermally generated, concentration fluctuation will not die away, as it would in the one-phase of the phase diagram; rather it will grow to form domains of the two coexisting phases. However, concentration fluctuations on different

length scales do not grow at equal rates. In the case of a fluctuation with a very long wavelength (*Figure 1.5.b*), the composition fluctuations can only grow by transport of material from the troughs to the peaks. Atoms have to diffuse over long distances as the wavelength becomes longer thus in the case of a fluctuation with a very long wavelength the composition fluctuation grows more slowly. On the other hand, for a fluctuation with a very low wavelength (*Figure 1.5.c*) there will be additional contributions to the free energy beyond simple Flory-Huggins terms. The concentration gradients which are steep compared with the length scale of the radius of gyration of a chain carry free energy penalty and this has the effect of suppressing fluctuations of very short wavelength. Thus there is some intermediate length scale of fluctuations that will grow the fastest and the morphology of the phase separating structure will be dominated by this length (*Figure 1.5.a*).

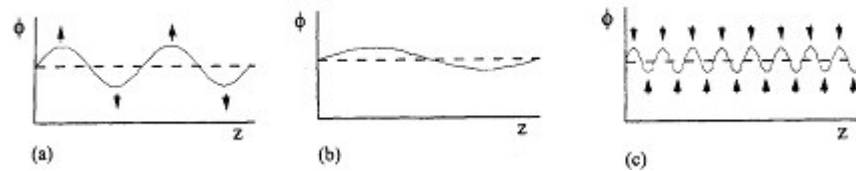


Figure 1.5. Spinodal decomposition. **A.** In the unstable part of the phase diagram, random concentration fluctuations are unstable and grow in amplitude. Long-wavelength fluctuations **(b)** grow slowly because of the large distances through which material needs to be transported, while short fluctuations **(c)** are suppressed, because of the free energy penalty associated with sharp concentration gradients [110].

The picture of spinodal decomposition assumed in *Figure 1.5*, in which composition fluctuations grows in amplitude but remaining with constant wavelength, cannot be sustained for long. As the peak coexisting compositions, the amplitude of composition wave cannot go on increasing, yet the system is still very far from equilibrium. The only possibility for the size of the domains is to grow. The process of spinodal decomposition consists of three stages: early, intermediate, and late. As shown in *Figure 1.6*, R characterizes the size of domains and their average separation, and w which characterizes the width of the interface between the domains. During early stage, both R and w are essentially constant and are related to the fastest growing wavelength λ_{\max} . when the peak compositions approach the coexisting compositions we enter a complicated, intermediate stage of phase separation, during which R increases while the

interfacial width decreases towards its equilibrium value. During the late stage of phase separation, discrete domains with compositions close to the coexisting compositions are separated by interfaces essentially at the equilibrium width w_1 . The only length scale characterizing the morphology is R , which characterizes both the average size and the separation of the domains.

The fact that the morphology at this late stage is characterized by only one length scale leads to the important idea that the domain pattern itself is self-similar in time. Statistically, the domain pattern at a later time is simply a blow-up of the pattern at an earlier time.

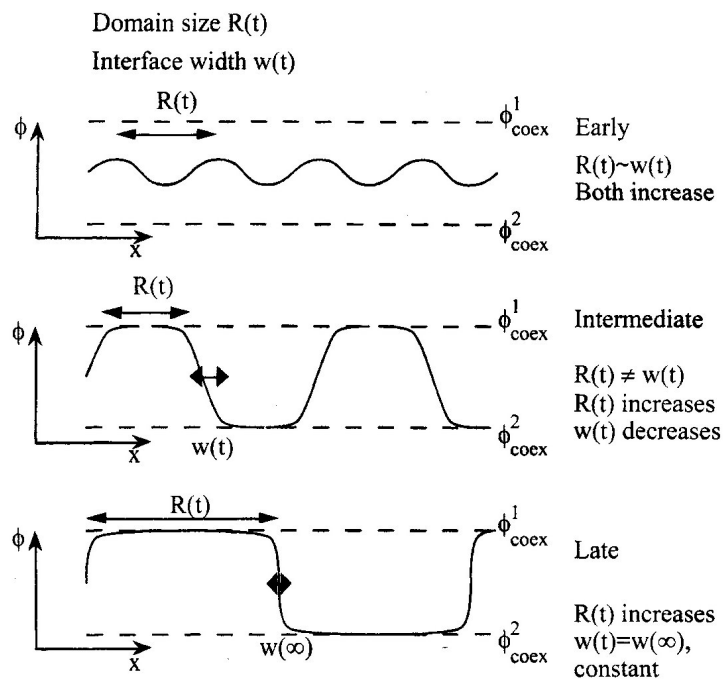


Figure 1.6. The behavior of the interface width w and the average domain size R at various stages of spinodal decomposition: (a) early stage, (b) intermediate stage, (c) late stage [110].

1.6.5 Surface directed phase separation

The presence of a surface profoundly modifies the mechanism of phase separation. The process of spinodal decomposition leads to superposition of composition waves of given wavelength but at random directions and phases; the effect of surface is to fix the direction and the phase of the waves at the surface, leading to the

real-space concentration wave near the surface. Material diffuses from regions of low concentration to high concentration, thus the depleted region is made deeper and deeper and a second layer of higher concentration is formed near the surface. However, in the presence of a surface with a preferential attractive interaction for one of the component to the surface, and in turn, propagation of a coherent concentration wave with a dominant wave vector normal to the surface is induced. In this way an oscillatory concentration profile is formed near the surface [110-118].

Chapter 2

SYNTHESIZING AND ANCHORING ORGANOSILOXANE FILM ON INJECTION MOLDED POLYPROPYLENE BY INTERCALATION STRATEGY

2.1 Introduction

One limitation to the formation of ceramic-polymer composites is the high processing temperature required to sinter organoceramics, during which time any organic component is typically destroyed. A promising amelioration is derived from the technique of hydrothermal processing, which permits formation of ceramics oxides from ceramic-hydrates at much lower temperatures and moderate pressures. Hydrothermal processing, involving the formation of materials in an aqueous medium, enables the processing of ceramics like BaTiO_3 and $(\text{Ba,Sr})\text{TiO}_3$ below 200°C , for electronic applications [119]. By this method, even preformed plastics can in principle undergo ceramic processing as passive bystanders. Another potential limitation to the formation of reliable composites is achieving good interfacial bonding. With low-surface-energy polymers in particular, improved interfacial bonding leading to specialty materials typically requires surface pre-activation using various physico-chemical methods.

Polymerized pre-glass laid upon polypropylene, for instance, may in principle be covalently anchored at the interface via a strategy in which bridging molecules bearing organic and inorganic moieties such as vinylic organosilanes are free-radical grafted onto the plastic surface through their vinylic moiety. In a following step, the hydrolysis products of tetraethoxysilane can be deposited and cured along the new surface, affording bonds with surface silanol adducts and adjacent hydrogen-bonded tetraethoxysilane hydrolysis products. It follows that the resultant pre-glass surface

could be hydrothermally processed to afford a glass surface and a successful composite. Each activation step, however, carries with it some drawback. Free-radical and oxidative methods do improve bondability for example, but they also potentially introduce peroxide intermediates into the matrix, thus accelerating the degradation of the polymer. It follows that a non-reactive approach which does not necessitate surface pre-activation is needed to alleviate polymer deterioration.

One strategy which has not been attempted in preformed polymers and which can be very useful to promote bonding is an intercalation-activation approach in which perfusion-based strategy was envisaged to promote interfacial bonding on low-surface-energy polymer without necessitating surface pre-treatment. The basic advantage over the free-radical method is that the latter would require no covalent modification of the plastic. In this non-reactive approach, polymerizable precursors would be co-perfused into the matrix alongside solvent molecules. The precursors, activated by reaction with an appropriate agent, would spontaneously polymerize to create an entangled network intertwined within the polymer. It follows that this strategy would not only preclude a need to covalently alter the surface, but it would also prevent modification-related side effects such as peroxide incorporation.

2.2 Materials

Injection-molded isotactic polypropylene tubes (2ml capacity) were purchased from Eppendorf Company. Analytical reagent grade toluene and propanol were purchased from Aldrich. Ninhydrin and 1,3-diaminopropane were obtained from Merck. Toluene was dried over 4Å molecular sieves.

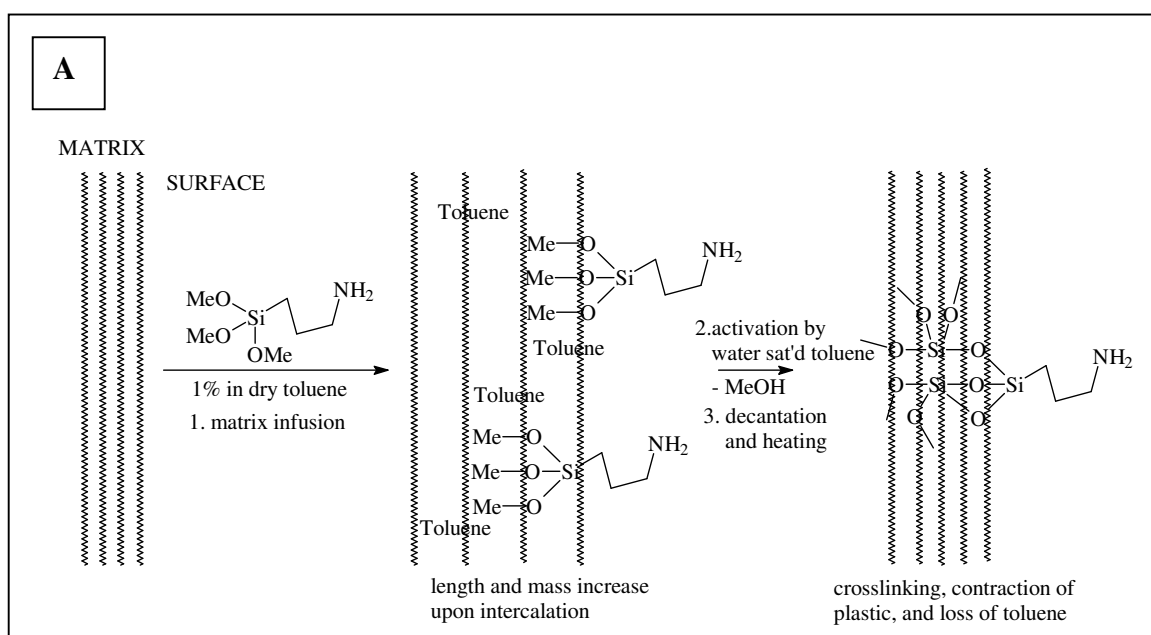
2.3 Methods

2.3.1 Rationale

The veracity and potential merit of a perfusion-crosslinking approach was tested upon the standard injection molded isotactic polypropylene Eppendorf tube using an organosilane precursors of the type $YSi(OR)_3$, where Y is an appropriate organic functional moiety and OR is an appropriate hydrolyzable alkoxide moiety.

Aminopropyltrimethoxysilane was preferred for a number of reasons in place of other organosilanes or tetraethoxysilane, the latter being a common precursor in sol-gel processes and of glass. Firstly, the hydrolysis and crosslinking of amine-bearing silanes in the presence of even trace moisture is autocatalytic. Secondly, the primary amino moiety is testable using propanolic ninhydrin solution, permitting easy visualization and localization of precursor-containing products in the pre-formed plastic.

The methodology devised is illustrated in *Figure 2.1*. In approach A (*Figure 2.1.a*), aminopropyltrimethoxysilane is co-perfused into polypropylene ahead of water, whereas in approach B, (*Figure 2.1.b*), co-perfusion, activation, and presumably crosslinking are simultaneously operative. Toluene, which is an established and mild matrix-swelling solvent of polypropylene, was used to encourage precursors to perfuse into polypropylene (Step 1 of Approach A). It was also used to deliver water to aminopropyltrimethoxysilane (Step 2 of Approach A; Step 1 of Approach B), the rationale being that water associated to toluene would also be carried into the polymer. Thus, trace water would be made available to sub-surface sites containing precursors as well as surface sites adsorbing precursors. It follows that dissolved, intercalated and surface adsorbed precursors should undergo hydrolysis to the active form and participate in siloxane bond formation. More importantly, if permitted to cross-link, the activated precursors should afford an aminopropylsiloxane-type network intertwined within the matrix of polypropylene and along its surface (Step 3 of Approach A; Step 2 of Approach B). Even though no formal covalent bond would exist across elements of the two networks, resultant double network would be bonded like two spider webs constructed within each other.



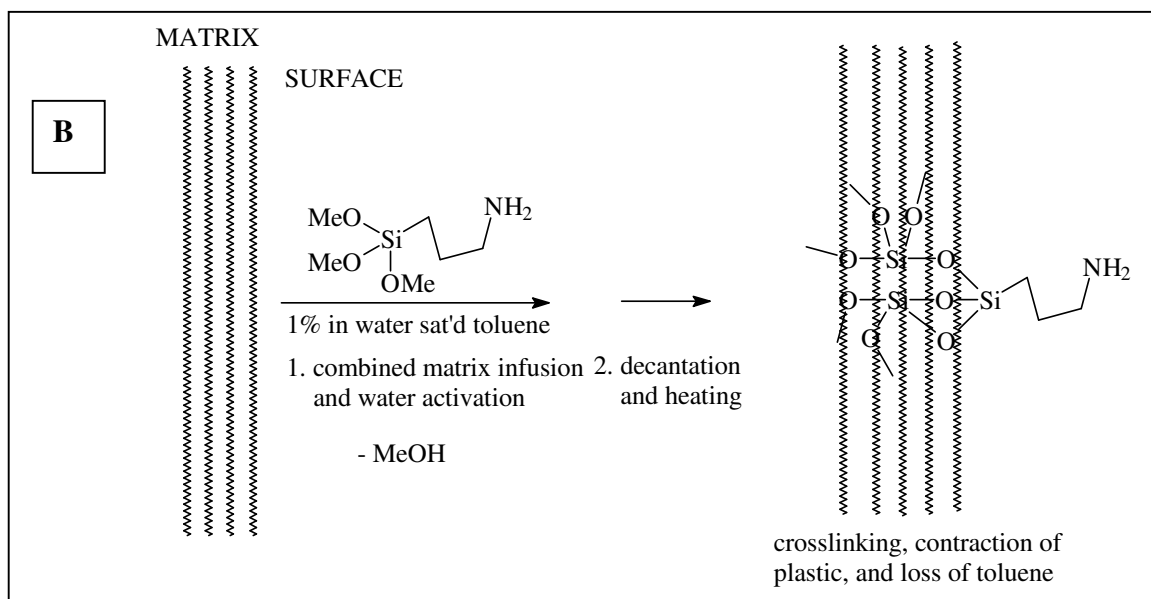


Figure 2.1. Two approaches to anchor organosilanes onto plastics using intercalation and activation. **A.** Aminopropyltrimethoxysilane in dry toluene is co-infused into the matrix (Step 1); water-saturated toluene is delivered to intercalated and surface-residing organosilanes (Step 2); reactive organosilanols form siloxane bridges to one another with heating and concomitant loss of toluene (Step 3). **B.** Simultaneous co-infusion and activation of aminopropyltrimethoxysilane (*Step 1*) followed by decantation and heat-induced cross-linking (*Step 2*).

It follows that if the mechanism of *Figure 2.1* is operative, the interfacial bond fastness displayed by ensuing film should be comparable to that obtained using surface pre-treatments, and in the case of free-radical grafted vinylsilanes. However, the difference is that, no alteration of polymer functional groups would be required and no covalent bond would exist across the elements of the two networks. In the case of polypropylene, the anticipated pre-glass layer should describe a thin sub-surface zone composed of polymer and pre-glass materials, and a second zone supra to the surface composed entirely of pre-glass. A logical progression would be to cure the hydrolysis products of silanes thereon and to hydrothermally process the material under mild conditions. In this manner, inorganic-organic glass hybrids or pure glass coatings may be bonded onto heat-sensitive, low-surface-energy polymers and molded plastics without necessitating surface pre-treatments to activate surface. In the particular case of the Eppendorf tube, greatly reduced oxygen permeability would be anticipated. Alternatively, high-temperature stable polymers such as Teflon could be processed at

atmospheric pressures and moderately high temperatures to afford glass surfaces. In this preliminary investigation, the veracity and feasibility of intercalating, activating and self-crosslinking of aminopropylsiloxane precursors as interfacial linker molecules are examined.

2.3.2 General methods

(i) Ninhydrin Reaction

The reaction between certain amino acids and ninhydrin results in formation of a brightly colored compound called Ruhemann's Purple [121]. In our case, ninhydrin color analysis can be used to detect the presence of surface accessible amino groups, thus the tubes that were reacted with aminosilanes were tested with ninhydrin solution. Tubes containing the one-percent propanolic ninhydrin solution were incubated for 40min at 70°C.

2.3.3 Synthetic Methods

In order to establish the prospect of a perfusion-activation-crosslinking mechanism four related experimental designs were devised. In the tube distention experiments, the ability of hot toluene to perfuse into the walls of an Eppendorf tube was established. In a second experiment, the ability of toluene to facilitate the perfusion of solvated aminopropylsiloxane precursors was also established. A third and fourth type of experiment was devised to show that intercalated aminopropylsiloxane precursors, once activated, were retained via crosslinking as opposed to physical entrapment or any other non-covalent association. Lastly, in order to identify the contribution of intercalation and crosslinking, a set of reaction tubes were incubated with a series of solutions and compared with the set of control tubes which were treated in a parallel way, the difference being that propanol was use in place of toluene.

(i) Characterizing tube extension due to toluene perfusion

The top-to-bottom length of native Eppendorf tubes containing toluene (1.8ml, 70°C) was measured (30min intervals, 3h total duration) with a Mitutoyo brand CD-6 B model digital caliper in order to determine tube expansion by solvent intercalation. The top-to-bottom length of propanol incubated Eppendorf Tube was also measured in the same way. Elongation versus time was graphed using Microsoft Excel and the graphical analyses were used to characterize the intercalation process. The images of Eppendorf Safe-Twist tubes, treated with toluene or propanol, was captured by laying the tubes upon a HP ScanJet 6300C scanner.

(ii) Verifying the co-perfusion of aminopropyltrimethoxysilane-toluene.

Tubes containing the reaction solution (2.0ml, 1:99 (v/v) aminopropyltrimethoxysilane/water-reduced toluene) were incubated (70°C, 3h) and flushed thereafter under a jet of distilled water to promote the removal of mechanically fixed surface residues. After a quick rinse with propanol, amino groups residing in the wall of the tubes were visualized by incubation with a propanolic solution of 1% ninhydrin (1.8ml, 70°C, 40min). The experiment was redone using propanol in place of water-reduced toluene for comparison. As propanol is incapable of distending polypropylene, a marked difference in color yield was anticipated.

(iii) Characterizing the product of co-perfusion and subsequent activation-crosslinking (*Figure 2.1.A*)

The extent that amino groups were retained in control tubes treated with aminopropyltrimethoxysilane/water-reduced toluene (2.0ml, 1:99 (v/v), 70°C, 3h) was compared to trial tubes treated initially with aminopropyltrimethoxysilane/water-reduced toluene (2.0ml, 1:99 (v/v), 70°C, 3h) and afterwards with water-saturated toluene (2.0ml, 70°C, 3h). All tubes were rinsed after with propanol, cured by heat treatment (70°C, 3h), flushed with water, dried, and tested with ninhydrin (1.8ml, 70°C, 40min).

(iv) Characterizing the product of concurrent co-perfusion-activation-crosslinking (Figure 2.1.B)

The extent that amino groups were retained in control tubes treated with aminopropyltrimethoxysilane/ water-reduced toluene (2.0ml, 1:99 (v/v), 70°C, 3h); no successive incubation in wet toluene) was compared to trial tubes treated with aminopropyltrimethoxysilane/water-saturated toluene (2.0ml, 1:99 (v/v)). All tubes were rinsed after with propanol, cured (70°C, 3h), water-flushed, dried, and ninhydrin-tested (1.8ml, 70°C, 40min). Images were captured by laying the tubes directly upon a scanner.

(v) Validating non-adsorptive mode of product retention.

To verify that aminopropyltrimethoxysilane hydrolysis products were indeed retained by covalent crosslinking, native tubes were treated with a non-crosslinkable diaminopropane in water-saturated toluene (2.0ml, 1:99 (v/v), 70°C, 3h). The non-crosslinkable diamine, with two amino groups instead of one amino and silane group, served to estimate the fraction of non-crosslinked aminopropyltrimethoxysilane hydrolysis products that might be retained by an adsorption only mechanism. The diamine, bearing a rough physico-chemical similarity to the activated target molecule, was anticipated to crudely mimic the retention profile of non-crosslinked aminopropyltrimethoxysilane hydrolysis products, which resided in the matrix. Following incubation, control tubes were rinsed with propanol and set aside, while trial tubes were rinsed and incubated in water-reduced toluene (70°C, 3h). Matrix-perfused diamine was anticipated to leach back into solution during the second incubation. In order to control the contribution of crosslink-promoted retention, native tubes were similarly treated in a parallel experiment using the crosslinkable target molecule, namely, aminopropyltrimethoxysilane with in place of diamine. Control and trial tubes, and contents remaining from spent solutions were tested using ninhydrin (1.8ml, 70°C, 40min). A potential revision to this experiment might have been to examine the degree to which aminopropyltrimethoxysilane perfused into the matrix and partitioned back into solution under anhydrous-only conditions. In practice, however, traces of water in toluene or the polypropylene matrix caused the experiment to be impractical.

2.4 Results

Top-to-bottom measurement of Eppendorf tubes by a digital caliper showed that the length of the native tube increased gradually during incubation with toluene and the change of length had stabilized after 3 hours of incubation. The incubation of Eppendorf tube with propanol did not result in increase of length. The length of a native tube treated with propanol (left) and another treated with toluene (right) is compared in *Figure 2.2.a*. After 3 hours of toluene incubation, a final length increase of approximately 5% was noted in the tube (*Figure 2.2.b*). Accordingly, an arbitrary reaction time of 3 hours was adopted for all subsequent experiments. Weight gains due to matrix-perfused toluene were approximately 4-5%. The original mass and length of tubes were restored most conveniently by heating *in vacuo*. No length increase was observed during treatment with propanol (graph not shown).

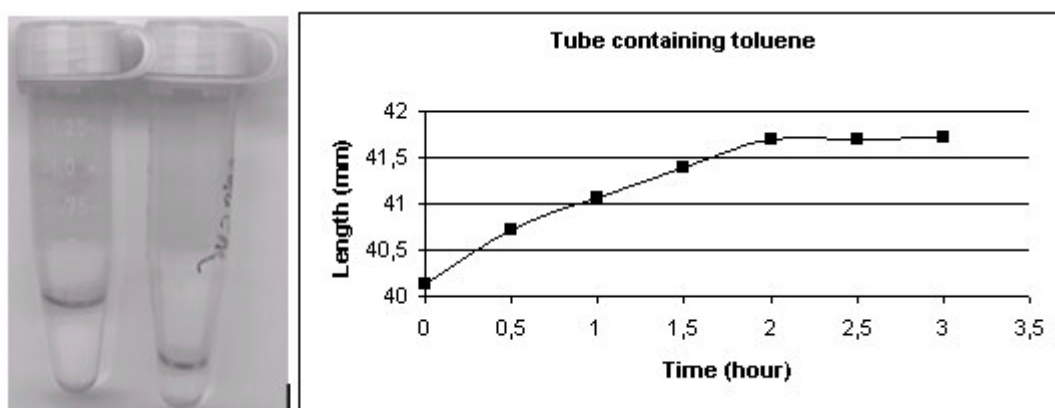


Figure 2.2. Distention of polypropylene during solvent treatment is depicted. **A.** Image of Eppendorf Safe-Twist tubes treated (3h) with propanol control (left) and water-reduced toluene (right); **B.** Graph of elongation versus time in toluene, reporting the top-to-bottom length of an Eppendorf Safe-Lock tube.

The ninhydrin yield of the experiment designed to verify the intercalation of toluene-reagent solution is shown in *Figure 2.3*. The solution-treated tubes were flushed with water and propanol. Matrix-perfusion was then tested using propanolic ninhydrin. The ninhydrin negative results were obtained for a native tube (*Figure 2.3.A*) and a control tube pre-incubated with aminopropyltrimethoxysilane in non-perfusing propanol (*Figure 2.3.B*). The trial tube (*Figure 2.3.C*), previously incubated in a water-reduced toluene solution of aminopropyltrimethoxysilane, tested ninhydrin positive and the

color was fixed in the walls of the tube. The ninhydrin reaction shows the ability of matrix-swelling toluene to facilitate entry of low-molecular-weight aminopropylsilyl species into polypropylene.

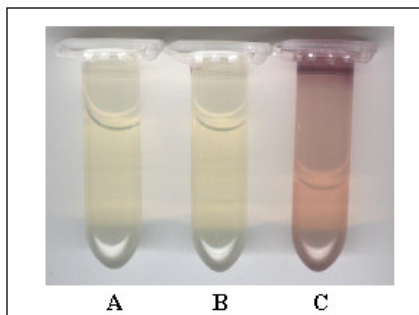


Figure 2.3. A. Native tube; B. Control tube incubated with aminopropyltrimethoxysilane in non-perfusing propanol; C. Trial tube incubated with aminopropyltrimethoxysilane in water-reduced toluene.

The ninhydrin color yields of tubes that were pre-treated in water-saturated or water-reduced toluene solutions containing aminopropyltrimethoxysilane are illustrated in *Figure 2.4*. The ninhydrin yield of native tube was negative (*Figure 2.4.A*). The walls of tubes treated aminopropyltrimethoxysilane in water-reduced toluene solution tested ninhydrin positive (*Figure 2.4.B*). Tubes treated with the silane dissolved in water-saturated toluene (*Figure 2.4.C*) were consistently more ninhydrin positive. Moreover, a fair portion of the total color was noted in solution.

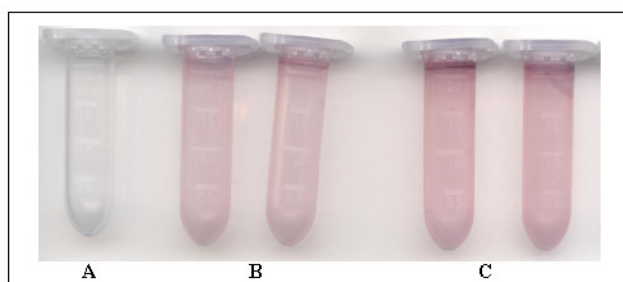


Figure 2.4. A. Native tube; B. Control tubes treated with aminopropyltrimethoxysilane in water-reduced toluene solution; C. Trial tubes treated with aminopropyltrimethoxysilane in water-saturated toluene solution.

In a last experiment, several tubes were incubated using a hydrated toluene solution of diaminopropane, and then rinsed with propanol. Those analyzed immediately with ninhydrin afforded a positive result along the walls and in solution (results not shown). Those re-incubated instead in water-reduced toluene afforded a ninhydrin negative result. The spent, water-reduced toluene solution tested ninhydrin positive. By comparison, native tubes incubated with aminopropyltrimethoxysilane in hydrated toluene solution not only afforded significant ninhydrin yields in the walls before the secondary treatment with water-reduced toluene, but also afterwards, in direct contrast to the result noted for the diamine perfusate. The water-reduced toluene solution tested ninhydrin negative.

2.5 Discussion

(i) Evidence supporting perfusion of toluene and co-perfusion of aminopropylsilyl species.

Figure 2.2 confirmed the polypropylene tubes had distended in the presence of hot toluene. The graphic profile reported a linear increase until 2 hours incubation time, followed by a plateau. These results indicated that toluene under the influence of heat, was able to perfuse into the plastic matrix. It followed that perfusion had increased the inter-chain separation of the polymer. Furthermore, a point was reached where a net influx of solvent was prevented by strains associated with the inter-chain separation. The results also implied that suitable solutes, such as silanes or toluene-associated water, might co-perfuse into the plastic by this approach. This deduction was supported by the results shown in *Figure 2.3*, which indicated that co-perfusion had occurred. The fact that tubes incubated with toluene/amimosilane solution tested ninhydrin positive, whereas those incubated with propanol/aminosilane solution tested negative proved that aminopropylsilyl species could only co-perfuse if a matrix-swelling solvent was applied.

More evidence related to establishing the matrix-localization of aminopropylsilane species may be inferred from the ninhydrin test. In particular, the chromophore produced with primary amines detaches during formation and is free to enter solution [121]. The fact that color remained fixed in the walls of the tube as opposed to freely dissolved in ninhydrin solution indicated that the ninhydrin reaction

likely occurred with matrix-perfused amino groups, affording a trapped chromophore. The color noted was red instead of violet, which may implicate constricted packing of chromophores in the confines of the matrix, solid-phase trapping of ninhydrin reaction intermediates, or any other matrix effect. All indications, therefore, supported perfusion of toluene and co-perfusion of aminopropylsilyl species into the polymer walls.

(ii) Evidence supporting co-perfusion, activation and crosslinking of aminopropylsilyl species in the matrix and pendant to the surface

The crosslinking of silane precursors along and under the polypropylene surface appeared influenced by water content, temperature, perfusability into the matrix, and leaching or partitioning of matrix-associated compounds back into solution. The stepwise perfusion-activation approach (*Figure 2.1.A*) apparently suffered from leaching of silane precursors. However, the likely formation of intra-matrix crosslinks, and a thin, if not negligible surface film, was nonetheless shown. While leaching of matrix species was not deemed an issue with the concurrent perfusion-activation attempt (*Figure 2.1.A*), findings suggested that surplus activation-crosslinking of precursors in solution could curb, for steric reasons, the effective penetration of anchor-forming units into the sub-layers of polypropylene. The overall results left little probability that a surface film had anchored only mechanically as opposed to having bonded chemically. Of the scenarios envisaged in *Figure 2.1.A*, the second approach proved more amenable in practice. However, either approach appeared to yield a surface potentially suitable to further modification.

Polypropylene that was co-perfused by aminopropyltrimethoxysilane in water-reduced toluene and treated subsequently with water-saturated toluene (*Figure 2.1.A*) afforded a lower color yield than polypropylene treated by the concurrent approach (*Figure 2.1.B*), particularly in the solution phase (results not shown). This finding was anticipated, as the potential for aminopropylsilyl species to associate without hydrolytic activation (i.e., *Figure 2.1.A, Step 1*) was unlikely. In the concurrent approach, the ninhydrin yield of tubes treated with aminopropyltrimethoxysilane in water-saturated toluene (*Figure 2.4.C*) was higher than tubes treated in water-reduced toluene (*Figure 2.4.B*). This superior color yield was an indication and consequence of more widespread activation by water. While some color entered solution, the rest remained fixed to the

plastic. This finding would likely be consistent for an aminopropylsiloxane coating that was part surface pendant and part buried. In the case of the water-reduced control experiment (*Figure 2.4.B*), the growth and immobilization of a surface coating was clearly limited by low water content, consistent with a ninhydrin positive yield in the matrix and a negative or near-negative yield in solution. In the case of all tailored tubes, ninhydrin positive results were obtained despite numerous pre-washings using water, further suggesting that surface-anchored populations (if applicable) and sub-surface anchor-like populations of activated monomers had collectively bonded together. A question remaining to be addressed was whether the aminopropylsilyl species had attached solely by non-covalent means.

(iii) Evidence ruling out non-covalent modes of aminopropylsilyl retention in the matrix and along the surface

The results of the diaminopropane-retention experiments indicated that diaminopropane had leached from the polypropylene matrix into water-reduced toluene. This finding supported the crosslinking idea, as it implied that non-covalent bonding alone should not be strong enough to retain activated yet non-crosslinked variants of aminopropyltrimethoxysilane in the polymer. Clearly, another mode of retention was likely operative that was consistent with the chemistry of hydrolyzed aminopropyltrimethoxysilane. Retention could be conceived, for instance, by the intra-matrix formation of dimeric to oligomeric anchor groups. The fact that tubes treated with aminopropyltrimethoxysilane in hydrated toluene gave similar ninhydrin yields after subsequent incubation with water-reduced toluene (comparison not shown), supported the likelihood that crosslinking facilitated the retention of aminopropylsilyl species within and along the matrix of the plastic. This finding was further supported by virtue that spent toluene recovered after the incubation tested ninhydrin negative. In view of the reversed partitioning that was noted for diaminopropane, tubes pre-treated in water-reduced toluene solutions of aminopropyltrimethoxysilane were also anticipated to show highly decreased matrix-phase color yields when subsequently incubated in water-reduced toluene. In practice, however, the principle was contradicted. The key reason is likely related to residual water and uncontrollable crosslinking.

2.6 Conclusion

The veracity of an intercalation-crosslinking approach as a novel means of activating and tailoring the surfaces of polypropylene without resorting to chemical modification of polymer surface groups was supported by experimental results. First advantage is that the original material is unaltered in the chemical sense, as the process physically combined two polymer networks, presumably by intertwining a growing polymer amidst individual chains of the plastic. Therefore, the surface formed is likely a thin layer as opposed to a monolayer. All the other methods chemically alter the polymer surface and this fact will potentially affect material longevity, particularly if the method introduces local regions bearing reactive meta-stable functional groups. A second very significant advantage is that the choice of surface modification is not limited to amino groups. In fact, several different functional groups may be deposited simultaneously and in precise ratios. One disadvantage of this method is that it is not particularly amenable to continuous flow processes. Another disadvantage is that this method is not as rapid as plasma methods.

The approach has great potential for polymers bearing relatively inert surfaces. The process is not dependent on any specific chemical reactivity but rather on choosing a suitable matrix-swelling solvent, thus if the procedure is generalized, it could be used to achieve organic-inorganic bonding in polymers regardless of the polymer. It follows that non-reactive bonding to surface functional groups could form a technology by which diverse surface-pendent functional groups in any organo-ceramic coating may be engineered.

CHAPTER 3

CHEMICAL MODIFICATION OF POLYPROPYLENE SURFACE BY AMMONIUM PEROXYDISULFATE OXIDATION AND OXIDATION INDUCED MESOPATTERN FORMATION

3.1 Introduction

Polypropylene, has excellent physico-chemical properties and it is becoming increasingly attractive materials for a series of engineering and biotechnological applications. Surface properties of polymers often do not meet the demands of industrially important applications and it is necessary to tailor the surface selectively while keeping the bulk characteristics unchanged. Typical methods to activate surfaces are based on nitrogen plasmas, oxidative/acidic chemical activation conditions, and free radical grafting and photografting. In the case of polypropylene, some chemical activation methods rest on treatment with nitric acid, chromic acid, peroxytrifluoroacetic acid, peracetic and aqueous peroxydisulfate.

In this study, not only the chemistry but also the topology after oxidation is under study since the topology of the surface in nanoscale is important in biological applications and also for the hydrophobicity studies. Nanoscale engineering of topology is severely limited with respect to many materials. Common methods of achieving small-scale topologies have required template approaches such as micro- and nanolithography. On the other hand, high loadings of surface functional groups are also desired, however plasma modifications, for example, typically quote sub- $\mu\text{mole}/\text{cm}^2$ derivatizations. This defines an effective upper limit in approaches that do not graft preformed multifunctional polymer chains onto a surface or do not polymerize monomers thereon. It follows that in the case of oxidation of polypropylene tubes under study, one way to manipulate mesoscale topologies and increase loading capacities

while maintaining original size constraints might be to roughen the accessible surface via chemical degradation. In this respect, treatment with aqueous ammonium peroxydisulfate was envisaged as a convenient method to simultaneously activate surfaces and roughen topologies at the mesoscale. Therefore, the strategy not only precludes costly equipment but also introduces the ability to subsequently attach a very diverse assortment of functional groups upon the activated topology.

3.2 Materials

Eppendorf Safe-Lock brand tubes (2ml capacity) were obtained from Eppendorf Company. Melt-blown polypropylene was obtained from Proctor and Gamble. Reagents were obtained from Sigma-Aldrich. Distilled water was produced in-house and reagent grade solvents were obtained from commercial suppliers.

3.3 Methods

3.3.1 Reaction method

The reactions were performed using a standard laboratory oven, a Savant Speedvac with the vacuum accessory disabled and an Eppendorf brand thermomixer. The chosen temperature was 70°C which is suitable for the activation of the ammonium peroxydisulfate and not so high as to potentially alter the morphological properties of PP.

(i) Time course reactions

The inner surface of commercial injection-molded isotactic polypropylene tubes was exposed to aqueous ammonium persulfate solution (1.8ml, 1M, 70°C) for 0h, 2h, 4h, 6h, 8h, 10h, 12h, 14h, 16h, 18h or 24h. Negative controls, which accounted for potential thermal oxidation at 70°C, were prepared by treatment with ammonium sulfate (1.8ml, 2M, 70°C, 16h). All tubes were rinsed thoroughly with distilled water and isopropanol, and dried in a vacuum oven (40°C, 2h). Melt-blown polypropylene fibers were oxidized for 16h and worked up in a parallel manner.

(ii) Gravimetric Analysis

The weight of Eppendorf tubes before and after oxidation with ammonium peroxydisulfate was compared in order to assess the loss by gravimetric analysis. Eppendorf tubes (10×2ml) were washed with distilled water and then dried in vacuum oven (70° C, 6h). Tubes were transferred to a desiccator to prevent them absorbing moisture while cooling down to room temperature. After tubes were weighed collectively, APS solution (1M, 1.8 ml) was delivered to each tube and allowed to react (70° C, 16h). The tubes were washed thoroughly after reaction, dried and weighed again.

3.3.2 General Methods

(i) Preparation of Persulfate and Control Solutions

Ammonium peroxydisulfate solution was prepared by dissolving the required amount of solute in deionized water and with the help of an ultrasonic bath. The control solutions were prepared by dissolving ammonium sulfate in deionized water. In the control solution there was no active agent but it maintained counter ions for comparability. The solutions were prepared freshly before each experiment to maintain consistency.

(ii) Washing and Drying Method for Modified Samples

At pre-selected times, samples were taken from the heating device and allowed to cool down to room temperature. The tubes were emptied and flushed thereafter under a jet of water to promote the removal of mechanically fixed surface residues. Samples were dried in a vacuum oven prior to analysis to remove potential moisture and other volatiles from the matrix of the polymers.

(iv) Preparation and ATR-FTIR Analysis of Samples

Samples were prepared in such a way that avoids incidental damage to the plastic matrix and permits the effective analysis using the attenuated total reflectance

equipment of the Fourier Infrared Instrument. As excessive bending of samples during the sample preparation yielded poor ATR-FTIR spectra, this modification to the method was introduced to protect the crystal structure of the polymer. For preparation of tube samples, a cylindrical piece with an approximate height of 3mm was cut just above the base of the tube using a heated razor blade. These ring-shaped pieces from the sample were immersed in liquid nitrogen and shattered while frozen, the effect being that undesirable cracking of the polymer was avoided. The cutting steps are illustrated in *Figure 3.1* shown below. The pieces chosen for analysis by FT-IR typically bore dimensions of 2x3mm. These pieces were then were dried in a vacuum oven (40⁰C, 2h) prior to analysis to remove potential moisture and other volatiles from the matrix of the plastic. The samples prepared in this way had little or no damage to the crystal structure but nevertheless some bore thick edges with scuff as a result of the cutting action with hot blade. These regions were carefully cut with a flat edged razor blade. Clear, scuff-free appearing regions were clamped over the window of the ATR accessory of a Bruker model Equinox 55 infrared spectrophotometer. Twenty scans were averaged using a 70-point rubber-band correction option that was part of the Bruker OPUSV 3.1 software package.

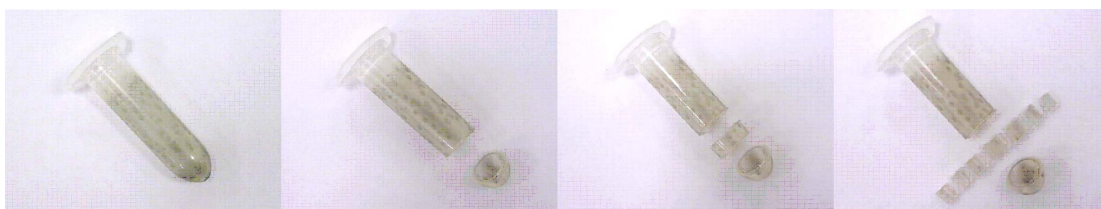


Figure 3.1 Cutting steps for sample preparation for ATR-FTIR.

(v) Preparation and Scanning Electron Spectroscopic Analysis of Samples

Sample tubes for SEM analysis were prepared by method used for the ATR-FTIR sample preparation. For melt-blown fibers and samples in sheet form no special sample preparation was done. Carbon coatings were employed in the case of the Eppendorf brand tubes and a tungsten-platinum mix was employed in the case of the melt-blown fibers. Either coating greatly improved the air to surface contrast. Scanning electron micrographs were obtained using a beam voltage of 5, 10 and 15kV. At least four areas per sample were examined at resolutions up to 70kX and analyzed using windows-

based imaging software. The former samples were analyzed using a JEOL model JSM-6500F instrument, whereas the latter were analyzed in a Hitachi S5200 Field Emission Scanning Electron Microscope.

3.4 Results

(i) FTIR measurements of time course and concentration course samples

The attenuated total reflectance signal of an Eppendorf Tube before and after reaction is shown in *Figure 3.2*. It should be noted that wavenumbers are generally shifted to lower frequencies and all high frequency absorbances are reduced in ATR mode of FTIR in comparison to transmission infrared spectroscopy. In case of our instrument, this shift was calibrated at 9cm^{-1} for native polypropylene. The wavenumbers reported in the results were not corrected by this amount in order to remain consistent with their spectral profiles, however, functional group assignments were made only after applying this correction.

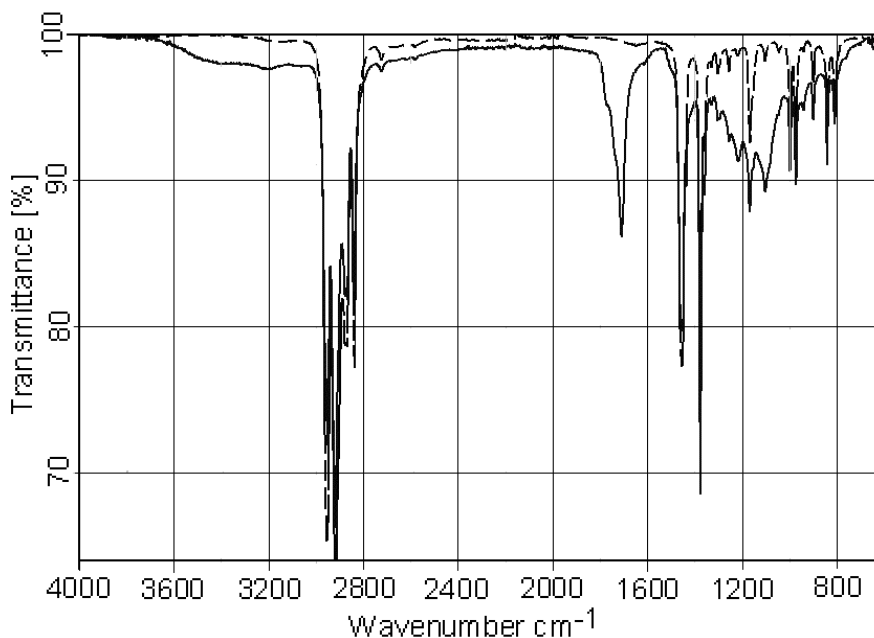


Figure 3.2 ATR FTIR spectrum of vacuum dried samples before (dashed line) and after (solid line) reaction (1M, 70°C , 16h).

Control and blank surfaces afforded spectra with methylene stretches at 2916cm^{-1} and 2838cm^{-1} and methyl stretches at 2949cm^{-1} and 2868cm^{-1} , as expected for polypropylene. The methine absorption is generally weak and obscured, however in this case a peak lying immediately to the left of 2868cm^{-1} was tentatively assigned to this stretch. In the fingerprint region, an asymmetric deformation was ascribed to the peak at 1379cm^{-1} for the methylene group. In fact, given that the starting material appeared pure, all absorptions below 1500cm^{-1} in the spectra were attributed to different vibrational modes of alkyl groups of varying hydrogen multiplicity, namely, deformation, rocking, torsion, scissoring, wagging and twisting. The peak at 1770cm^{-1} was previously identified as $-\text{CHCH}_3$ absorbance mode and the peak at 975cm^{-1} was assigned to a methyl group absorbance. The spectral mode responsible for strong absorbance at 998cm^{-1} is rather complex and it disappears in low molecular weight polypropylenes.

Spectral profiles differed notably in the functional group region ($4000\text{-}1300\text{cm}^{-1}$), fingerprint region ($1300\text{-}900\text{cm}^{-1}$) and remaining low-frequency region ($900\text{-}600\text{cm}^{-1}$). Native surfaces revealed a minor dip in the O-H stretching region from 3600cm^{-1} to 3050cm^{-1} which corresponds to surface bound and intermolecular H-bonded water. Two other possibilities for this absorbance are carboxylic acid and alcohol groups. However, O-H stretching is extremely broad for carboxylic acids, moreover a carbonyl stretch and C-OH deformation absorbance at $1440\text{-}1400\text{cm}^{-1}$ were expected but they are not observed on the spectra profile. Similarly, strong C-OH stretching would be anticipated in the presence of significant alcohol groups, with the highest frequencies of $1150\text{-}1130\text{cm}^{-1}$ attributed to tertiary alcohols. A C-H frequency of an unsaturated carbon would be expected just above 3000cm^{-1} and C=C stretch in the range of $1680\text{-}1600\text{cm}^{-1}$, but such were not the case, so it can be concluded that carbon-carbon unsaturations were also not apparent. The peak at 2721cm^{-1} could have been attributed to one of the Fermi doublets of an aldehyde group, however the carbonyl stretching region was completely clean and moreover this peak would certainly be consumed by persulfate initiated tertiary peroxides. This peak remains unvalidated, but it was observed in many different polypropylene preparations. There were no carbonyl absorbances ruling out the presence of any significant amount of aldehyde, carboxylic acid, ketone and ester.

Following persulfate treatment, a broad absorbance spanning the region from 1300cm^{-1} to 1000cm^{-1} was noted. Similar spectral profiles were afforded in the

photochemical oxidation of polypropylene and ethylene-propylene-diene monomer as measured by transmission infrared spectroscopy and in related thermooxidative investigations. In interpreting the spectrum between 3640cm^{-1} and 3200cm^{-1} , consideration was given to the scenario that both hydroperoxide groups and hydroxyl groups may be present, with their absorbances potentially superimposed and displaying comparable extinction coefficients. Under the mediation of persulfate, the net content of isolated and hydroperoxide-, hydroxyl- or otherwise associated hydroperoxides was presumed to accumulate during the course of a reaction. Therefore, the absorbance from 3640cm^{-1} to 3200cm^{-1} was assigned to hydroxylation of the polypropylene and the absorbance continuing to the right of 3200cm^{-1} and extending down to 2400cm^{-1} was assigned to O-H stretching absorbance of carboxylic acids. The strongest stretching frequencies amongst the derivatives were found in the carbonyl region, of which the expanded spectra clearly showed a composite peak bearing at least three populations of carbonyl groups, namely, a main peak centered at 1706cm^{-1} and two apparent shoulders centered at 1728cm^{-1} and 1765cm^{-1} . These peaks potentially described ketone, carboxylic acid and ester products.

Ruling out candidates such as peracid, peroxide, hydroperoxide and aldehyde, the products most likely formed alcohol, ketone, carboxylic acid, ether and ester. The immediate goal was to summarize by means of an overly simplified mechanism that the products stated above could in fact be afforded.

Figure 3.3 shows the carbonyl region FTIR spectra of a tube that was oxidatively activated for up to 24 hour. The increase of signal was gradual and the maximum intensity was reached after 16 hours of oxidation (*Figure 3.3*, balls & solid lines). At least three signals, denoting three types of carbonyl products, were apparent. On the basis of the measurements, products likely formed included alcohol, ketone, carboxylic acid and possibly ether and ester. The products obtained were consistent with established radical-induced transformation pathways, which could potentially be accelerated or altered via aqueous acid catalysis. The contribution of potential ether and ester products along solvent-accessible regions was deemed inconsequential in the matter of affecting surface adhesion. In fact, the existence of solvent-accessible ether and ester groups was essentially discounted in view of the highly reactive conditions at

the surface, which might have discouraged their formation and certainly encouraged their removal through secondary transformations. In keeping with this logic and the fact that aqueous persulfate is ultra-reactive, only surface carboxyl, ketone, and possibly hydroxyl groups were anticipated in significant number.

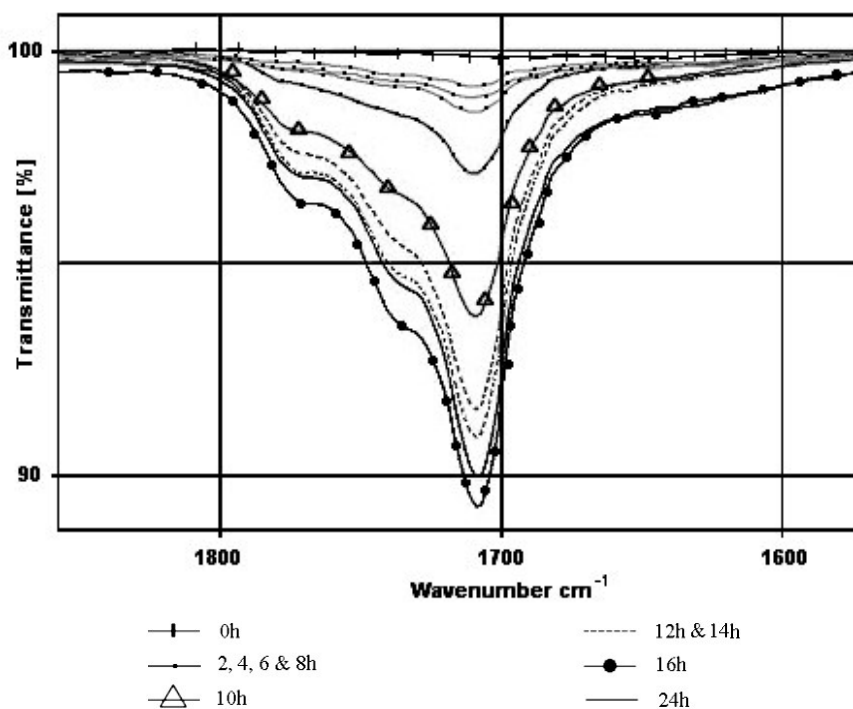


Figure 3.3 ATR- FTIR spectra of the time course reaction.

(ii) Scanning Electron Microscope Analyses

Surface of native, ammonium sulfate and ammonium persulfate treated Eppendorf tubes were analyzed by scanning electron microscope in order to investigate the change in the topology after each treatment. The micrograph of oxidized Eppendorf Tubes (1M APS, 70°C, 16h) showed the development of parallel cracks along inside walls of the tube (*Figure 3.4.C*). On the other hand, the micrograph showed no such cracks for native tube surface heated for 16 hours (*Figure 3.4.A*) and for the polypropylene tube treated with ammonium sulfate (*Figure 3.4.B*). However, small cracks appeared on both surfaces which resulted from sample preparation step for scanning electron microscopy analysis. The beam of electrons is highly negative, so during analysis it will cause the sample to become negatively charged and this charging will deflect the beam resulting disruption of image quality. Thus, in order to avoid this problem, all the samples were coated with a thin layer of either with carbon, gold or tungsten that will conduct the electrical charge on the surface to ground. However, in the case of carbon

coating when the coating is not thin and formation of cracks on the carbon coating is observed. This condition explains the presence of small cracks on native and ammonium sulfate treated polypropylene surfaces.

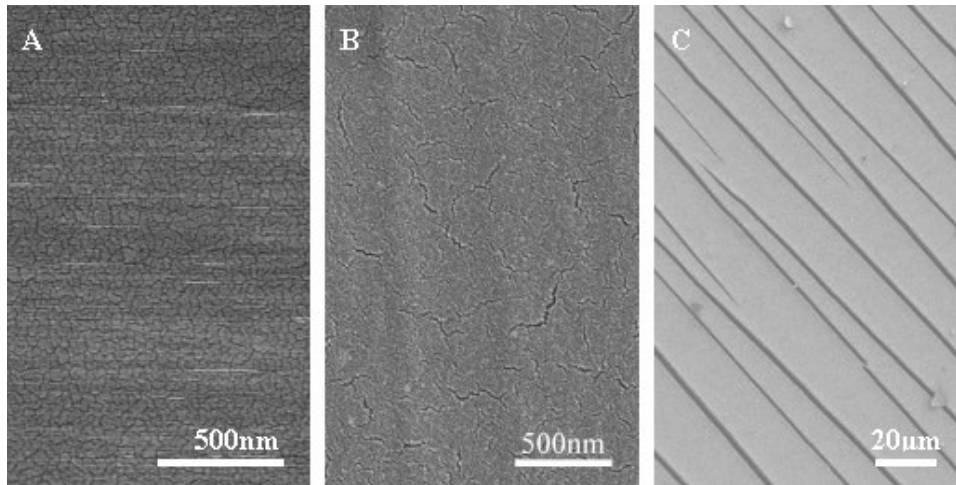


Figure 3.4 SEM image of **A.** Native Eppendorf tube; **B.** Eppendorf Tube treated with ammonium sulfate(1M, 70°C, 16h) ; **C.** Eppendorf Tube treated with ammonium persulfate (1M, 70°C, 16h).

In polypropylene, the incident light is scattered on crystallites, spherulites and also the interface between the amorphous and the crystalline phases having different refractive phases and as a result light scattered on different units of the structure makes this polymer opaque in its native form. The opacity of the polypropylene tube increased after oxidation reaction, as a result of change on the surface. The cracks formed upon oxidation resulted in loss of optical clarity yielding increased opacity which is easily observable by naked eye. The photograph taken on a dark background opacity (*Figure 3.5*) clearly shows that the oxidized Eppendorf tube is more opaque compared to native tube.

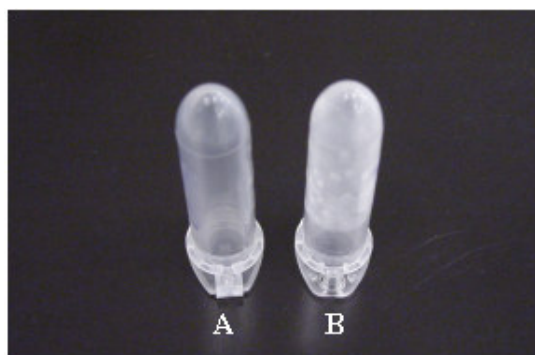


Figure 3.5 Photograph of **A. Native Eppendorf tube; B. Oxidized Eppendorf Tube**, showing the change in optical clarity after oxidation

The *Figure 3.6.A* shows the schematic drawing of an Eppendorf tube half-full with persulfate solution. A piece of sample from the middle of the tube bearing the air-solution boundary cut and analyzed by optical microscope to investigate the changes on surface where one part is oxidized and the other not. The fact that the crack formation is dependent on oxidation is clearly seen in *Figure 3.6.B*, illustrating the air-solution boundary of an Eppendorf Tube where the changes on both the oxidized and non-oxidized part of the surface are observable. Upper half of the image, showing the part of the tube surface which was not in contact with the APS solution, appeared normal. In contrast, the densely clustered cracks are observed on the surface which was in contact with persulfate solution (lower part of the image). This figure clearly shows that cracks were restricted to areas having had direct contact with the persulfate solution.

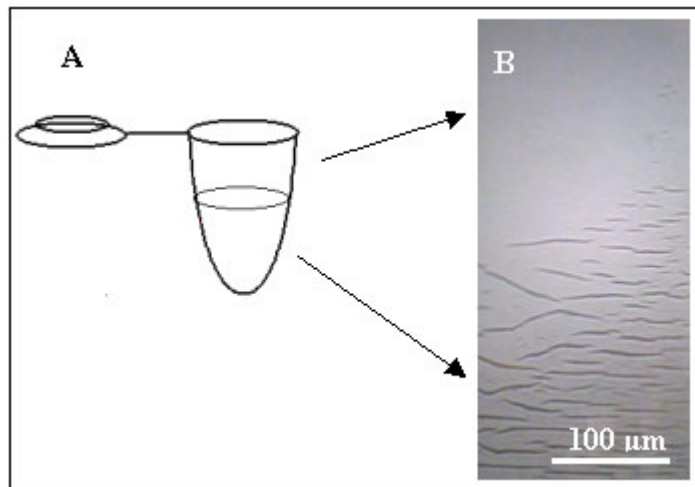


Figure 3.6 **A.** Schematic drawing of an Eppendorf half-full with the oxidant solution ammonium peroxydisulfate; **B.** Optical microscope image of oxidized Eppendorf Tube showing the air-solution boundary

Scanning electron micrograph given in *Figure 3.7* shows the depth of the cracks along the broken edge of APS treated tube. The image shows that the cracks are limited to depth of 20 μ m, which represents the skin layer of the injection molded polypropylene.



Figure 3.7 Scanning electron micrograph of APS treated Eppendorf tube taken from the cross-sectional viewpoint, tilted slightly towards the inner face

Figure 3.8 given below shows the scanning electron micrograph of an oxidized Eppendorf tube (1M APS, 70°C, 42h) at four different magnifications in increasing order. As the magnification was increased, a mesoscopic pattern formation between the cracks were observed.

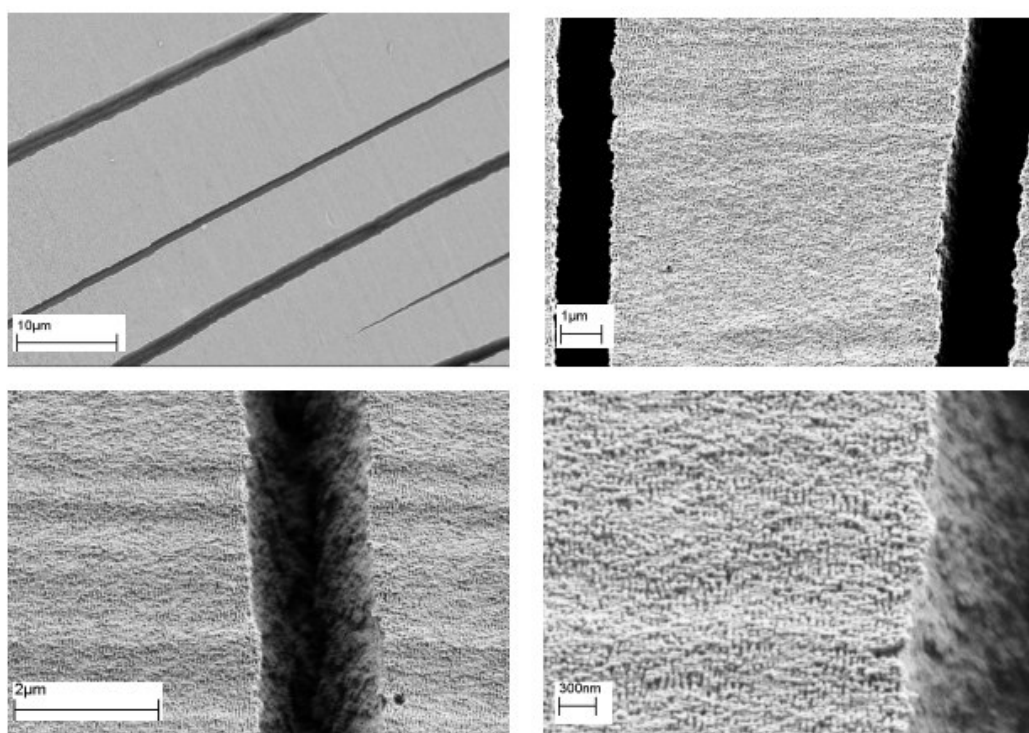


Figure 3.8 Scanning electron micrographs of gold-coated surfaces of Eppendorf tubes oxidized with APS (1M, 70°C, 42h) at different magnifications.

Scanning electron micrographs in *Figure 3.9* illustrate the development of mesoscale topology during the course of oxidizing Eppendorf Tubes. No significant change of appearance was noted at early times of oxidation. The topology appeared to

remain native like after 8 hours of oxidation (*Figure 3.9.A*). On the other hand, minor changes had developed by 10 hours, in the form of sparsely distributed bulges of approximate 400nm diameter (*Figure 3.9.B*). These two images implied a latent period of oxidation, in which topological changes were suppressed for the most part. In contrast, a relatively brief period of dramatic change was noted thereafter, vis-à-vis the sponge-like mesoscale topology shown at 12h reaction time (*Figure 3.9.C*). Further reaction did not appear to alter the landscape (*Figure 3.9.D*).

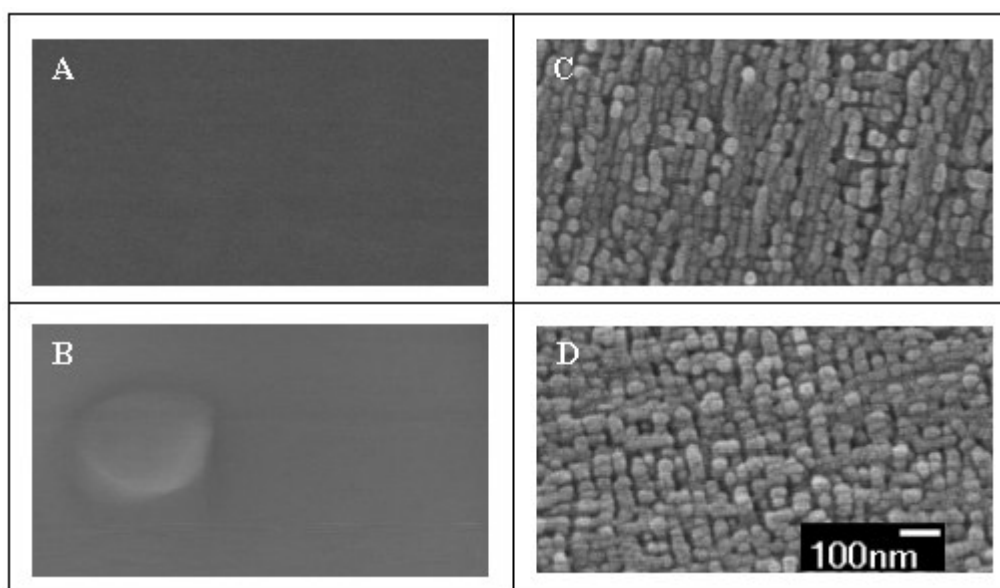


Figure 3.9 Scanning electron micrographs of injection-molded polypropylene oxidized for: (A) 8h; (B) 10h; (C) 12h; and (D) 16h. The negative reaction control surface appeared identical to the 8h time point (A).

Oxidized melt blown fibers were also analyzed by SEM to observe the changes following oxidation. *Figure 3.10.A* and *Figure 3.10.B* showed that material formation had occurred above the surface of the melt blown polypropylene fibers following oxidation. The material formed above the surface also has a sponge-like appearance (*Figure 3.10.C*). In order to assure that the material observed on the surface is not adsorbed but connected to surface, the fibers were rinsed very well with water and analyzed again by SEM. The presence of material on the surface was observed on the micrographs after washing (result not shown).

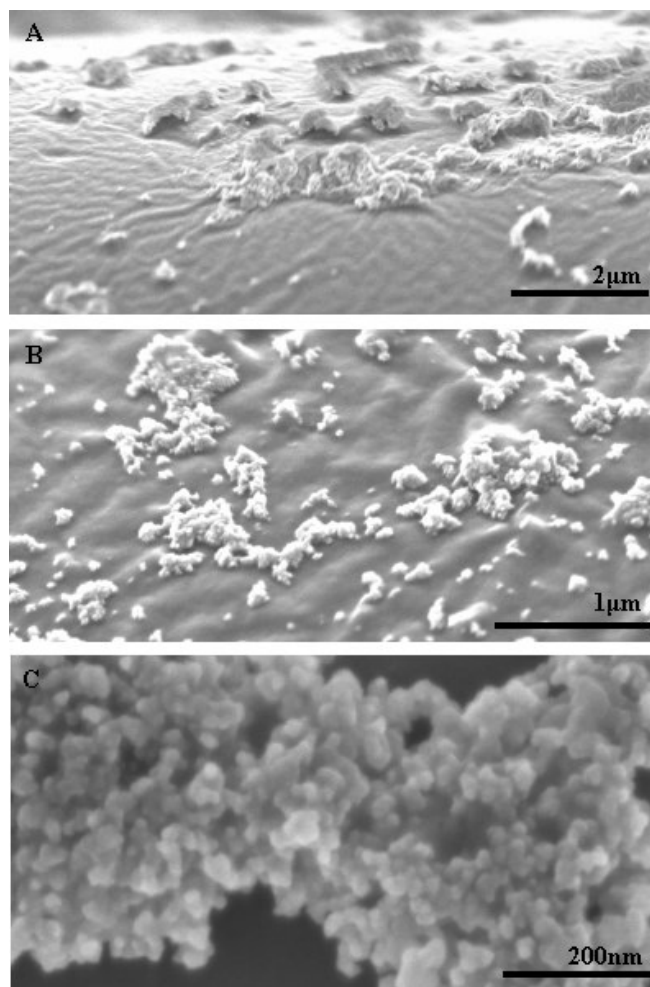


Figure 3.10 Scanning electron micrographs of oxidized melt-blown polypropylene at different magnifications

The elemental composition of the melt blown polypropylene fiber at three different points; base, amorphous part, particles, namely, was analyzed by means of energy dispersive X-ray analysis (SEM-EDS) (*Figure 3.11*). The elemental composition of the base fiber and amorphous part was same. The intensity of hydrogen, carbon, and oxygen on these sites had same magnitude. On the other hand, analysis of the elemental composition of the particles on the surface showed that the intensity oxygen peak was higher corresponding to this area was higher compared to base fiber. The fact that the oxygen content of the particles is higher indicates the presence of higher amount of oxygen containing groups in this area. This implies that the oxidized fiber, having a lower surface energy than base fiber segregates to surface and form as a phase containing hydrophilic groups and phase separates.

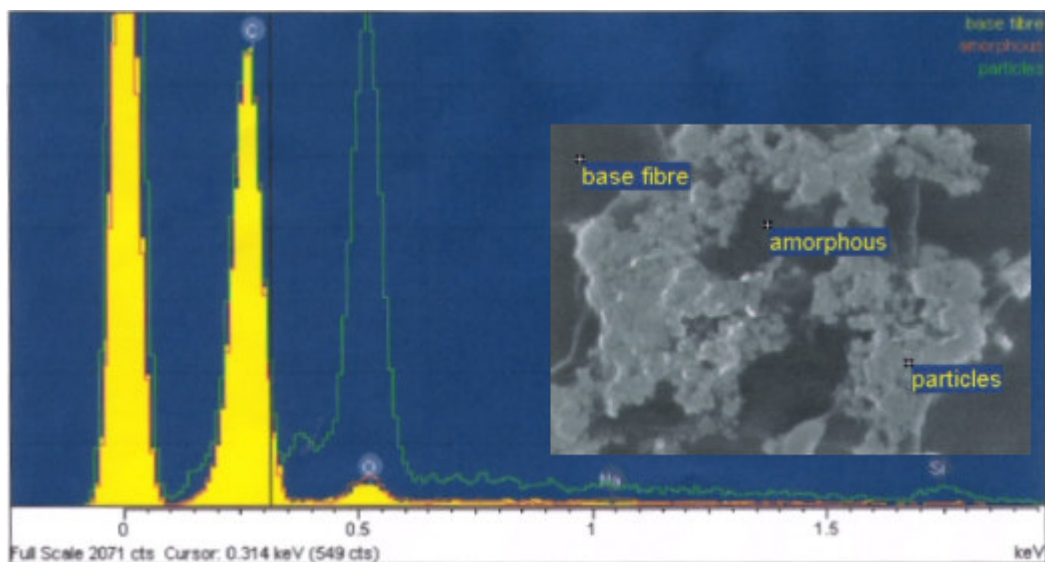


Figure 3.11 Scanning electron micrographs and EDS analysis of oxidized PP fiber; lines intensities corresponding to: yellow line: base fibre; redline: amorphous, green line: particles on the surface.

The micrographs in *Figure 3.12* shows the surface of oxidized melt blown polypropylene fiber and polypropylene Eppendorf Tube. Both micrographs captured, the presence of two structures separated by a boundary on the oxidized surface. A transition zone in which structures have developed along the lower portion of the photograph, whereas, others are about to emerge along the upper portion, is shown in both case. The topology shown in *Figure 3.12.A* is also patterned, although substantially different than in the case of the tubes. The difference of appearance was attributed to the inherent morphological differences between the top layers of injection-molded and melt-blown polypropylene. *Figure 3.12.B* clearly shows the surface-pendent mesostructures from a slightly oblique angle.

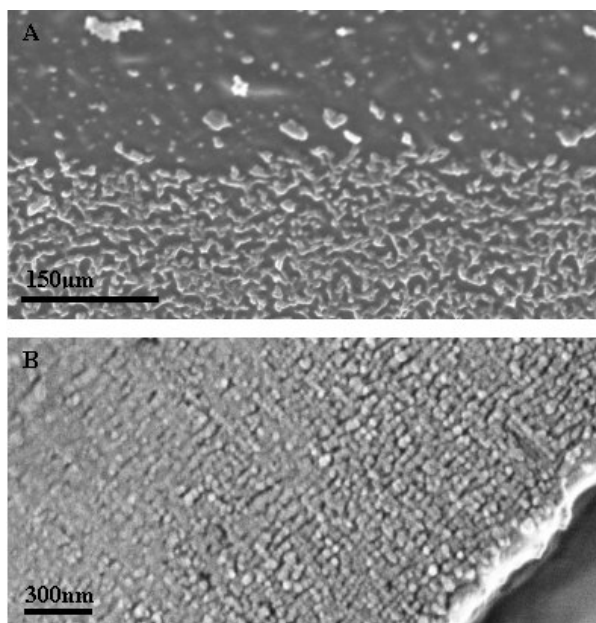


Figure 3.12 Scanning electron micrographs **A.** Polypropylene fiber, **B.** Polypropylene tubes, treated with APS showing two structures separated by a boundary.

3.5 Discussion

(i) Persulfate-initiated surface reactions and spectroscopic characterization

The chemistry employed and FTIR spectra of oxidized tube was consistent with a number of functional groups. The oxidation may be generally viewed as a partially ordered, weight-averaged summation of radical-mediated propagation, transfer, scission, and termination pathways, as well as radical, thermal and acid-catalyzed peroxide decomposition pathways. The immediate goal was to show that the products stated in results of FTIR interpretation could be afforded as a result of several mechanism taking place during oxidation.

The *Figure 3.13* outlines several immediate products and hydroperoxide intermediates. Thermal decomposition of persulfate ion yields sulfate radical and it abstracts hydrogen from water molecule, affording hydroxyl radical. The hydroxyl radical generated affords several products and hydroperoxide intermediates (*Figure 4.16.A*). After generation of hydroxyl radical, tertiary carbon center is generated as a result of abstraction of hydrogen preferentially from the tertiary carbon center (*Figure 4.16.B*). The relative rate of hydrogen by bromine are for primary, secondary and tertiary hydrogens are given as 1:82: 1640 respectively. The relative rates in hydrogen

abstraction vary considerably with the attacking agent but the given abstraction rates can still be used to compare relative hydrogen abstraction rates during oxidation since the activation energies for the reaction of bromine atoms with hydrocarbons are comparable to activation energy for the reaction of oxidizing agent, chromic acid, with hydrocarbons.

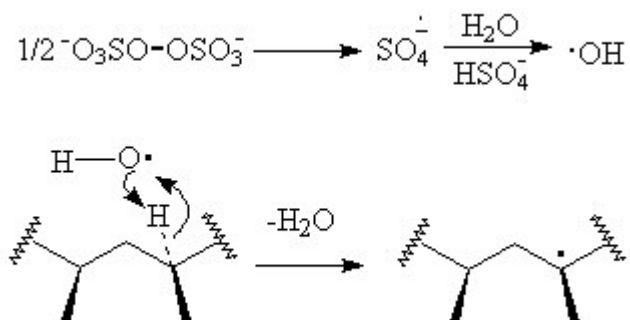


Figure 3.13 A. Homolytic decomposition of persulfate B. Hydrogen abstraction from a tertiary carbon.

Under anoxic conditions tertiary radical affords vinylidene group and a secondary carbon radical as a result of chain scission.

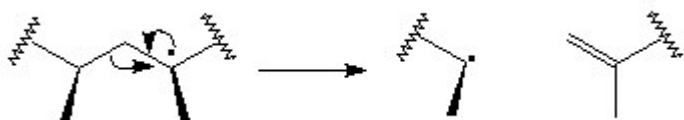


Figure 3.14 Chain scission under anoxic conditions.

In the propagation step, peroxy radical formation and a subsequent hydroperoxidation predominates in the presence of an oxygen and accessible hydrogen source such as water or a neighboring polymer moiety. The oxygen is present as a result of hydroxyl radical disproportionation. The reaction of the alkyl radical with the oxygen afford peroxy radical and then it abstracts hydrogen either from water or neighboring polymer moiety. In this respect, the ability of oxygen to diffuse into sublayers would govern the ease by which radical reactions can propagate via the hydroperoxide way. Propagation can lead either isolated or clustered hydroperoxides. The extent of clustering is influenced by the efficiency of an intramolecular backbiting reaction that leads to the generation of new tertiary, secondary and primary radicals. Secondary carbon centers may be converted into hydroperoxide in a similar way.

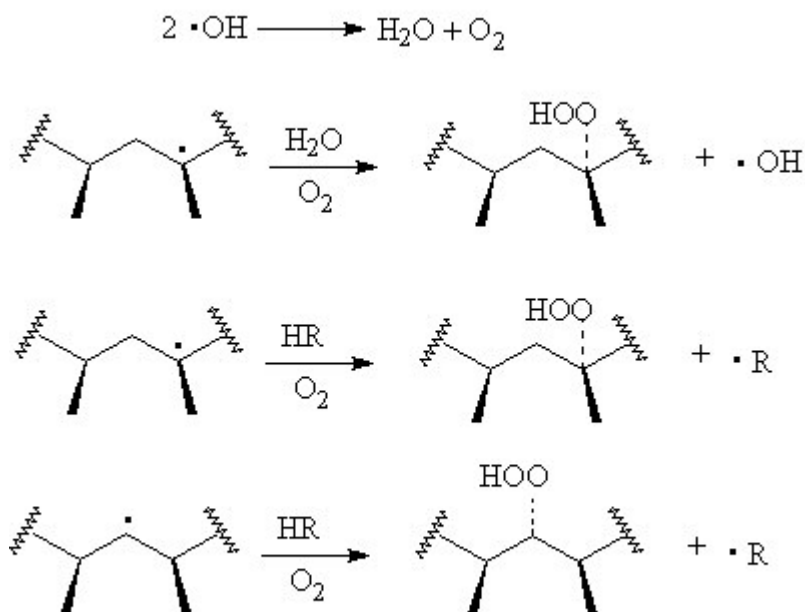


Figure 3.15 Hydroperoxidation of primary and secondary carbon centers.

Hydroperoxide decompositions appear to be potentially the most important sources of free radicals in the initial stages of polypropylene oxidation. Hydroperoxide decompositions may proceed by thermal decomposition, acid catalyzed decomposition, radical decomposition and radical abstraction of α -carbon hydrogen. Unimolecular and bimolecular thermolysis are both plausible pathways for thermal decomposition. Thermolysis of hydroperoxides result in efficient cleavage to give hydroxyl and tertiary macroalkoxyl and macroperoxyl radical. In solution, alkoxy radicals are known to abstract hydrogen from many substrates to combine with available free radicals and to decompose by β -scission processes which will play important role in backbone scission and alkyl radical formation.

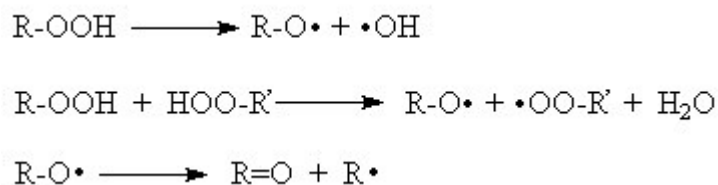


Figure 3.16 A. Unimolecular thermolysis of hydroperoxides B. Bimolecular thermolysis of hydroperoxides C. Decomposition of alkoxy radical by β -scission.

Acid catalyzed heterolytic bond cleavage affords chain scission, ketone and primary alcohol groups or dehydration with in-chain ketone. Under the reaction conditions, it is conceivable that the alcohols oxidize further to the carboxylic acid via an aldehyde intermediate. Acid-catalyzed rearrangements of hydroperoxides have been observed in polar and non-polar solvents. Protic solvents are the most effective catalysts of the rearrangement. The *Figure 4.20* shows the most general reaction sequence for acid-catalyzed hydroperoxide rearrangement.

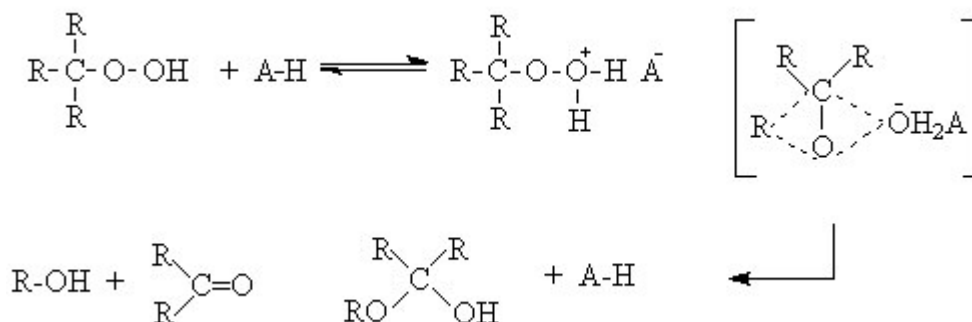


Figure 3.17 General acid catalyzed hydroperoxide decomposition.

Protonation of the hydroperoxide is a rapid and reversible reaction. It is followed by the rate-determining rearrangement where the electron density is redistributed and the nucleophile is migrating to one of the peroxide atoms. It has been found that acids can decompose primary and secondary hydroperoxides according to two different pathways shown in *Figure 3.18*. Heterolytic bond cleavage via acid catalysis affords chain scission, an end-chain ketone fragment and end-chain alcohol fragment (*Figure 3.18.A*), or dehydration with in-chain ketone (*Figure 3.18.B*).

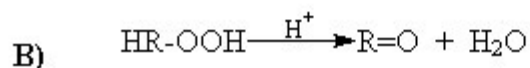
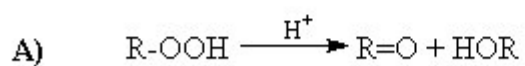
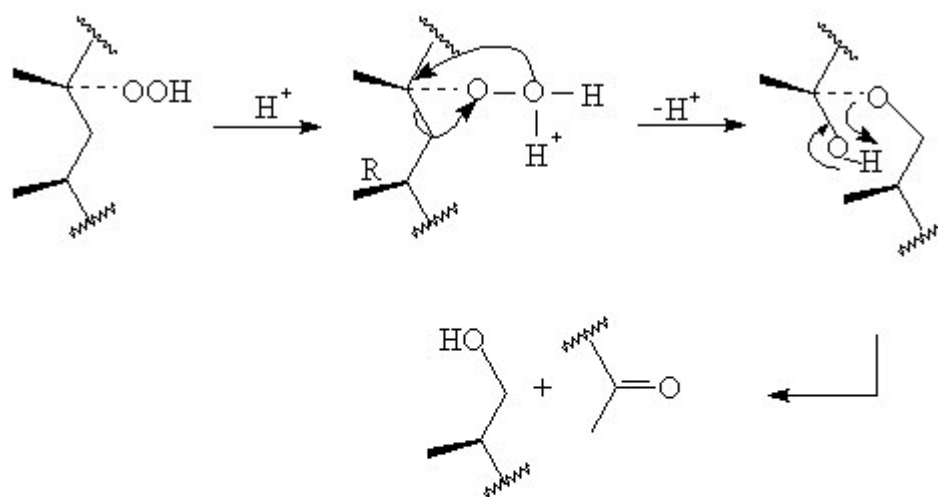


Figure 3.18 Acid catalyzed decomposition of polypropylene hydroperoxides.

Hydrogen abstraction by peroxy radical leads to spontaneous free-radical induced hydroperoxide decomposition and affords ketone formation. The tertiary hydrogen atom of secondary hydroperoxides is labile and easily abstracted by free radicals such as peroxy and alkoxy radicals. The reaction yields α -alkyl-hydroperoxy radical, and after scission of the peroxy bond a ketone and hydroxyl radical is generated (*Figure 3.19.A*). It follows that a similar reaction mediated by hydroxyl radical or alkoxy radical may occur in selected regions of polypropylene (*Figure 3.19.B*).

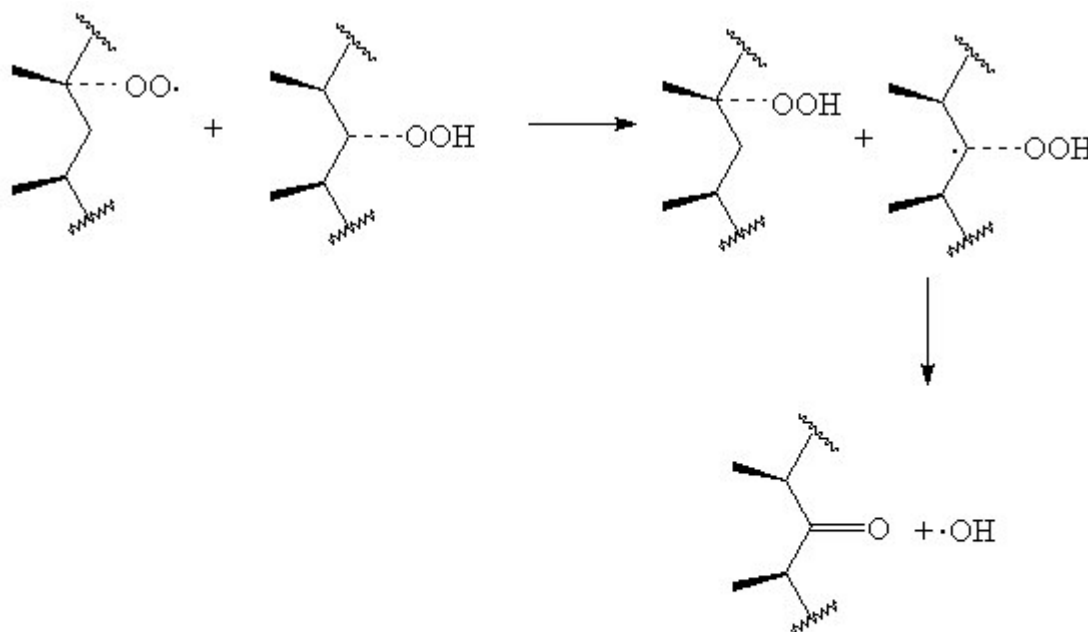


Figure 3.19 Decomposition of peroxides induced by **A.** peroxy radical **B.** hydroxyl radical.

As hydroxyl radical and ketone are co-produced, they could promote the formation of carboxylic acid. The effectiveness of this transformation is anticipated as the two components maybe unable to separate quickly and therefore mimic the cage effect that is known for viscous polymer melts. By a similar transfer process, esters can be produced. In addition to ester and ketone formation, the alkoxy radical contributes to formation of alcohol via hydrogen abstraction and radical transfer.

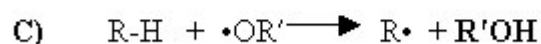


Figure 3.20 Reaction model illustrating formation of carboxylic acid , ester and alcohol via transfer pathway

In general, radicals have to terminate bimolecularly. Polymer radicals may decay intramolecularly with another radical situated at the same polymer molecule or intermolecularly with a radical at another polymer molecule. With a large number of radicals at the same macromolecule, such as are produced at the high dose rate of pulse radiolysis with low polymer concentrations, the former process is usually favored. The recombination of radical with hydroxyl, alkyl, alkoxy and peroxy radical also results in termination. The recombination of alkyl radicals with alkoxy radicals yield ethers (*Figure 3.21.A*) whereas the recombination with hydroxyl radicals yield alcohols (*Figure 3.21.B*). Secondary and tertiary peroxy radicals may co-terminate to afford alcohol and ketone (*Figure 3.21.C*). Intermolecular hydrogen abstraction by alkoxy radical at β -carbon of a secondary hydroperoxide affords alcohol, ketone, aldehyde, with concomitant chain scission (*Figure 3.21.D*). Secondary alkoxy radicals in particular can also terminate via hydroxyl-assisted dehydration (*Figure 3.21.E*).

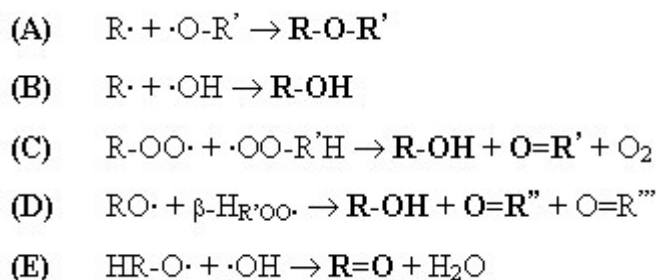


Figure 3.21 Important reactions of termination step.

The observed yields are of course subject to variation by any number of alternate pathways. Alcohol, for example, may be transformed by oxidation to carbonyl and even to carboxylic acid. Short-lived aldehydes are known to easily proceed to the carboxylic acid. Esters can also be produced by reaction of aldehyde and hydroperoxide precursors. Persulfate concentration, local oxygen availability, pH, temperature and polymer structure are some parameters that can influence the absolute and regional distribution of the four radical types (*vide infra*) and the final product distribution. The initiation, propagation, termination and other important reaction mechanisms are outlined in *Figure 3.22*.

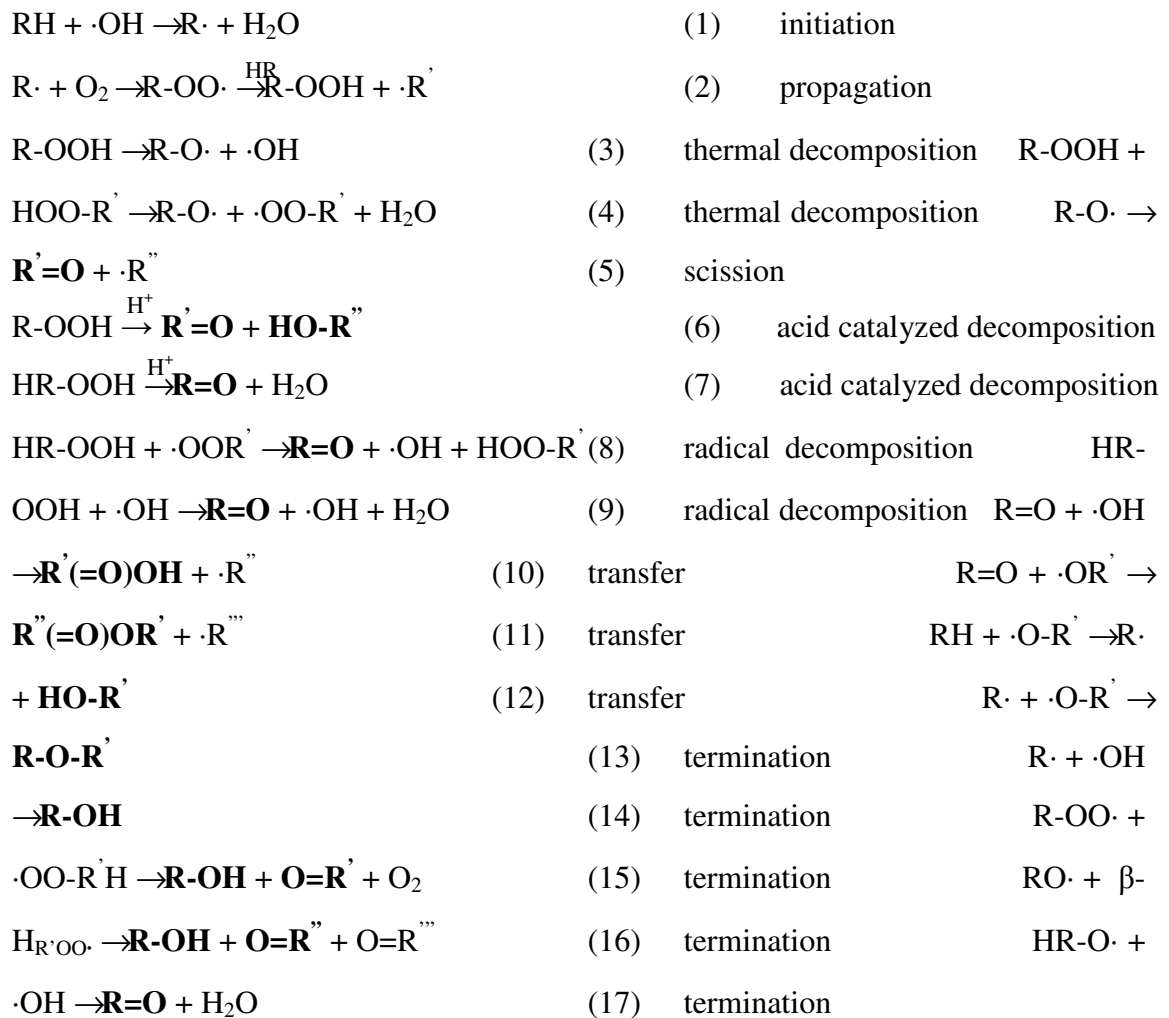


Figure 3.22 Reaction model illustrating formation of functional groups in polypropylene during oxidation.

(ii) Rationalizing Cracking Mechanism

The scanning electron micrographs revealed the presence of crack formation along the oxidized polypropylene surface after certain oxidation time had passed. The crack formation can be rationalized by three mechanisms: release of internal stress, chemicrystallization, coalescence of voids.

In a solid, just as in a liquid, the bounding surfaces possess a surface tension which implies the existence of a corresponding amount of potential energy. If a crack is formed as a result of applied stress, or a pre-existing crack is caused to extend, therefore, a quantity of energy proportional to the area of the new surface must be added. The condition that this shall be possible is that such addition of energy shall take place without any increase in the total potential energy of the system. This means that the increase in the potential energy due to the surface tension of the crack must be balanced by the decrease in the potential of the strain energy and the applied forces. The Griffith's energy release rate criteria states that the crack growth can occur if the energy required to create new crack surface area can be delivered by the system.

In the system under study, the crack formation may be related to the release of stress which may reside in polymer during its manufacture or accumulate gradually over time under the influence of external factors. The injection molded polypropylene may be subjected to stress during its processing. It is known that during injection molding, very complex thermal and flow conditions prevail in the cavity. The surface layer of the flowing melt is subjected to extensional stresses, and the subsurface layers are subjected to shear stresses. This results in a molecular orientation in the melt flow direction and a skin-core morphology where little or no orientation can be detected in the core. The skin has a complex morphology and its characteristics depend on processing parameters including the heat transfer conditions in the mold. The injection molded Eppendorf tube particularly the skin layer may have accumulated stress during the heat transfer when the polymer is quenched against a cold mold during processing. The hot isotactic polypropylene melt contacting with the cold walls of the die experiences high stresses, strain rates and cooling rates and subsequently the final structures are inhomogeneous and anisotropic.

Another possible explanation is that, during oxidation the wall was etched away to the point of structural failure. The gravimetric analysis of test tubes before and after oxidation indicated loss of 2.6mg on the average. This value corresponds to 4 μ m loss of

skin thickness and when compared to the thickness of wall, 900 μm , it is not significant enough to weaken the tube wall to the point of failure. However, when the cracking mechanism is explained in terms of coalescence of voids mechanisms, this amount of mass loss becomes important.

Oxidative degradation leading to creation and coalescence of voids is another mode of stress generation. In oxidized Eppendorf tubes, the depth of cracks were found to be restricted to a depth of 20 μm . Moreover, most of the degradation and voiding is expected to predominate near the surface and not deeper than the skin due to diffusion limitations. It follows that if the degradation is the cause of the cracking, then the mass loss must be restricted to the skin layer and it represents 20% voiding. In this case the skin layer must occupy the same surface area with a less amount of material, since the tube dimensions are constant. As a result, the skin is subjected to stress and in order to reduce it voids would migrate around the polymer chains under the influence of thermal motion, and unite near surface. Volume variations due to oxidation have been established as a possible explanation of cracking mechanism by Fayolle [94].

Cracks also could form if the density of regionally constrained material within the plastic was to increase. Extrusion-molded isotactic polypropylene is potentially composed of amorphous as well as α , β , γ and smectic crystalline regions. The densities of polymorphs measure 0.858, 0.936, 0.921, 0.936 and 0.88 g/cm^3 , respectively. In theory, β -to- α recrystallization could result in cracking. However, the process would only occur at temperatures above 140 $^{\circ}\text{C}$ in non-nucleated systems. The contribution of smectic polypropylene falls under more suspicion as it often defines the outermost 10-50 μm of plastics, and anneals to the much denser α form if elevated to at least 70 $^{\circ}\text{C}$, namely, the temperature at which tubes were incubated. Moreover, edge-on views obtained by scanning electron microscopy indicate that the penetration depth is consistent with the skin thickness and highest concentration of the smectic form. If temperature-induced densification was indeed a contributor, a comparable persulfate reaction at 60 $^{\circ}\text{C}$ would likely produce less cracks than could be accounted for by the slowing of chemical kinetics. When performed, an incubation of 32h at 60 $^{\circ}\text{C}$ afforded the same patterning as 16h at 70 $^{\circ}\text{C}$, so no marked contribution of densification could be identified. Moreover, for densification to be valid, cracks would be anticipated on the inner walls of control tubes that were incubated in ammonium sulfate, but this was not the case. A possible explanation for the absence of cracks at 70 $^{\circ}\text{C}$ in sulfate solution points to recent studies, which have indicated that

smectic polypropylene anneals completely at considerably higher temperatures than once thought.

Another mode of densification could also be operative if chemicrystallization was to occur under the influence of persulfate. In this process, after chemical degradation, segments of entangled and tie chain molecules are released via chain scission, thus permitting localized regions at the surface to undergo a secondary crystallization. The most important consequence of chemicrystallization is the spontaneous formation of surface cracks caused by the contraction of the surface layers. The volumetric contraction at the surface again would introduce stresses and enhance vulnerability to cracking. The relevance of this mode of densification is currently under investigation, however, it appears conclusive that non-chemically assisted densification could not be a contributor to the cracking.

(iii) Rationalizing Pattern formation

The possible modes of transformation proposed to rationalize the topology included; spatially organized pitting or damage to the surface as a result of chemical oxidation from above or within; an oxidation-mediated phase separation or a combination of the two mechanisms.

It is well established that oxidative degradation of isotactic polypropylene initiates in the crystalline interphase and spreads out the amorphous region where oxygen can diffuse easily. While chemical oxidation is clearly involved, preferential chemical etching of the surface, or exit of degradation products from within, by themselves cannot be responsible. Indeed, the FTIR profile of showed a gradual increase of the carbonyl signals, whereas, the SEM images clearly pointed to a delayed and dramatic change of topology (*Figure 3.23*). If selective chemical etching or any form of material loss were truly operative, then a gradual change of topology would be expected to occur in time as opposed to a sudden change. In this respect, a quick phase separation would be more consistent with the observations.

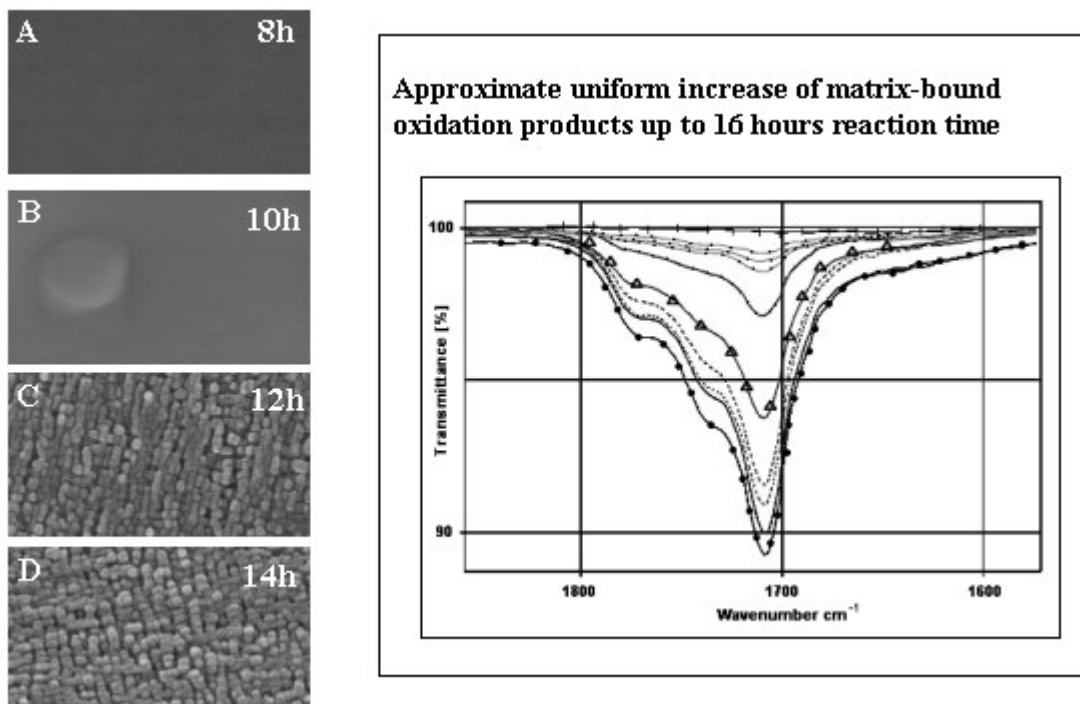


Figure 3.23 Comparison of SEM micrographs(left) and FTIR(right) of time course samples.

Scanning electron micrographs of oxidized melt blown (*Figure 4.13.A* and *Figure 4.13.B*) showed the development of material formation above the surface of the melt blown polypropylene fibers following oxidation. The material formed above the surface also has a sponge-like appearance (*Figure 4.13.C*). SEM micrographs taken after rinsing proved that the material on the surface not adsorbed on the surface. SEM-EDS result showed that the material formed above the surface was another phase different than the fiber and contained oxygen functional groups indicating that the surface was enriched in one component and the composition near the surface is different than the bulk.

The fact that the topology changed dramatically late in the oxidation process and a different phase having lower surface energy formed on the surface indicated oxidation induced, surface-phase separation as a possible mechanism for the topology change. The formation of a layer containing functional groups is consistent with the surface segregation and uphill diffusion phenomena in surface-directed spinodal decomposition and micro-phase separation in diblock copolymers.

The formation of the material above the surface can be attributed to surface segregation as result of free energy trade-off. The driving force for the segregation of oxidized material to the surface of polypropylene may be related to the lowering system's free energy that is possible by having a larger concentration of the material of low surface energy at the surface. Another possible explanation for material formation above the surface could be up-hill diffusion. The mutual diffusion of a polymer mixture is important for the mechanism that is operative in the unstable part of the phase diagram. During up-hill diffusion material diffuses from regions of low concentration to high concentration, thus the depleted region is made deeper and deeper and a second layer of higher concentration is formed near the surface. However, surface energy differences are by no means the only factor determining the extent of surface degradation, so the free energy cost also should be taken into account.

Micro-phase separation in diblock copolymers is another possible explanation for the pattern formation. In the case of diblock copolymers, consisting of two sub-chains a and b made of different monomers A and B respectively, even a weak repulsion between unlike monomers induces a strong repulsion between sub-chains. As a result, different sub-chains tends to segregate below some temperature, but as they are chemically bonded, even a complete segregation cannot lead to a macroscopic phase separation as in mixtures of two polymers. Only a local micro-phase separation occurs and micro-phases rich in A or B are formed. There is a close connection between spinodal decomposition and diblock copolymer micro-phase separation and it is established that different mesoscale structures are observed depending the ratio of block sizes.

To summarize the results of the initial investigation, the pattern noted was likely a product of chemical oxidation induced phase separation by surface directed spinodal decomposition mechanism and release of internal stress that had accumulated during oxidation. The presence of a surface profoundly modified the mechanism of phase separation and the course of spinodal decomposition, by breaking the translational and rotational symmetry. Material diffused from regions of low concentration to high concentration, thus the depleted region is made deeper and deeper and; in the presence of a surface with a preferential attractive interaction for one of the component to the surface, a second layer of higher concentration is formed near the surface.

3.6 Conclusion

In this work, revised methods to engineer polypropylene surface were investigated using aqueous ammonium peroxydisulfate. The scanning electron micrographs showed that the oxidation process not only yielded polar functional groups along the new surface, but more importantly, it produced dramatic changes of topology on the order of the mesoscopic length scale. A preliminary objective was to characterize the surface-pendant functional group composition and new topology, since either factor is known to govern wetting-related adhesivity. More importantly, potential explanations for the oxidation-induced pattern formation were proposed and discussed. While the specific mechanism leading to this change of topology remains outstanding, noteworthy candidates include modes of pitting or rupture of the surface in a spatially regular manner, oxidation-mediated phase separation, or a combination of both elements. Clearly, an understanding of the mechanism underlying this new topology could potentially introduce promising alternatives of achieving physico-chemically engineered surfaces and chemically active surfaces.

REFERENCES

1. Somorjai, G.A., *Introduction to Surface Chemistry and Catalysis*, John Wiley and Sons, NY, 1994.
2. Burakowski, T., Wierzchon, T., *Surface Engineering of Metals: Principles, Equipment, Technologies*; CRC Press, NY, 1999.
3. Chan, C.-M., *Polymer Surface Modification and Characterization*, Hanser Gardner Publications, Cincinnati, 1994.
4. Stokes, R.J., Evans, D.F., *Fundamentals of Interfacial Engineering*, Wiley-VCH, NY, 1997.
5. Richards, R.W.; Peace, S.K., *Polymer Surfaces and Interfaces III*; John Wiley and Sons, NY, 1999.
6. Batchelor, A.W., Lam, L.N., Chandrasekaran, M., *Materials Degradation and its Control by Surface Engineering*; World Scientific Publishing, Singapore, 1999.
7. Arkles, B., *Tailoring surfaces with silanes*, Chemtech, (1977) 7: 766-778.
8. Plueddemann, E.P., *Silane Coupling Agents*, Plenum Press, NY, 1982.
9. Van Der Voort, P., Vrancken, K.C., *Characterization and Chemical Modification of the Silica Surface: In Studies in Surface Science and Catalysis*, Elsevier, NY, 1995, Vol. 93.
10. Wu, S., *Polymer Interface and Adhesion*, Marcel Dekker, NY, 1982.
11. Grill, A., *Cold Plasma in Materials Fabrication: From Fundamentals to Applications*, IEEE Press, NY, 1994.
12. Tsujii, K., *Surface Activity - Principles, Phenomena, and Applications: In Polymers, Interfaces, and Biomaterials*, Academic Press: NY, 1998.
13. Korach, Ł., Czaja, L., "Synthesis and activity of zirconocene catalysts supported on silica-type sol-gel carrier for ethylene polymerization", *Polymer Bulletin*, (2001) 46: 175-182
14. Levi, M., Ferro, C., Regazzoli, D., Dotelli, G., Lo presti A., "Comparative evaluation method of polymer surface treatments applied on high performance concrete", *Journal of Materials Science*, (2002) 37(22): 4881-4888
15. Pesek, J.J., Matyska, M.T., "Modified aluminas as chromatographic supports for high-performance liquid chromatography", *Journal of Chromatography A*, (2002) 952(1-2): 1-11

16. Electronics: Uemura, S., Yoshida, M., Hoshino, S., Kodzasa, T., Kamata, "Investigation for surface modification of polymer as an insulator layer of organic FET", *Thin Solid Films*, (2003), 438-439: 378-381
17. Electrochemistry: Pastor-Moreno, G., Riley, J.D., "Influence of surface preparation on the electrochemistry of boron doped diamond: A study of the reduction of 1,4-benzoquinone in acetonitrile", *Electrochemistry Communications*, (2002) 4(3): 218-221
18. Stoneham, A.M., Itoh, N., "Materials modification by electronic excitation", *Applied Surface Science*, 168(1-4), 186-193
19. Mao-Sung Wu, M.-S., Wu, H., Wang, Y., Wan, C., "Electrochemical investigation of hydrogen-storage alloy electrode with duplex surface modification", *International Journal of Hydrogen Energy*, (2004) 29(12): 1263-1269
20. Taga, Y., "Review of plasma thin-film technology in automobile industry", *Surface and Coating Technology*, (1999) 112(1-3): 339-346
21. LaPorte, R.J., *Hydrophilic Polymer Coatings for Medical Devices: Structure/properties, Development, Manufacture, and Applications*, Technomic Publishing: Lancaster, 1997.
22. Toebes, M.L., van Dillen, J.A., de Jong, K.P. "Synthesis of supported palladium catalysts", *Journal of Molecular Catalysis A: Chemical*, (2001) 173: 75-98.
23. Shiraishi, S., Kanamura, K., Takehara, Z-I. "Influence of initial surface condition of lithium metal anodes on surface modification with HF", *Journal of Applied electrochemistry*, (1999), 29: 869-881
24. Wang, M., Bonfield, W., "Chemically coupled hydroxyapatite-polyethylene composites: structure and properties", *Biomaterials*, (2001) 22(11): 1311-1320.
25. Ismail, A.F., David, L.I.B., "A review on the latest development of carbon membranes for gas separation", *Journal of Membrane Science*, (2001) 193(1): 1-18.
26. Dörwald, F.Z., *Organic Synthesis on Solid Phase: Supports, Linkers, Reactions*, Wiley-VCH, Weinheim, 2000.
27. Seneci, P., *Solid-Phase Synthesis and Combinatorial Technologies*, John Wiley and Sons, NY, 2000.
28. Harris, D.C., *Quantitative Chemical Analysis*, 2nd Ed., Freeman and Company, NY, 1987.

29. Pelka, A., Ostrowski, G., Niedzielski, P., Mitura, S., Stroz, D., "Carbon coatings on shape memory alloys", *Journal of Wide Bandgap Materials*, (2001) 8(3-4): 189-194
30. Kannan, S., Balamurugan, A., Rajeswari, S., Subbaiyan, M., "Metallic implants: approach for long term applications in bone related defects", *Corrosion Reviews*, (2003), 20-(4-5): 339-358
31. Faust, V., Heidenau, F., Schmidgall, J., Stenzel, F., Lipps, G., Ziegler G., "Biofunctionalized biocompatible titania coatings for implants", *Key Engineering Materials*, (2002) 206-213(3): 1547-1550
32. Mao, C., Zhao, W.B., Zhu, A.P., Shen, J., Lin, S.C. "A photochemical method for the surface modification of poly(vinyl chloride) with *O*-butyrylchitosan to improve blood compatibility", *Process Biochemistry*, (2004) 39(9): 1151-1157
33. Korach, Ł., Czaja, L., "Synthesis and activity of zirconocene catalysts supported on silica-type sol-gel carrier for ethylene polymerization", *Polymer Bulletin*, (2001) 46: 175-182
34. Sinfelt, J.H., "Role of surface science in catalysis", *Surface Science* (2002) 500 (1-3): 923-946
35. Paul, H., Basu, S., Bhaduri, S. and Lahiri, G.K., "Platinum carbonyl derived catalysts on inorganic and organic supports: a comparative study", *Journal of Organometallic Chemistry*, (2004) 689(2): 309-316
36. Jin, C., Lan, H., Lu, Y., Huang, M., "Research on boronisation of bearing pins for motor timing chains", *Heat. Treat. Met.*, (2002) 7: 45-47
37. Lou, Y., Zou, X.-J., Ouyang, B.-S., Shi, S.-H., Fan, X.-F., "Analysis of laser hardening for tablet punch pin", *Heat. Treat. Met.*, (2002) 7:37-39
38. Balamurugan, S., Mandale, A.B., Badrinarayanan, S., Vernekar, S.P. "Photochemical bromination of polyolefin surfaces", *Polymer*, (2001) 42(6): 2501-2512
39. Long, J., Chen, P. "Surface characterization of Hydrosilyated Polypropylene: Contact Angle Measurement and Atomic Force Microscopy", *Langmuir*, (2001) 17(10): 2965 -2972
40. Shearer, G., Tzoganakis, C., "Free radical hydrosilylation of polypropylene", *Journal of Applied Polymer Science*, (1997) 65: 439-447.
41. Karger-Kocsis, J. *Polypropylene: An A-Z Reference*, Kluwer Academic Publishers, New York, 1999.

42. Öztürk, G.İ., Vakos, H.T., Voelter, W., Taralp, A., “A simple approach to synthesize and bond organosiloxane films on injection-molded polyolefins”, *Key Engineering Materials*, (2004), 264-268: 637-642.
43. Bamford, C.H., Al-Lamee, K.G., “Studies in polymer surface functionalization and grafting for biomedical and other applications”, *Polymer*, (1996) 35(13): 2844-2852
44. Garbassi, F., Morra, M., Occhiello, E., *Polymer Surfaces: From Physics to Technology*, John Wiley & Sons, Chichester, 1998.
45. Garbassi, F., Occhiello, E., Polato, F., Brown, A., “Surface effect of flame treatments on polypropylene”, *Journal of Materials Science*, (1987) 22: 1450-1456
46. Sheng, E., Sutherland, I., Brewis, D.M., Heath, R.J., “An X-ray photoelectron spectroscopy study of flame treatment of polypropylene”, *Applied Surface Science*, (1994) 78(3): 249-254
47. Strobel, M., Branch, M.C., Ulsh, M., Kapaun, R.S., Kirk, S., Lyons, C.S., “Flame surface modification of polypropylene film”, *Journal of Adhesion Science and Technology*, (1996) 10(6): 515-539
48. Pijpers, A.P., Meier, R.J., “Adhesion behavior of polypropylenes after flame treatment determined by XPS(ESCA) spectral analysis”, *Journal of Electron Spectroscopy and related phenomena*, (2001) 121: 299-313
49. 34. Mark Strobel et al., “Gas-phase modeling of impinging flames used for the flame surface modification of polypropylene film” *Journal of Adhesion Science and Technology*, (2001) 15(1): 1-21
50. 35. Mark Strobel et al “Surface modification of polypropylene film using N₂O-containing flames”, *Journal of Adhesion Science and Technology*, (2000) 14-10: 1243-1264
51. Garbassi, F., Occhiello, E., Polato, F., Brown, A., *Journal of Material Science*, (1987) 22: 1450
52. A. Lanauze, J.A., Myers, D.L., “Ink adhesion on corona treated polyethylene studied by chemical derivatization of surface functional groups”, *Journal of Applied Polymer Science*, (2003) 40(3-4): 595-611

53. Ogawa, T., Mukai, H., Osawa, S., "Improvement of the mechanical properties of an ultrahigh molecular weight polyethylene fiber/epoxy composite by corona discharge treatment", *Journal of Applied Polymer Science*, (2000) 79(7): 1162-1168
54. C. Xu, W., Liu, X., "Surface modification of polyester fabric by corona discharge irradiation", *European Polymer Journal*, (2003) 39(1): 199-202
55. Massines, F., Gouda, G., Gherardi, N., Duran, M., Croquesel, E., "The role of dielectric barrier discharge atmosphere and physics on polypropylene surface treatment", *Plasmas and Polymers*, (2001) 6: 35-49
56. Meiners, S., Salge, J.G.H., Prinz, E., Forster, F., "Surface modification of polymer materials by transient gas discharges at atmospheric pressure", *Surface and Coating Technology*, (1998) 98: 1121-1127
57. Strobel, M., Jones, V., Lyons, C.S., Ulsh, M., Kushner, M.J., Dorai, R., Branch, M.C. "A comparison of corona treated and flame-treated polypropylene films", *Plasmas and Polymers*, (2003) 8(1): 61-95
58. Liu, C.Z., Wu, J.Q., Ren, L.Q., Li, J.Q., Cui, N., Brown, N.M.D., Meenan, B.J., "Comparative study on the effect of RF and DBD plasma treatment on PTFE surface modification", *Materials Chemistry and Physics*, (2004) 85(2-3): 340-346
59. Noeske, M., Degenhardt, Strudthoff, S., Lommatzsh, U., "Plasma jet treatment of five polymers at atmospheric pressure: surface modifications and relevance for adhesion", *International Journal of Adhesion and Adhesives*, (2004) 24(2): 171-177
60. Oehr, C., "Plasma surface modification of polymers for biomedical use", *Nuclear Instruments and Methods in Physics Section B: Beam Interactions with Materials and Atoms*, (2003) 208: 40-47
61. Kim, K.S., Lee, K.H., Cho, K., Park, C.E., "Surface modification of polysulfone ultrafiltration membrane by oxygen plasma treatment", *Journal of Membrane Science*, (2002) 199(1-2): 135-145
62. Poncin-Epaillard, F., Chevet, B., Brosse, J.C., "Reactivity of a polypropylene surface modified in a nitrogen plasma", *Journal of Adhesion Science and Technology*, (1994) 8(4): 455-468

63. Aouinti, M., Bertrand, P., Poncin-Epaillard, F. "Characterization of polypropylene surface treated in a CO₂ plasma", *Plasmas and Polymers*, (2003) 8-4: 225-236
64. France, R.M., Short, R.D., "Plasma treatment of polymers: The effects of energy transfer from an argon plasma on the surface chemistry of polystyrene, and polypropylene. A high-energy resolution X-ray photoelectron spectroscopy study", *Langmuir*, (1998) 14(17): 4827-4835
65. Kamińska, A., Kaczmarek, H., Kowalonek, J., "Influence of side groups and polarity of polymers on the kind and effectiveness of their surface modification by air plasma action", *European Polymer Journal*, (2002) 38(9): 1915-1919
66. Hong, J., Truica-Marasescu, F., Martinu, L., Wertheimer, M.N. "An investigation of plasma-polymer interactions by mass spectrometry", *Plasmas and Polymers*, (2002) 7(3): 245-260
67. Riekerink, M.B.O., Terlingen, J.G.A., Engbers, G.H.M., Feijen J., "Selective etching of semicrystalline polymers: CF₄ gas plasma treatment of poly(ethylene)", *Langmuir*, (1999) 15(14): 4847-4856
68. Favia, P., Sardella, E., Gristina, R., "Novel plasma processes for biomaterials: micro-scale patterning of biomedical polymers", *Surface Coatings and Technology*,(2003) 169-170: 707-711.
69. Poncin-Epaillard, F., Brosse, J.C., Falher, T., "Cold plasma treatment: surface or bulk modification of polymer films?", *Macromolecules*, (1997) 30(15): 4415–4420
70. Olde Riekerink, M.B., Terlingen, J.G.A., Engbers, G.H.M., Feijen, J., "Selective Etching of Semicrystalline Polymers: CF₄ Gas Plasma Treatment of Poly(ethylene)", *Langmuir*, (1999) 15(14): 4847-4856,
71. Laurens, P., Petit, S., Arefi-Khonsari, F. "Study of PET surfaces after laser or plasma treatment: Surface modifications and adhesion properties towards Al deposition", *Plasma and Polymers*, (2003) 8(4): 281-295
72. Lippert, T., Nakamura, T., Niino H., Yabe A. "Laser induced chemical and physical modifications of polymer films: dependence on the irradiation wavelength", *Applied Surface Science*, (1997) 109-110: 227-231
73. Frerichs, H., Stricker, J., Wesner, D. A., Kreutz, E.W., "Laser-induced surface modification and metallization of polymers", *Applied Surface Science*, (1995) 86(1-4): 405-410

74. Davidson, M.R., Mitchell, S.A., Bradley, R.H., "UV-ozone modification of plasma-polymerized acetonitrile films for enhanced cell attachment", *Colloids and Surfaces B: Biointerfaces*, (2004) 34(4): 213-219
75. Chen, W., Zhang, J., Fang, Q., Hu, K., Boyd, I.W., "Surface modification of polyimide with excimer UV radiation at wavelength of 126 nm", *Thin Solid Films*, (2004) 453-454: 3-6
76. Bertrand, P., Lambert, P., Travaly, Y., "Polymer metallization: Low energy ion beam surface modification to improve adhesion", *Nuclear Instruments and Methods in Physics Research Section B: Beam Interactions with Materials and Atoms*, (1997) 131(1-4): 71-78
77. Biederman, H., "RF sputtering of polymers and its potential application", *Vacuum*, (2000) 59(2-3): 594-599
78. Wu, G.M, Hung, C.H., Liu, S.J., "Surface modification of reinforcement fibers for composites by acid treatments", *Journal of Polymer Research*, (2004) 11: 31-36
79. Vasconcellos, A.S., Oliveira, J.A.P., Baumhardt-Neto, R., "Adhesion of polypropylene treated with nitric and sulfuric acid", *European Polymer Journal*, (1997) 33: 1731-1734
80. Idage, S.B., Badrinarayanan, S., Vernekar, S.P., Sivaram, S., "X-ray photoelectron spectroscopy of sulphonated polyethylene", *Langmuir*, (1996) 12(4): 1018-1022.
81. Gibson, H.W., Bailey, F.C., "Chemical modification of polymers. 13. sulfonation of polystyrene surfaces", *Macromolecules*, (1980) 13(1): 34-41
82. Yang, P., Deng, J.Y., Yang, W. T., "Confined photo-catalytic oxidation: a fast surface hydrophilic modification method for polymeric materials", *Polymer*, (2003) 44(23): 7157-7164
83. Kubota, H., Hariya, Y., Kuroda, S., Kondo, T., "Effect of photoirradiation on potassium persulfate-surface oxidation of low-density polyethylene film", *Polymer Degradation and Stability*, (2001) 72: 223-227
84. Price, G.J., Clifton, A.A., Keen, F., "Ultrasonically enhanced persulfate oxidation of polyethylene surfaces", *Polymer*, (1996) 37(26): 5825-5829
85. Szreder, T., Wolszczak, M., Mayer, J. "Study of fast processes in oxidized polypropylene in the presence of pyrene", *Journal of photochemistry and Photobiology A: Chemistry*, (1998) 113: 265-270

86. Lee, K-W., McCarthy, T.J., "Surface-selective hydroxylation of polypropylene", *Macromolecules*, (1988) 21(2): 309-313
87. Wiberg, K.B., Foster, G., "The Stereochemistry of the Chromic Acid Oxidation of Tertiary Hydrogens", *Journal of American Chemical Society* (1961) 83(2): 423-429
88. Gensler, R., Plummer, C.J.G., Kausch, H.-H., Kramer, E., Pauquet, J.-R., Zweifel, H., "Thermo-oxidative degradation of isotactic polypropylene at high temperatures: phenolic antioxidants versus HAS", *Polymer Degradation and Stability*, (2000) 67(2): 195-208
89. Gugumus, F., "Re-examination of the thermal oxidation reactions of polymers 3. Various reactions in polyethylene and polypropylene", *Polymer Degradation and Stability*, (2002), 77(1): 147-155
90. Zaikov, G.E., *Degradation and Stabilization of Polymers: Theory and Practice*, Nova Science Publishers, 1995, New York
91. Hinske, H.S., Moss, S., Pauquet, J., Zweifel, H., "Degradation of polyolefins during melt processing", *Polymer Degradation Stability*, (1991) 34(1-3): 279-293.
92. Canevarolo, S.V., "Chain scission distribution function for polypropylene degradation during multiple extrusions", *Polymer Degradation and Stability*, (2000) 70(1): 71-76
93. Elvira, M., Tiemblo, P., Elvira, J. M., "Changes in the crystalline phase during the thermo-oxidation of a metallocene isotactic propylene. A DSC study", *Polymer Degradation and Stability*, (2004) 83(3): 509-518
94. Fayolle, B., Audouin, L., George, G.A., Verdu, J., "Macroscopic heterogeneity in stabilized polypropylene thermal oxidation", *Polymer Degradation and Stability*, (2002) 77(3): 515-522
95. Tehrani, A.R., Shoushtari, A.M., Malek, R.M.A., Abdous, M., "Effect of chemical oxidation treatment on dyeability of polypropylene", *Dyes and Pigments*, (2004) 63(1): 95-100
96. Liu, Q., deWijn, J.R., deGroot, K., Blitterswijk, C.A., "Surface modification of nano-apatite by grafting organic polymer", *Biomaterials*, (1998) 19(11-12): 1067-1072
97. Liu, Q., Spears, D.A., Liu, Q., "MAS NMR study of surface-modified calcined kaolin", *Applied Clay Science*, (2001) 19(1-6): 89-94

98. Picard, C., Larbot, A., Guida-Pietrasanta, F., Boutevin, B., Ratsimihety, “Grafting of ceramic membranes by fluorinated silanes: hydrophobic features”, *Separation and Purification Technology*, (2001) 25(1-3): 65-69
99. Song, K., Sandí, G., “Characterization of montmorillonite surfaces after modification by organosilane”, *Clays and Minerals*, (2001) 49(2): 119-125
100. Jesionowski, T., “Influence of aminosilane surface modification and dyes adsorption on zeta potential of spherical silica particles formed in emulsion system”, *Colloids and Surfaces A: Physicochemical and Engineering Aspects*, (2003) 222(1-3): 8794
101. Domka, L., Krysztafkiewicz, A., Kozak, M., “Silane modified fillers for reinforcing polymers”, *Polymer and Polymer Composites*, (2002) 10(7): 541-552
102. Matsuda, T., Magoshi, T., “Terminally Alkylated Heparin. 1. Antithrombogenic Surface Modifier”, *Biomacromolecules*, (2001) 2(4): 1169 – 1177
103. Malmstadt, N., Yager, P., Hoffman, A. S., Stayton, P.S., “A Smart Microfluidic Affinity Chromatography Matrix Composed of Poly(*N*-isopropylacrylamide)-Coated Beads”, *Analytical Chemistry* (2003) 75(13): 2943-2949
104. Wang, Z-H., Gang, J., “Silicon surface modification with a mixed silanes layer to immobilize proteins for biosensor with imaging ellipsometry”, *Colloids and Surfaces B: Biointerfaces*, (2004) 34(3): 173-177
105. Ratner, BD., *Biomaterials Science: An introduction to materials in medicine*, Academic Press, USA, 1996.
106. Halliwell, C.M., Cass, A.E.G., “A Factorial Analysis of Silanization Conditions for the Immobilization of Oligonucleotides on Glass Surfaces”, *Analytical Chemistry*,(2001) 73(11): 2476-2483
107. Strobl, G., *The Physics of Polymers*, 2nd Edition, Springer, 1997
108. Lipatov, Y.S., Nesterov, A.E., *Thermodynamics of polymer blends*, Polymer Thermodynamics Library, Volume1, ChemTec Publishing, Lancaster, 1997
109. Lo, C.-T., Seifert, S., Thiyagarajan, P., Narasimhan, B., “Phase behavior of semicrystalline polymer blends”, *Polymer*, (2004) 45: 3671-3679
110. Jones, R.A.L., Richards, R.W., *Polymers at Surfaces and interfaces*, Cambridge University Press, Cambridge, 1999.

111. Unpublished data: "Thermodynamic interactions and phase separation in a polyolefin blend", An experiment using the NG3 SANS instrument at the NIST NCNR summer school, June 3-7, 2002
112. MacDougall, A.J, Righy, N.M., Ring, S.G. "Phase separation of plant cell wall polysaccharides and its implications for cell assembly", *Plant Physiology*, (1997), 114(1): 353-362
113. Schugens, C., Maquet, Grandfils, Jerome, V.C.R., Teyssie, Ph., "Biodegradable and macroporous polylactide implants for cell transplantation: 1. Preparation of macroporous polylactide supports by solid-liquid phase separation", *Polymer*, (1996) 37(6): 1027-1038
114. Tanaka, T., Lloyd, D.R., "Formation of poly(lactic acid) microfiltration membranes via thermally induced phase separation", *Journal of Membrane Science*, Article in Press
115. Kwok, A.Y., Prime, E.L., Qiao, G.G., Solomon, D.H., "Synthetic hydrogels 2. Polymerization induced phase separation in acrylamide systems", *Polymer*, (2003) 44(24): 7335-7344
116. Elicabe, G.E., Larrondo, H.A., Williams R.J J., "Polymerization-Induced Phase Separation: A Maximum in the Intensity of Scattered Light Associated with a Nucleation-Growth Mechanism", *Macromolecules*, (1997) 30(21): 6550–6555
117. Kim, E., Krausch, G., Kramer, E.J. "Surface-directed spinodal decomposition in the blend of polystyrene and tetramethyl-bisphenol-A polycarbonate" *Macromolecules*, (1994) 27:5927-5929
118. Jones, R.A.L., Norton, L.J., Kramer, E.J., Bates, F.S., Wiltzius, P., "Surface-directed spinodal decomposition", *Physical Review Letters*, (1991) 66(10): 1326-1329
119. Schertz, T.D., Reiter, R.C., Stevenson, C.D., "Zwitterion Radicals and anion radicals from electron transfer and solvent condensation with fingerprint developing agent ninhydrin", *Journal of Organic Chemistry*, (2001) 66: 7596-7603

REFERENCES

1. Somorjai, G.A., *Introduction to Surface Chemistry and Catalysis*, John Wiley and Sons, NY, 1994.
2. Burakowski, T., Wierzchon, T., *Surface Engineering of Metals: Principles, Equipment, Technologies*; CRC Press, NY, 1999.
3. Chan, C.-M., *Polymer Surface Modification and Characterization*, Hanser Gardner Publications, Cincinnati, 1994.
4. Stokes, R.J., Evans, D.F., *Fundamentals of Interfacial Engineering*, Wiley-VCH, NY, 1997.
5. Richards, R.W.; Peace, S.K., *Polymer Surfaces and Interfaces III*; John Wiley and Sons, NY, 1999.
6. Batchelor, A.W., Lam, L.N., Chandrasekaran, M., *Materials Degradation and its Control by Surface Engineering*; World Scientific Publishing, Singapore, 1999.
7. Arkles, B., *Tailoring surfaces with silanes*, Chemtech, (1977) 7: 766-778.
8. Plueddemann, E.P., *Silane Coupling Agents*, Plenum Press, NY, 1982.
9. Van Der Voort, P., Vrancken, K.C., *Characterization and Chemical Modification of the Silica Surface: In Studies in Surface Science and Catalysis*, Elsevier, NY, 1995, Vol. 93.
10. Wu, S., *Polymer Interface and Adhesion*, Marcel Dekker, NY, 1982.
11. Grill, A., *Cold Plasma in Materials Fabrication: From Fundamentals to Applications*, IEEE Press, NY, 1994.
12. Tsujii, K., *Surface Activity - Principles, Phenomena, and Applications: In Polymers, Interfaces, and Biomaterials*, Academic Press: NY, 1998.
13. Korach, Ł., Czaja, L., "Synthesis and activity of zirconocene catalysts supported on silica-type sol-gel carrier for ethylene polymerization", *Polymer Bulletin*, (2001) 46: 175-182
14. Levi, M., Ferro, C., Regazzoli, D., Dotelli, G., Lo presti A., "Comparative evaluation method of polymer surface treatments applied on high performance concrete", *Journal of Materials Science*, (2002) 37(22): 4881-4888
15. Pesek, J.J., Matyska, M.T., "Modified aluminas as chromatographic supports for high-performance liquid chromatography", *Journal of Chromatography A*, (2002) 952(1-2): 1-11

16. Electronics: Uemura, S., Yoshida, M., Hoshino, S., Kodzasa, T., Kamata, “Investigation for surface modification of polymer as an insulator layer of organic FET”, *Thin Solid Films*, (2003), 438-439: 378-381
17. Electrochemistry: Pastor-Moreno, G., Riley, J.D., “Influence of surface preparation on the electrochemistry of boron doped diamond: A study of the reduction of 1,4-benzoquinone in acetonitrile”, *Electrochemistry Communications*, (2002) 4(3): 218-221
18. Stoneham, A.M., Itoh, N., “Materials modification by electronic excitation”, *Applied Surface Science*, 168(1-4), 186-193
19. Mao-Sung Wu, M.-S., Wu, H., Wang, Y., Wan, C., “Electrochemical investigation of hydrogen-storage alloy electrode with duplex surface modification”, *International Journal of Hydrogen Energy*, (2004) 29(12): 1263-1269
20. Taga, Y., “Review of plasma thin-film technology in automobile industry”, *Surface and Coating Technology*, (1999) 112(1-3): 339-346
21. LaPorte, R.J., *Hydrophilic Polymer Coatings for Medical Devices: Structure/properties, Development, Manufacture, and Applications*, Technomic Publishing: Lancaster, 1997.
22. Toebes, M.L., van Dillen, J.A., de Jong, K.P. “Synthesis of supported palladium catalysts”, *Journal of Molecular Catalysis A: Chemical*, (2001) 173: 75-98.
23. Shiraishi, S., Kanamura, K., Takehara, Z-I. “Influence of initial surface condition of lithium metal anodes on surface modification with HF”, *Journal of Applied electrochemistry*, (1999), 29: 869-881
24. Wang, M., Bonfield, W., “Chemically coupled hydroxyapatite-polyethylene composites: structure and properties”, *Biomaterials*, (2001) 22(11): 1311-1320.
25. Ismail, A.F., David, L.I.B., “A review on the latest development of carbon membranes for gas separation”, *Journal of Membrane Science*, (2001) 193(1): 1-18.
26. Dörwald, F.Z., *Organic Synthesis on Solid Phase: Supports, Linkers, Reactions*, Wiley-VCH, Weinheim, 2000.
27. Seneci, P., *Solid-Phase Synthesis and Combinatorial Technologies*, John Wiley and Sons, NY, 2000.
28. Harris, D.C., *Quantitative Chemical Analysis*, 2nd Ed., Freeman and Company, NY, 1987.

29. Pelka, A., Ostrowski, G., Niedzielski, P., Mitura, S., Stroz, D., "Carbon coatings on shape memory alloys", *Journal of Wide Bandgap Materials*, (2001) 8(3-4): 189-194
30. Kannan, S., Balamurugan, A., Rajeswari, S., Subbaiyan, M., "Metallic implants: approach for long term applications in bone related defects", *Corrosion Reviews*, (2003), 20-(4-5): 339-358
31. Faust, V., Heidenau, F., Schmidgall, J., Stenzel, F., Lipps, G., Ziegler G., "Biofunctionalized biocompatible titania coatings for implants", *Key Engineering Materials*, (2002) 206-213(3): 1547-1550
32. Mao, C., Zhao, W.B., Zhu, A.P., Shen, J., Lin, S.C. "A photochemical method for the surface modification of poly(vinyl chloride) with *O*-butyrylchitosan to improve blood compatibility", *Process Biochemistry*, (2004) 39(9): 1151-1157
33. Korach, Ł., Czaja, L., "Synthesis and activity of zirconocene catalysts supported on silica-type sol-gel carrier for ethylene polymerization", *Polymer Bulletin*, (2001) 46: 175-182
34. Sinfelt, J.H., "Role of surface science in catalysis", *Surface Science* (2002) 500 (1-3): 923-946
35. Paul, H., Basu, S., Bhaduri, S. and Lahiri, G.K., "Platinum carbonyl derived catalysts on inorganic and organic supports: a comparative study", *Journal of Organometallic Chemistry*, (2004) 689(2): 309-316
36. Jin, C., Lan, H., Lu, Y., Huang, M., "Research on boronisation of bearing pins for motor timing chains", *Heat. Treat. Met.*, (2002) 7: 45-47
37. Lou, Y., Zou, X.-J., Ouyang, B.-S., Shi, S.-H., Fan, X.-F., "Analysis of laser hardening for tablet punch pin", *Heat. Treat. Met.*, (2002) 7:37-39
38. Balamurugan, S., Mandale, A.B., Badrinarayanan, S., Vernekar, S.P. "Photochemical bromination of polyolefin surfaces", *Polymer*, (2001) 42(6): 2501-2512
39. Long, J., Chen, P. "Surface characterization of Hydrosilyated Polypropylene: Contact Angle Measurement and Atomic Force Microscopy", *Langmuir*, (2001) 17(10): 2965 -2972
40. Shearer, G., Tzoganakis, C., "Free radical hydrosilylation of polypropylene", *Journal of Applied Polymer Science*, (1997) 65: 439-447.
41. Karger-Kocsis, J. *Polypropylene: An A-Z Reference*, Kluwer Academic Publishers, New York, 1999.

42. Öztürk, G.İ., Vakos, H.T., Voelter, W., Taralp, A., “A simple approach to synthesize and bond organosiloxane films on injection-molded polyolefins”, *Key Engineering Materials*, (2004), 264-268: 637-642.
43. Bamford, C.H., Al-Lamee, K.G., “Studies in polymer surface functionalization and grafting for biomedical and other applications”, *Polymer*, (1996) 35(13): 2844-2852
44. Garbassi, F., Morra, M., Occhiello, E., *Polymer Surfaces: From Physics to Technology*, John Wiley & Sons, Chichester, 1998.
45. Garbassi, F., Occhiello, E., Polato, F., Brown, A., “Surface effect of flame treatments on polypropylene”, *Journal of Materials Science*, (1987) 22: 1450-1456
46. Sheng, E., Sutherland, I., Brewis, D.M., Heath, R.J., “An X-ray photoelectron spectroscopy study of flame treatment of polypropylene”, *Applied Surface Science*, (1994) 78(3): 249-254
47. Strobel, M., Branch, M.C., Ulsh, M., Kapaun, R.S., Kirk, S., Lyons, C.S., “Flame surface modification of polypropylene film”, *Journal of Adhesion Science and Technology*, (1996) 10(6): 515-539
48. Pijpers, A.P., Meier, R.J., “Adhesion behavior of polypropylenes after flame treatment determined by XPS(ESCA) spectral analysis”, *Journal of Electron Spectroscopy and related phenomena*, (2001) 121: 299-313
49. 34. Mark Strobel et al., “Gas-phase modeling of impinging flames used for the flame surface modification of polypropylene film” *Journal of Adhesion Science and Technology*, (2001) 15(1): 1-21
50. 35. Mark Strobel et al “Surface modification of polypropylene film using N₂O-containing flames”, *Journal of Adhesion Science and Technology*, (2000) 14-10: 1243-1264
51. Garbassi, F., Occhiello, E., Polato, F., Brown, A., *Journal of Material Science*, (1987) 22: 1450
52. A. Lanauze, J.A., Myers, D.L., “Ink adhesion on corona treated polyethylene studied by chemical derivatization of surface functional groups”, *Journal of Applied Polymer Science*, (2003) 40(3-4): 595-611

53. Ogawa, T., Mukai, H., Osawa, S., "Improvement of the mechanical properties of an ultrahigh molecular weight polyethylene fiber/epoxy composite by corona discharge treatment", *Journal of Applied Polymer Science*, (2000) 79(7): 1162-1168
54. C. Xu, W., Liu, X., "Surface modification of polyester fabric by corona discharge irradiation", *European Polymer Journal*, (2003) 39(1): 199-202
55. Massines, F., Gouda, G., Gherardi, N., Duran, M., Croquesel, E., "The role of dielectric barrier discharge atmosphere and physics on polypropylene surface treatment", *Plasmas and Polymers*, (2001) 6: 35-49
56. Meiners, S., Salge, J.G.H., Prinz, E., Forster, F., "Surface modification of polymer materials by transient gas discharges at atmospheric pressure", *Surface and Coating Technology*, (1998) 98: 1121-1127
57. Strobel, M., Jones, V., Lyons, C.S., Ulsh, M., Kushner, M.J., Dorai, R., Branch, M.C. "A comparison of corona treated and flame-treated polypropylene films", *Plasmas and Polymers*, (2003) 8(1): 61-95
58. Liu, C.Z., Wu, J.Q., Ren, L.Q., Li, J.Q., Cui, N., Brown, N.M.D., Meenan, B.J., "Comparative study on the effect of RF and DBD plasma treatment on PTFE surface modification", *Materials Chemistry and Physics*, (2004) 85(2-3): 340-346
59. Noeske, M., Degenhardt, Strudthoff, S., Lommatzsh, U., "Plasma jet treatment of five polymers at atmospheric pressure: surface modifications and relevance for adhesion", *International Journal of Adhesion and Adhesives*, (2004) 24(2): 171-177
60. Oehr, C., "Plasma surface modification of polymers for biomedical use", *Nuclear Instruments and Methods in Physics Section B: Beam Interactions with Materials and Atoms*, (2003) 208: 40-47
61. Kim, K.S., Lee, K.H., Cho, K., Park, C.E., "Surface modification of polysulfone ultrafiltration membrane by oxygen plasma treatment", *Journal of Membrane Science*, (2002) 199(1-2): 135-145
62. Poncin-Epaillard, F., Chevet, B., Brosse, J.C., "Reactivity of a polypropylene surface modified in a nitrogen plasma", *Journal of Adhesion Science and Technology*, (1994) 8(4): 455-468

63. Aouinti, M., Bertrand, P., Poncin-Epaillard, F. "Characterization of polypropylene surface treated in a CO₂ plasma", *Plasmas and Polymers*, (2003) 8-4: 225-236
64. France, R.M., Short, R.D., "Plasma treatment of polymers: The effects of energy transfer from an argon plasma on the surface chemistry of polystyrene, and polypropylene. A high-energy resolution X-ray photoelectron spectroscopy study", *Langmuir*, (1998) 14(17): 4827-4835
65. Kamińska, A., Kaczmarek, H., Kowalonek, J., "Influence of side groups and polarity of polymers on the kind and effectiveness of their surface modification by air plasma action", *European Polymer Journal*, (2002) 38(9): 1915-1919
66. Hong, J., Truica-Marasescu, F., Martinu, L., Wertheimer, M.N. "An investigation of plasma-polymer interactions by mass spectrometry", *Plasmas and Polymers*, (2002) 7(3): 245-260
67. Riekerink, M.B.O., Terlingen, J.G.A., Engbers, G.H.M., Feijen J., "Selective etching of semicrystalline polymers: CF₄ gas plasma treatment of poly(ethylene)", *Langmuir*, (1999) 15(14): 4847-4856
68. Favia, P., Sardella, E., Gristina, R., "Novel plasma processes for biomaterials: micro-scale patterning of biomedical polymers", *Surface Coatings and Technology*,(2003) 169-170: 707-711.
69. Poncin-Epaillard, F., Brosse, J.C., Falher, T., "Cold plasma treatment: surface or bulk modification of polymer films?", *Macromolecules*, (1997) 30(15): 4415–4420
70. Olde Riekerink, M.B., Terlingen, J.G.A., Engbers, G.H.M., Feijen, J., "Selective Etching of Semicrystalline Polymers: CF₄ Gas Plasma Treatment of Poly(ethylene)", *Langmuir*, (1999) 15(14): 4847-4856,
71. Laurens, P., Petit, S., Arefi-Khonsari, F. "Study of PET surfaces after laser or plasma treatment: Surface modifications and adhesion properties towards Al deposition", *Plasma and Polymers*, (2003) 8(4): 281-295
72. Lippert, T., Nakamura, T., Niino H., Yabe A. "Laser induced chemical and physical modifications of polymer films: dependence on the irradiation wavelength", *Applied Surface Science*, (1997) 109-110: 227-231
73. Frerichs, H., Stricker, J., Wesner, D. A., Kreutz, E.W., "Laser-induced surface modification and metallization of polymers", *Applied Surface Science*, (1995) 86(1-4): 405-410

74. Davidson, M.R., Mitchell, S.A., Bradley, R.H., "UV-ozone modification of plasma-polymerized acetonitrile films for enhanced cell attachment", *Colloids and Surfaces B: Biointerfaces*, (2004) 34(4): 213-219
75. Chen, W., Zhang, J., Fang, Q., Hu, K., Boyd, I.W., "Surface modification of polyimide with excimer UV radiation at wavelength of 126 nm", *Thin Solid Films*, (2004) 453-454: 3-6
76. Bertrand, P., Lambert, P., Travaly, Y., "Polymer metallization: Low energy ion beam surface modification to improve adhesion", *Nuclear Instruments and Methods in Physics Research Section B: Beam Interactions with Materials and Atoms*, (1997) 131(1-4): 71-78
77. Biederman, H., "RF sputtering of polymers and its potential application", *Vacuum*, (2000) 59(2-3): 594-599
78. Wu, G.M, Hung, C.H., Liu, S.J., "Surface modification of reinforcement fibers for composites by acid treatments", *Journal of Polymer Research*, (2004) 11: 31-36
79. Vasconcellos, A.S., Oliveira, J.A.P., Baumhardt-Neto, R., "Adhesion of polypropylene treated with nitric and sulfuric acid", *European Polymer Journal*, (1997) 33: 1731-1734
80. Idage, S.B., Badrinarayanan, S., Vernekar, S.P., Sivaram, S., "X-ray photoelectron spectroscopy of sulphonated polyethylene", *Langmuir*, (1996) 12(4): 1018–1022.
81. Gibson, H.W., Bailey, F.C., "Chemical modification of polymers. 13. sulfonation of polystyrene surfaces", *Macromolecules*, (1980) 13(1): 34-41
82. Yang, P., Deng, J.Y., Yang, W. T., "Confined photo-catalytic oxidation: a fast surface hydrophilic modification method for polymeric materials", *Polymer*, (2003) 44(23): 7157-7164
83. Kubota, H., Hariya, Y., Kuroda, S., Kondo, T., "Effect of photoirradiation on potassium persulfate-surface oxidation of low-density polyethylene film", *Polymer Degradation and Stability*, (2001) 72: 223-227
84. Price, G.J., Clifton, A.A., Keen, F., "Ultrasonically enhanced persulfate oxidation of polyethylene surfaces", *Polymer*, (1996) 37(26): 5825-5829
85. Szreder, T., Wolszczak, M., Mayer, J. "Study of fast processes in oxidized polypropylene in the presence of pyrene", *Journal of photochemistry and Photobiology A: Chemistry*, (1998) 113: 265-270

86. Lee, K-W., McCarthy, T.J., "Surface-selective hydroxylation of polypropylene", *Macromolecules*, (1988) 21(2): 309-313
87. Wiberg, K.B., Foster, G., "The Stereochemistry of the Chromic Acid Oxidation of Tertiary Hydrogens", *Journal of American Chemical Society* (1961) 83(2): 423-429
88. Gensler, R., Plummer, C.J.G., Kausch, H.-H., Kramer, E., Pauquet, J.-R., Zweifel, H., "Thermo-oxidative degradation of isotactic polypropylene at high temperatures: phenolic antioxidants versus HAS", *Polymer Degradation and Stability*, (2000) 67(2): 195-208
89. Gugumus, F., "Re-examination of the thermal oxidation reactions of polymers 3. Various reactions in polyethylene and polypropylene", *Polymer Degradation and Stability*, (2002), 77(1): 147-155
90. Zaikov, G.E., *Degradation and Stabilization of Polymers: Theory and Practice*, Nova Science Publishers, 1995, New York
91. Hinske, H.S., Moss, S., Pauquet, J., Zweifel, H., "Degradation of polyolefins during melt processing", *Polymer Degradation Stability*, (1991) 34(1-3): 279-293.
92. Canevarolo, S.V., "Chain scission distribution function for polypropylene degradation during multiple extrusions", *Polymer Degradation and Stability*, (2000) 70(1): 71-76
93. Elvira, M., Tiemblo, P., Elvira, J. M., "Changes in the crystalline phase during the thermo-oxidation of a metallocene isotactic propylene. A DSC study", *Polymer Degradation and Stability*, (2004) 83(3): 509-518
94. Fayolle, B., Audouin, L., George, G.A., Verdu, J., "Macroscopic heterogeneity in stabilized polypropylene thermal oxidation", *Polymer Degradation and Stability*, (2002) 77(3): 515-522
95. Tehrani, A.R., Shoushtari, A.M., Malek, R.M.A., Abdous, M., "Effect of chemical oxidation treatment on dyeability of polypropylene", *Dyes and Pigments*, (2004) 63(1): 95-100
96. Liu, Q., deWijn, J.R., deGroot, K., Blitterswijk, C.A., "Surface modification of nano-apatite by grafting organic polymer", *Biomaterials*, (1998) 19(11-12): 1067-1072
97. Liu, Q., Spears, D.A., Liu, Q., "MAS NMR study of surface-modified calcined kaolin", *Applied Clay Science*, (2001) 19(1-6): 89-94

98. Picard, C., Larbot, A., Guida-Pietrasanta, F., Boutevin, B., Ratsimihety, “Grafting of ceramic membranes by fluorinated silanes: hydrophobic features”, *Separation and Purification Technology*, (2001) 25(1-3): 65-69
99. Song, K., Sandí, G., “Characterization of montmorillonite surfaces after modification by organosilane”, *Clays and Minerals*, (2001) 49(2): 119-125
100. Jesionowski, T., “Influence of aminosilane surface modification and dyes adsorption on zeta potential of spherical silica particles formed in emulsion system”, *Colloids and Surfaces A: Physicochemical and Engineering Aspects*, (2003) 222(1-3): 8794
101. Domka, L., Krysztafkiewicz, A., Kozak, M., “Silane modified fillers for reinforcing polymers”, *Polymer and Polymer Composites*, (2002) 10(7): 541-552
102. Matsuda, T., Magoshi, T., “Terminally Alkylated Heparin. 1. Antithrombogenic Surface Modifier”, *Biomacromolecules*, (2001) 2(4): 1169 – 1177
103. Malmstadt, N., Yager, P., Hoffman, A. S., Stayton, P.S., “A Smart Microfluidic Affinity Chromatography Matrix Composed of Poly(*N*-isopropylacrylamide)-Coated Beads”, *Analytical Chemistry* (2003) 75(13): 2943-2949
104. Wang, Z-H., Gang, J., “Silicon surface modification with a mixed silanes layer to immobilize proteins for biosensor with imaging ellipsometry”, *Colloids and Surfaces B: Biointerfaces*, (2004) 34(3): 173-177
105. Ratner, BD., *Biomaterials Science: An introduction to materials in medicine*, Academic Press, USA, 1996.
106. Halliwell, C.M., Cass, A.E.G., “A Factorial Analysis of Silanization Conditions for the Immobilization of Oligonucleotides on Glass Surfaces”, *Analytical Chemistry*,(2001) 73(11): 2476-2483
107. Strobl, G., *The Physics of Polymers*, 2nd Edition, Springer, 1997
108. Lipatov, Y.S., Nesterov, A.E., *Thermodynamics of polymer blends*, Polymer Thermodynamics Library, Volume1, ChemTec Publishing, Lancaster, 1997
109. Lo, C.-T., Seifert, S., Thiyagarajan, P., Narasimhan, B., “Phase behavior of semicrystalline polymer blends”, *Polymer*, (2004) 45: 3671-3679
110. Jones, R.A.L., Richards, R.W., *Polymers at Surfaces and interfaces*, Cambridge University Press, Cambridge, 1999.

111. Unpublished data: "Thermodynamic interactions and phase separation in a polyolefin blend", An experiment using the NG3 SANS instrument at the NIST NCNR summer school, June 3-7, 2002
112. MacDougall, A.J, Righy, N.M., Ring, S.G. "Phase separation of plant cell wall polysaccharides and its implications for cell assembly", *Plant Physiology*, (1997), 114(1): 353-362
113. Schugens, C., Maquet, Grandfils, Jerome, V.C.R., Teyssie, Ph., "Biodegradable and macroporous polylactide implants for cell transplantation: 1. Preparation of macroporous polylactide supports by solid-liquid phase separation", *Polymer*, (1996) 37(6): 1027-1038
114. Tanaka, T., Lloyd, D.R., "Formation of poly(lactic acid) microfiltration membranes via thermally induced phase separation", *Journal of Membrane Science*, Article in Press
115. Kwok, A.Y., Prime, E.L., Qiao, G.G., Solomon, D.H., "Synthetic hydrogels 2. Polymerization induced phase separation in acrylamide systems", *Polymer*, (2003) 44(24): 7335-7344
116. Elicabe, G.E., Larrondo, H.A., Williams R.J J., "Polymerization-Induced Phase Separation: A Maximum in the Intensity of Scattered Light Associated with a Nucleation-Growth Mechanism", *Macromolecules*, (1997) 30(21): 6550–6555
117. Kim, E., Krausch, G., Kramer, E.J. "Surface-directed spinodal decomposition in the blend of polystyrene and tetramethyl-bisphenol-A polycarbonate" *Macromolecules*, (1994) 27:5927-5929
118. Jones, R.A.L., Norton, L.J., Kramer, E.J., Bates, F.S., Wiltzius, P., "Surface-directed spinodal decomposition", *Physical Review Letters*, (1991) 66(10): 1326-1329
119. Schertz, T.D., Reiter, R.C., Stevenson, C.D., "Zwitterion Radicals and anion radicals from electron transfer and solvent condensation with fingerprint developing agent ninhydrin", *Journal of Organic Chemistry*, (2001) 66: 7596-7603